Geosci. Model Dev. Discuss., https://doi.org/10.5194/gmd-2018-309
Manuscript under review for journal Geosci. Model Dev.
Discussion started: 17 January 2019

Geoscientific Model Development Discussions

The DeepMIP contribution to PMIP4: methodologies for selection, compilation and analysis of latest Paleocene and early Eocene climate proxy data, incorporating version 0.1 of the DeepMIP database

Christopher J. Hollis[1], Tom Dunkley Jones[2], Eleni Anagnostou[3,4], Peter K. Bijl[5], Margot J. Cramwinckel[5], Ying Cui[6], Gerald R. Dickens[7], Kirsty M. Edgar[2], Yvette Eley[2], Davide Evans[8], Gavin L. Foster[3], Joost Frieling[5], Gordon N. Inglis[9], Elizabeth M. Kennedy[1], Reinhard Kozdon[10], Vittoria Lauretano[9], Caroline H. Lear[11], Kate Littler[12], Nele Meckler[13], B. David A. Naafs[9], Heiko Pälike[14], Richard D. Pancost[9], Paul Pearson[11], Dana L. Royer[15], Ulrich Salzmann[16], Brian Schubert[17], Hannu Seebeck[1], Appy Sluijs[5], Robert Speijer[18], Peter Stassen[18], Jessica Tierney[19], Aradhna Tripati[20], Bridget Wade[21], Thomas Westerhold[14], Caitlyn Witkowski[22], James C. Zachos[23], Yi Ge Zhang[24], Matthew Huber[25] and Daniel J. Lunt[26].

[1] GNS Science, Lower Hutt, New Zealand

[2] School of Geography, Earth and Environmental Sciences, University of Birmingham, UK

[3] Ocean and Earth Science, National Oceanography Centre Southampton, University of Southampton, UK

[4] GEOMAR Helmholtz Centre for Ocean Research, Kiel, Germany

[5] Institute for Marine and Atmospheric Research, Utrecht University, Netherlands

6 Department of Earth Sciences, Dartmouth College, New Hampshire, USA

7 Department of Earth Sciences, Rice University, Texas, USA

[8] Institute of Geosciences, Goethe University Frankfurt, Frankfurt am Main, Germany

[9] School of Chemistry & School of Earth Sciences, University of Bristol, UK

[10] Lamont–Doherty Earth Observatory of Columbia University, USA

[11] School of Earth and Ocean Sciences, Cardiff University, UK

[12] Camborne School of Mines & Environment and Sustainability Institute, University of Exeter, UK

[13] Bjerknes Centre for Climate Research and Department of Earth Science, University of Bergen, Norway

[14] MARUM, University of Bremen, Germany

[15] Department of Earth & Environmental Sciences, Wesleyan University, USA

[16] Department of Geography, Northumbria University, UK

[17] School of Geosciences, University of Louisiana at Lafayette, Louisiana, USA

[18] Department of Earth and Environmental Sciences, KU Leuven, Belgium

[19] Department of Geosciences, University of Arizona, USA

[20] Institute of the Environment and Sustainability, University of California, Los Angeles, USA

[21] Department of Earth Sciences, University College London, UK

Geosci. Model Dev. Discuss., https://doi.org/10.5194/gmd-2018-309
Manuscript under review for journal Geosci. Model Dev.
Discussion started: 17 January 2019

[22] Department of Marine Microbiology and Biogeochemistry (MMB), NIOZ Royal Netherlands Institute for Sea Research and Utrecht University, Den Burg, The Netherlands
[23] Earth and Planetary Sciences Department, University of California, Santa Cruz, USA
[24] Department of Oceanography, Texas A&M University, USA
[25] Department of Earth, Atmospheric, and Planetary Sciences, Purdue University, USA
[26] School of Geographical Sciences, University of Bristol, UK

Correspondence to: Christopher J. Hollis (c.hollis@gns.cri.nz)

Abstract. The early Eocene (56 to 48 million years ago) is inferred to have been the most recent time that Earth's atmospheric CO_2 concentrations exceeded 1000 ppm. Global mean temperatures were also substantially warmer than present day. As such, study of early Eocene climate provides insight into how a super-warm Earth system behaves and offers an opportunity to evaluate climate models under conditions of high greenhouse gas forcing. The Deep Time Model Intercomparison Project (DeepMIP) is a systematic model-model and model-data intercomparison of three early Paleogene time slices: latest Paleocene, Paleocene-Eocene thermal maximum and early Eocene climatic optimum. A previous article outlined the model experimental design for climate model simulations. In this article, we outline the methodologies to be used for the compilation and analysis of climate proxy data, primarily proxies for temperature and CO_2. This paper establishes the protocols for a concerted and coordinated effort to compile the climate proxy records across a wide geographic range. The resulting climate "atlas" will be used to constrain and evaluate climate models for the three selected time intervals, and provide insights into the mechanisms that control these warm climate states. We provide version 0.1 of this database, in anticipation that this will be expanded in subsequent publications.

1 Introduction

Over much of the last 100 million years of Earth history, greenhouse gas levels and global temperatures were higher than present (Zachos et al., 2008; Foster et al. 2017). Because greenhouse gas levels are currently well above anything experienced during the modern climate mode, ancient climate archives hold important clues to our future climate (IPCC, 2013). This is particularly true for those times when climate was considerably warmer and greenhouse gas levels considerably higher than present. For instance, such intervals can provide information about the sensitivity of the climate to greenhouse gas forcing (e.g. PALAEOSENS Project Members, 2012; Zeebe, 2013; Caballero and Huber, 2013; Anagnostou et al., 2016) or reveal the behaviour of carbon cycle feedbacks under super-warm climate states (e.g. Carmichael et al., 2017). These times of past warmth also provide a powerful means to test the outputs of climate models because they represent actual realisations of how the Earth system functions under conditions of greenhouse forcing comparable to the coming century and beyond. If the models can match the geological evidence of the prevailing climatic conditions, we can have greater confidence in their skill in

predicting our future climate. Similarly, differences between models and data could indicate aspects of models and/or data that require further development.

This is the rationale behind DeepMIP – the Deep-time Model Intercomparison Project (www.deepmip.org) – which brings together climate modellers and paleoclimate scientists from a wide range of disciplines in a coordinated, international effort to improve understanding of the climate of these time intervals, to improve the skill of climate models, and to improve the accuracy and precision of climate proxies. The term "Deep-time" as applied here refers to the history of the Earth prior to the Pliocene, i.e. prior to about 5 million years ago (Ma). DeepMIP is a working group in the wider Paleoclimate Modelling Intercomparison Project (PMIP4), which itself is a part of the sixth phase of the Coupled Model Intercomparison Project (CMIP6). In DeepMIP, we focus on three warm greenhouse time periods in the latest Paleocene and early Eocene (~57–48 Ma), and for the first time, carry out a formal coordinated model–model and model-proxy intercomparison.

We have previously outlined the model experimental design of this project (Lunt et al., 2017). Here we outline the recommended methodologies for selection, compilation and analysis of climate proxy data sets for three selected time intervals: latest Paleocene (LP), Paleocene-Eocene thermal maximum (PETM) and early Eocene climatic optimum (EECO). Section 2 outlines previous compilations, and Section 3 formally defines the time periods of interest. Sections 4 and 5 describe the proxies for sea surface and land air temperature (SST and LAT), respectively. Section 6 describes the proxies for atmospheric carbon dioxide (CO_2). For each proxy, we highlight their underlying mechanisms, their strengths and weaknesses, and recommendations for analytical methodologies. We focus on temperature in this article because it is the most commonly and readily reconstructed climatic variable and it is one of the best represented variables in climate models. When combined with CO_2, it allows assessment of climate sensitivity, a key metric of climate models. However, the DeepMIP database will provide a structure for future compilations of other climate proxies, such as precipitation, evaporation, salinity, upwelling, bathymetry, circulation, currents and vegetation cover, but these are not discussed or compiled here. Section 7 outlines the structure of the planned DeepMIP database, which will accommodate the data presented in Supplementary Data Files 2–7 (which constitute Version 0.1 of the database) and additional datasets as they become available. Section 8 presents a preliminary synthesis of the paleotemperature data from these tables and includes a discussion of the geographic coverage and quality of existing paleotemperature data for the three selected time intervals.

2 Previous climate proxy compilations

The first global climate proxy compilations for the Cenozoic were based on deep-sea records of stable isotopes from benthic foraminifera (e.g., Shackleton, 1986; Miller et al., 1987, 2005; 2011; Zachos et al., 1994, 2001, 2008; Cramer at al., 2009), which are proxies for deep-sea temperature and ice volume (oxygen isotopes, expressed as $\delta^{18}O$) and carbon cycle changes (carbon isotopes, expressed as $\delta^{13}C$). This work has culminated in studies in which $\delta^{18}O$ and Mg/Ca ratios of benthic

Geosci. Model Dev. Discuss., https://doi.org/10.5194/gmd-2018-309
Manuscript under review for journal Geosci. Model Dev.
Discussion started: 17 January 2019

foraminifer tests (Lear et al., 2000) were combined to derive an independent estimate of bottom water temperature (BWT) and thus separate the temperature and ice volume/sea level components in the $\delta^{18}O$ record (Cramer et al., 2011).

Early attempts at comparable compilations for sea surface temperature (SST) were complicated by seafloor alteration of the oxygen isotope composition of planktic foraminifera (Schrag et al., 1995; Schrag, 1999). For the early Paleogne, the discovery that robust SST reconstructions could be derived from well-preserved foraminifera in clay-rich sediments (Pearson et al., 2001; Sexton et al., 2006), coupled with the development of the organic biomarker-based TEX_{86} SST proxy (Schouten et al., 2002), shifted attention away from the deep sea to continental margin settings where $\delta^{18}O$-based SST reconstructions could be compared with SSTs derived from Mg/Ca, clumped isotopes and TEX_{86} (Zachos et al., 2006; Pearson et al., 2007; John et al., 2008; Hollis et al., 2009; Keating-Bitonti et al., 2011). These relatively few Paleogene sites have formed the basis of several SST compilations, which were undertaken as part of previous model-proxy intercomparison efforts (Sluijs et al., 2006; Bijl et al., 2009; Hollis et al., 2009, 2012; Lunt et al., 2012; Dunkley Jones et al., 2013). In recent years, new compilations have been presented as part of targeted efforts to fill the geographic gaps identified by this earlier work (e.g. Frieling et al., 2014, 2017, 2018; Cramwinckel et al., 2018; Evans et al., 2018a). In comparison, there have been fewer compilations of land air temperature (LAT) proxy data (Huber and Caballero, 2011; Jaramillo and Cardenas, 2013; Naafs et al., 2018a). In our study, we have compiled and reviewed existing datasets for SSTs and LAT, calibrated them to a consistent time scale in order to identify the time intervals of interest, and recalculated SST and LAT using the methodologies outlined below (Supplementary Data Files 2–7). This represents the most comprehensive compilation of early Paleogene paleotemperature data published to date.

Compilations of atmospheric CO_2, the only greenhouse gas for which any proxy-based constraints exist, have tended to deal with the Cenozoic in its entirety (e.g. Beerling and Royer, 2011) or as part of longer compilations focused on the Phanerozoic (e.g. Royer et al., 2001; Royer, 2006; Foster et al., 2017). Here we review the latest understanding of the available proxies and summarize estimates of atmospheric CO_2 for the three focus intervals. These estimates will provide constraints for climate simulations and climate sensitivity studies.

3 Time intervals, correlation and variability

We have chosen to focus on three time intevals in the latest Paleocene and early Eocene (Fig. 1). These time intervals are the climate state immediately before (latest Paleocene, LP) and at the peak of a short-lived but high amplitude warming event (Paleocene-Eocene thermal maximum, PETM) and the subsequent longer-term peak of Cenozoic warmth (early Eocene climatic optimum, EECO). These time intervals are selected because they are the most extreme warm climates of the Cenozoic, and thus represent a warm climate end member for PMIP model experiments. They are also advantageous as they are readily identifiable in the stratigraphic record, the climate signal has a high signal-to-uncertainty ratio, the uncertainties in non-greenhouse gas boundary conditions (e.g. ocean gateways etc.) between the three intervals are thought to be small, and a large

amount of climate data has been generated by numerous studies over the last two decades. The latest Paleocene provides a reference "background" point for both the PETM and the EECO.

Latest Paleocene (LP): In the most complete deep-sea isotope records (Westerhold et al., 2011, 2017, 2018; Littler et al., 2014), a gradual warming trend is evident in the lead-up to the PETM from ~59 Ma. Several records also indicate rapid warming directly preceding the CIE (e.g. Sluijs et al., 2007b). However, there is a ~1 million year (my) interval between this end-Paleocene warming (<10 ky duration – Sluijs et al., 2007b) and the base of magnetochron C24r in which the benthic $\delta^{18}O$ record is realtively stable (Westerhold et al., 2011, 2017, 2018; Littler et al., 2014). This is the preferred interval to adopt as representing background latest Paleocene conditions, although it is recognized that hiatuses occur in the uppermost Paleocene in several shelf sections (e.g. Hollis et al., 2012) and that many terrestrial sections lack the age control to identify this interval. In practice, many datasets for this LP interval come from the pre-PETM stratigraphy of studies that have good recovery of the onset of the PETM climate event (e.g. Dunkley Jones et al. 2013). These sections can be screened for any rapid warming associated with the onset of the PETM (Dunkley Jones et al. 2013), and although the age of the base of these successions is sometimes poorly constrained, they are assumed to be well within the ~1 my LP interval defined here. For reference, the LP interval is shown on Fig. 1 in relation to the benthic stable isotope compilation for north Pacific ODP Site 1209 (Westerhold et al., 2011, 2017, 2018) and south Atlantic IODP Site 1262 (Littler et al. 2014).

PETM: The PETM spans the first ~220 ky of the Eocene (55.93–55.71 Ma – Westerhold et al., 2017) and is associated with a negative excursion in the $\delta^{13}C$ of the global exogenic carbon pool (Koch et al., 1992; Dickens et al., 1995; Zachos et al., 2008). Although the magnitude and shape of the carbon isotope excursion (CIE) exhibits variation between sites and measured substrate, in the most complete records it is characterized by a rapid shift to peak negative values within the first ~20 ky of the event (Westerhold et al. 2018). Peak negative $\delta^{13}C$ values within the CIE are closely coupled to PETM peak temperatures, as evident from geochemical proxies (Fig. 2) and the abundance of warm-climate fossil species at higher latitudes (Sluijs et al., 2007a, 2011; McInerney and Wing, 2011; Sluijs and Dickens, 2012; Dunkley Jones et al., 2013) and the disappearance of some fossil groups, such as corals and dinoflagellates, in low latitudes (Speijer et al., 2012; Freiling et al. 2017). We recognise that each record will comprise onset, peak and recovery intervals that may vary in timing and duration (Fig. 2). In keeping with Dunkley Jones et al. (2013) and Frieling et al. (2017), our compilation identifies the peak PETM interval in each record based on the shape of the $\delta^{13}C$ excursion (interval of minimum values) and temperature proxies (interval of maximum values).

EECO: The EECO is identified in global compilations of benthic foraminiferal $\delta^{18}O$ as a prolonged episode of deep-sea warming between ~53 and ~50 Ma (Zachos et al., 2008; Cramer et al., 2009; Kirtland-Turner et al., 2014). The effect of local temperature regime complicates site-to-site correlations based on $\delta^{18}O$ alone, and for this reason, several studies have also used $\delta^{13}C$ stratigraphies for high temporal resolution correlations. Studies of pelagic carbonate sequences in New Zealand (Slotnick et al., 2012, 2015) place the base of the EECO at the "J" event (Cramer et al., 2003), a rather subdued CIE that lies

between the well-defined hyperthermals ETM2 (H event) and ETM3 (K event), which coincides with a marked increase in terrigenous clay abundance (Fig. 3). Lauretano et al. (2015) show that the J event is associated with a small negative $\delta^{18}O$ excursion in benthic foraminifera that is followed by a baseline negative shift in $\delta^{18}O$ at south Atlantic ODP Sites 1262 and 1263 (Fig. 1). The J event is also associated with a rapid turnover from planktic foraminiferal assemblages dominated by the genus *Morozovella* to assemblages dominated by *Acarinina* (Frontalini et al., 2016; Luciani et al., 2016, 2017). The J event equates to CIE C24n.2rH1 in the notation developed by Sexton et al. (2011), and corresponds approximately to the onset of the EECO previously indicated in global benthic $\delta^{18}O$ compilations (Zachos et al., 2008; Cramer et al., 2009; Kirtland-Turner et al., 2014). Slotnick et al. (2012, 2015) suggested that the top of the EECO may coincide with the top of the clay-rich interval in the New Zealand sequence, which lies within Chron 22n (Dallanave et al., 2014) (Fig. 3). This is consistent with the global benthic $\delta^{18}O$ record, in which cooling begins at ~50 Ma (Zachos et al., 2008; Cramer et al., 2009; Kirtland-Turner et al., 2014; Lauretano et al., 2015, 2018). At mid-Atlantic ODP Site 1258, the termination of the EECO is placed at the base of a positive shift in benthic $\delta^{18}O$ that follows a hyperthermal event identified as CIE C22nH3 (Sexton et al., 2011).

A new high-resolution, astronomically-calibrated, benthic foraminiferal record at Site 1209, in the north Pacific (Westerhold et al., 2017, 2018), provides further support for these correlations (Fig. 1). Based on these studies, we use a wide definition of the EECO interval as the benthic $\delta^{18}O$ minimum that extends from the J event (CIE CH24n.2rH1; 53.26 Ma) to the uppermost Chron C22n CIE, C22nH5 (49.14 Ma), an interval of 4.12 Myrs. The top of the EECO is well-defined by the onset of a cooling trend that follows CIE C22nH5. The base of the EECO is less well-defined. Oscillations in $\delta^{18}O$ occur from ~54 to ~52 Ma, with the most distinct negative shift in $\delta^{18}O$ coinciding with the M event (CIE C23rH2) at 51.97 Ma.

All of the above intervals are defined with timescale-independent stratigraphic markers: the LP from the base of magnetochron C24r to the first sign of pre-PETM warming; the PETM interval based on the identification of the CIE and associated characteristic warming patterns; and the EECO is bounded by CIEs CH24n.2rH1 (J event) and C22nH5. For an absolute timescale, our study benefits from ongoing efforts to complete the astronomical tuning of the geological timescale for the Paleocene and early Eocene (Lourens et al., 2005; Westerhold et al., 2008, 2017, 2018; Littler et al., 2014; Lauretano et al., 2015), as shown in Figs. 1 and 3. We recognise, however that most existing age models and biostratigraphic schemes are referenced to the GTS2012 timescale (Gradstein et al., 2012), and this is what we use for the purposes of data compilation. However, the DeepMIP database includes stratigraphic levels (depth or height) for all samples and information on age control for each site, which will facilitate updates to new age models as they become available.

4 Marine proxies for sea temperature

In this section, we outline the four main approaches for reconstructing Paleocene and Eocene sea temperatures: oxygen isotopes, Mg/Ca ratios, clumped isotopes and TEX_{86}. For each proxy, we outline (1) the underlying theoretical background, (2) strengths, (3) weaknesses, and (4) recommendations on methodologies. We focus on sea surface temperatures (SST) and

have compiled data from published studies of planktic foraminiferal $\delta^{18}O$ (Supplementary Data File 3) and Mg/Ca ratios (Supplementary Data File 4), clumped isotopes from benthic foraminifera and molluscs (Supplementary Data File 5) and TEX_{86} (Supplementary Data File 6).

4.1 Oxygen isotopes

4.1.1 Theoretical background of oxygen isotopes

Oxygen isotope paleothermometery is based on the temperature-dependent fractionation of the stable isotopes of oxygen (^{16}O and ^{18}O, expressed as $\delta^{18}O$) into biogenic calcite from its growth medium, typically seawater. Pearson (2012) provides more details on the development of the $\delta^{18}O$ proxy. The temperature dependence of $\delta^{18}O$ is a combination of thermodynamic and vital effects (e.g., Kim and O'Neil, 1997; Bemis et al., 1998). Most $\delta^{18}O$ paleotemperature reconstructions use the shells of marine foraminifera, a group of protists that live and calcify either as plankton in the ocean's surface mixed layer, thermocline or sub-thermocline depths, or as benthos on or just below the sea floor. Temperature is calculated by an empirical calibration to quantify the fractionation between the $\delta^{18}O$ of ancient seawater and biogenic calcite (Bemis et al., 1998).

4.1.2 Strengths of oxygen isotopes

Foraminiferal oxygen isotopes have been the primary proxy for reconstructing ocean temperatures spanning the past ~120 million years, largely due to the low analytical cost, small sample size requirements and relative ease of measurement. Moreover, the theoretical basis for temperature-dependent fractionation is firmly tied to field- and laboratory-based relationships between foraminifer test $\delta^{18}O$ values and temperature (e.g., Kim and O'Neil, 1997; Bemis et al., 1998; Lynch-Stieglitz et al., 1999). The range of planktic foraminiferal depth habitats also allows for the reconstruction of water column profiles and thermocline structure (e.g., Birch et al., 2013; John et al., 2013), which can be compared to modelled upper ocean structure (e.g., Lunt et al., 2017).

4.1.3 Weaknesses of oxygen isotopes

The dissolution and subsequent replacement of primary biogenic calcite by inorganic calcite (recrystallization/ diagenesis) in pelagic, carbonate-rich sediments during early diagenesis is known to shift planktic foraminiferal calcite to higher values (Schrag et al., 1995), with the effect that most low and mid-latitude $\delta^{18}O$-derived Paleogene SSTs from deep-ocean carbonate-rich successions may be systematic underestimates (Pearson et al., 2001; Tripati et al., 2003; Sexton et al., 2006; Pearson and Burgess, 2008; Kozdon et al., 2011; Edgar et al., 2015). The effect of seafloor recrystallization and diagenesis on SST estimates will be proportionally less significant in areas where cooler surface waters are closer to deep ocean temperatures, which may be the case in some Paleogene high-latitude or upwelling regions, and is considered to be insignificant for benthic foraminifera because temperatures during early diagenesis are very close to growth temperatures (Schrag et al., 1999; Edgar et al., 2013; Voigt et al., 2016). During diagenesis, foraminifer tests may also become overgrown and/or infilled with calcite precipitated

from sediment pore waters. Where marine sediments are exposed on land, those secondary precipitates can incorporate oxygen from isotopically light meteoric waters and hence yield artificially warm apparent temperatures. For these reasons, temperature estimates from foraminiferal $\delta^{18}O$ are only considered to be reliable where a good state of preservation has been confirmed by SEM examination and illustration. Well-preserved (non-recrystallized or glassy) late Paleocene to early Eocene foraminifera have been reported from low permeability clay-rich facies in shallow marine or hemipelagic settings from Tanzania (Pearson et al., 2004; 2009; Sexton et al., 2006), the New Jersey margin and California (Zachos et al., 2006; John et al., 2008; Makarova et al., 2017), New Zealand (Hollis et al., 2012), and Nigeria (Frieling et al., 2017).

One key assumption for $\delta^{18}O$-based temperatures is that foraminifera precipitate their tests in isotopic equilibrium with seawater. However, foraminiferal physiology (e.g., respiration, metabolism, biomineralization, photosymbiosis) and ecology (e.g., depth migration during life cycle, seasonality), often termed 'vital effects', commonly lead to isotopic offsets that can bias temperature reconstructions (e.g., Urey, 1984; Birch et al., 2013). The biology and ecology of foraminifera may also vary in either time or space. For instance, the depth habitat of a species may change in response to rapid environmental change, or due to evolution within a lineage. Foraminifera that host algal photosymbionts may also be subject to bleaching events, which can substantially alter the test micro-environment within which calcification, and the associated isotopic fractionation, occurs (Edgar et al., 2015; Luciani et al., 2016; Si and Aubry, 2018).

Calculating ancient SST from foraminiferal $\delta^{18}O$ requires an estimation of the oxygen isotopic composition of seawater ($\delta^{18}O_{SW}$) at the time of precipitation. This is not straightforward because $\delta^{18}O_{SW}$ varies spatially in the surface ocean, largely following patterns of salinity (Zachos et al., 1994; Rohling, 2013), and temporally due to changes in the cryosphere (Broecker, 1989; Cramer et al., 2009). Large and spatially variable changes in the intensity of the hydrological cycle are inferred across the PETM (Bowen et al., 2004; Zachos et al., 2006; Pagani et al., 2006; Carmichael et al., 2017), hence it is unlikely that $\delta^{18}O_{sw}$ at any single location remained constant through the Paleocene–Eocene interval. Continental margin settings, where foraminifera are typically well preserved, may be particularly sensitive to changes in $\delta^{18}O_{sw}$ related to the hydrological cycle.

Finally, culture studies and field observations demonstrate that the $\delta^{18}O$ value of foraminiferal calcite decreases as the pH of the culture medium increases (Spero et al., 1997; Bijma et al., 1999; Zeebe, 1999, 2001; Russell and Spero, 2000). This 'pH effect' can influence ancient SST reconstructions if seawater pH varied rapidly or was significantly different from today (Zeebe, 2001). Studies suggest that early Paleogene surface ocean pH was as much as ~0.5 units lower than today (Penman et al., 2014; Anagnostou et al., 2016; Gutjahr et al., 2017), which implies that background $\delta^{18}O$-based SST estimates for this time interval could be ~3°C too low, or even more so for the PETM when pH may have declined by a further ~0.3 units (Uchikawa and Zeebe, 2010; Aze et al., 2014).

4.1.4 Recommended methodologies for oxygen isotopes

Geosci. Model Dev. Discuss., https://doi.org/10.5194/gmd-2018-309
Manuscript under review for journal Geosci. Model Dev.
Discussion started: 17 January 2019

Here we outline our recommendations for generating $\delta^{18}O$ data from fossil foraminifera, and for converting $\delta^{18}O$ values into temperature estimates. We have compiled available planktic $\delta^{18}O$ data from ten DSDP, ODP and IODP sites and nine onshore sections (Supplementary Data File 3). Using the methods outlined below, we have calculated SSTs and error values and compiled a summary of proxy-specific SST estimates for each time slice (LP, PETM, EECO).

To expand on the $\delta^{18}O$ database, we propose a three-pronged approach. First, analysis of new and classic carbonate-rich sites containing partially recrystallized foraminiferal tests should involve the novel technique that uses a Secondary Ion Mass Spectrometer (SIMS). Pioneering SIMS studies by Kozdon et al. (2011, 2013) show that recrystallization of planktic foraminiferal tests is indeed partial and that areas furthest from the test exterior are less susceptible to diagenetic overprinting. These areas yield SSTs up to ~8°C warmer than conventional analyses from the same sample and are in better agreement with $\delta^{18}O$-based SSTs from glassy tests (Kozdon et al., 2011). On a cautionary note, a recent study by Wycech et al. (2018) has reported an offset between SIMS and traditional IRMS analyses for modern foraminifer, with SIMS $\delta^{18}O$ values being ~0.9‰ lower. Further study is needed to determine if this offset also affects fossil foraminifera. The SIMS technique provides hope for recovering reliable SSTs from recrystallized foraminiferal tests but it is time intensive and is not a practical approach for the analysis of all samples. Thus, our second recommendation is that whole specimen analyses are undertake together with the SIMS analysis, in order to constrain the magnitude of diagenetic bias on IRMS $\delta^{18}O$ values. For lithologically uniform sediments, quantitative estimates of this diagenetic biasin a few widely spaced samples could provide calibration points for higher resolution data generated by conventional whole shell methods. Whole specimen isotopic analyses should be species-specific and use a prescribed size fraction (e.g., 250-300 µm or 300-355 µm) to minimise variations in vital effects (Birch et al., 2013). Our third recommendation is that new sites that contain glassy foraminifera are sought out to provide the material for whole specimen analysis, as well as SIMS analysis of selected samples to further validate the two methods. All samples included within the database are categorized as either glassy or recrystallized, using the criteria of Sexton et al. (2006) and Pearson and Burgess (2008), as a guide to reconstructed SST reliability.

Empirically derived $\delta^{18}O$–temperature calibrations can differ by several degrees Celsius (Bemis et al., 1998; Pearson, 2012). Use of multiple equations may capture a range of plausible temperature values but our preference is the calibration of Kim and O'Neil (1997) for inorganic calcite, which is appropriate for the Paleogene because it is based on inorganic calcite precipitated from water temperatures between 10–40°C. Both epifaunal benthic and asymbiotic planktic foraminifera yield values close to the resulting regression (Bemis et al., 1998; Costa et al., 2006). Field or laboratory studies only include calcite precipitated up to 30°C (e.g., Bemis et al., 1998; Lynch-Stieglitz et al., 1999, Pearson, 2012), yet Paleogene SSTs likely fall close to or above the upper limit of these studies. The recommended calibration, as modified by Bemis et al. (1998), derives temperature from Eq. (1):

$$T = 16.1\text{-}4.64(\delta^{18}O_C\text{-}\delta^{18}O_{SW}) + 0.09(\delta^{18}O_C\text{-}\delta^{18}O_{SW})^2 \quad (1)$$

Geosci. Model Dev. Discuss., https://doi.org/10.5194/gmd-2018-309
Manuscript under review for journal Geosci. Model Dev.
Discussion started: 17 January 2019

where T is the water temperature in ˚C, $\delta^{18}O_C$ and $\delta^{18}O_{SW}$ are the $\delta^{18}O$ of calcite (‰ VPDB) and ambient seawater (‰ VSMOW), respectively. This equation may overestimate SST for symbiont-hosting planktic foraminifera by ~1.5°C based on the consistent 0.3‰ offset observed between *Orbulina universa* grown under high vs. low light conditions (Spero and Williams, 1988; Pearson, 2012). This offset is likely caused by algal photsymbionts modifying the pH in the calcifying microenvironment (Zeebe et al., 1999). *Orbulina universa* is inferred to share a similar ecology to the dominant Eocene genera *Morozovella* and *Acarinina* typically analysed for Paleogene SSTs (e.g., Shackleton et al., 1985; D'Hondt and Zachos, 1993) and is currently the best modern analogue for which calibration data are available. However, we do not recommend applying a symbiont correction to these genera because of uncertainties in photosymbiont activity levels in Paleogene conditions.

It is assumed that these $\delta^{18}O$ calibrations are insensitive to evolving seawater chemistry, unlike some trace element proxies (e.g., Evans and Müller, 2012). These calibrations do, however, require an appropriate estimate of $\delta^{18}O_{SW}$ at the time of test formation. Changes in global mean $\delta^{18}O_{SW}$ are largely driven by continental ice volume and isotopic composition. Here we use the value -0.89‰ for early Paleogene $\delta^{18}O_{sw}$ under ice-free conditions, which was calculated by Cramer et al. (2011). A correction for the local effects of salinity and hydrology on $\delta^{18}O_{sw}$ should also be incorporated into SST estimates where possible. Zachos et al. (1994) developed a correction using present-day $\delta^{18}O_{sw}$ latitudinal gradients, which is widely used despite acknowledged shortcomings. The correction is applied globally but is only based on Southern Hemisphere data and does not incorporate local freshwater runoff effects on continental margins or the influence of boundary currents. It also ignores expected changes in the relationship between latitude and $\delta^{18}O_{sw}$ through time. Isotope-enabled climate models have been used to generate predictions of early Paleogene surface ocean $\delta^{18}O_{sw}$, distributions, following an assumption of mean average $\delta^{18}O_{sw}$ conditions (e.g., Tindall et al., 2010; Roberts et al., 2011), but the $\delta^{18}O_{sw}$ fields generated are dependent on the surface climatology of the model concerned (Hollis et al., 2012). The use of model-derived $\delta^{18}O_{sw}$ to generate proxy estimates of SST also introduces a problematic model-dependency within the proxy data set. Here, we chose to update the approach of Zachos et al. (1994) using the more highly-resolved global gridded (1° x 1°) data set of modern $\delta^{18}O_{sw}$ produced by LeGrande and Schmidt (2006). We calculated $\delta^{18}O_{sw}$ for each site by relating the site's paleolocation to 10° latitudinal bins in the modern data set (see Supplementary Data File 3). Values were calculated using paleolocations derived from both paleomagnetic and mantle-based reference frames (see Sect. 7.2). Uncertainty was calculated using a Monte Carlo algorithm. We encourage future studies to improve the empirical fit to the modern spatial variability in $\delta^{18}O_{sw}$ but also recognise that the modern system only provides a first-order estimate of spatial $\delta^{18}O_{sw}$ patterns in deep-time. With improved data coverage, paired $\delta^{18}O$–Mg/Ca and $\delta^{18}O$–$\Delta47$ analyses hold promise for direct reconstructions of ancient $\delta^{18}O_{sw}$ variability.

We do not recommend applying a pH correction to $\delta^{18}O$ data because of significant uncertainty in the magnitude of the effect below pH 8 (Uchikawa and Zeebe, 2010), which is inferred to be the upper limit for most of our Paleogene records (Anagnostou

et al., 2016; Penman et al., 2014; Gutjahr et al., 2017). Further, the pH–$\delta^{18}O_C$ sensitivity of asymbiotic planktic and benthic foraminifera are not well known (e.g., Anagnostou et al., 2016; McCorkle et al., 2008; Mackensen, 2008).

4.2 Mg/Ca ratios

4.2.1 Theoretical background of Mg/Ca ratios

The sensitivity of foraminiferal Mg/Ca ratios to temperature has a basis in thermodynamics (Lea et al., 1999) through the exponential temperature dependence of any reaction for which there is an associated change in enthalpy. However, most species do not conform to theoretical calculations (Rosenthal et al., 1997), being characterised by a temperature sensitivity of Mg-incorporation around 2-3 times greater than for inorganic calcite. The reasons for this remain elusive (e.g., Bentov and Erez 2006), necessitating empirical calibration of foraminiferal Mg/Ca to temperature (e.g., Anand et al., 2003).

4.2.2 Strengths of Mg/Ca

As with $\delta^{18}O$ paleothermometry, Mg/Ca paleothermometry can be applied to both benthic and planktic foraminifera and be used to constrain the past thermal structure of the water column (Tripati and Elderfield, 2005). The long residence time of Ca and Mg in the ocean means that the Mg/Ca of seawater (Mg/Ca_{sw}) can be treated as constant over short timescales ($<10^6$ yrs), which removes one source of uncertainty in calculating relative changes in temperature (e.g., Zachos et al., 2003; Tripati and Elderfield, 2004). A major advantage of Mg/Ca is its use in paired measurements with $\delta^{18}O$ on the same substrate, which allows for the deconvolution of $\delta^{18}O_{sw}$ and temperature effects on measured foraminiferal $\delta^{18}O$. As Mg/Ca measurements are increasingly routine in many laboratories, are relatively inexpensive to produce, and have low sample-size requirements, high-resolution time series are readily achievable. Technological developments in laser ablation-ICPMS and other spatially-resolved methodologies, such as Electron Probe Microanalysis (EPMA) and SIMS, allows for Mg/Ca measurements on or within a single individual test, providing new information on foraminiferal ecology and short-term environmental variability (e.g., Eggins et al., 2004; Evans et al., 2013; Spero et al., 2015). Planktic foraminiferal Mg/Ca may also be more robust to shallow burial diagenetic recrystallization than $\delta^{18}O$, based on values measured in the same material (Sexton et al., 2006).

4.2.3 Weaknesses of Mg/Ca

A long-standing challenge for the deep-time application of the Mg/Ca temperature proxy is that the seawater Mg/Ca ratio (Mg/Ca_{sw}) also exerts a control on shell Mg/Ca, yet precise reconstructions of the secular evolution of Mg/Ca_{sw} are challenging to produce (Horita et al., 2002; Coggon et al., 2010; Broecker and Yu, 2011; Evans and Müller, 2012). Non-thermal influences on foraminiferal Mg/Ca ratios can also be difficult to account for, including pH, bottom water carbonate saturation state, and sample contamination (Barker et al., 2003; Regenberg et al., 2014; Evans et al., 2016b). Determining the reliability of Mg/Ca paleotemperatures requires an understanding of these challenges, and the use of independent paleoenvironmental proxies where available, such as boron isotopes to constrain carbonate system parameters (Anagnostou et al., 2016).

Geosci. Model Dev. Discuss., https://doi.org/10.5194/gmd-2018-309
Manuscript under review for journal Geosci. Model Dev.
Discussion started: 17 January 2019

***Impact of foraminiferal preservation on the Mg/Ca paleothermometer*:** Many foraminifer tests from deep ocean sediments are affected by diagenetic alteration (Pearson et al., 2001; Edgar et al., 2015), with the type and extent of alteration controlled by original test morphology, biostratinomic processes, the characteristics of the host sediment and burial history. For example, planktic foraminifera tests can undergo immediate post-mortem or post-gametogenic dissolution as they sink into deeper, less carbonate saturated waters (Brown and Elderfield, 1996). In general, $MgCO_3$ is more soluble than $CaCO_3$ such that dissolution tends to decrease foraminiferal Mg/Ca. This may result in artificially low Mg/Ca-based temperature estimates if unaccounted for (e.g., Rosenthal and Lohmann, 2002; Regenberg et al., 2014; Fehrenbacher and Martin, 2014), although not in all cases (e.g., Sadekov et al., 2010; Fehrenbacher and Martin, 2014). The effects of dissolution can be minimized by selecting sites with relatively shallow paleodepths, above the calcite lysocline (e.g., <2000 m). Foraminiferal shells can also be subject to diagenetic overgrowths of various mineral phases, including oxy-hydroxides and authigenic carbonates, depending on seafloor and sub-seafloor conditions (e.g., Boyle, 1983). Recent work suggests that some textural recrystallization of planktic foraminiferal tests may occur in semi-closed chemical conditions, potentially allowing original geochemical signals to be retrieved using microsampling techniques (e.g., Kozdon et al., 2011, 2013, see Sect. 5.2.5).

***Challenges for benthic foraminiferal Mg/Ca paleothermometry*:** The temperature sensitivity of Mg incorporation into benthic foraminiferal calcite varies between species, necessitating genus- or species-specific temperature calibrations (Lear et al., 2002). Fortunately, some extant species are common throughout the Cenozoic (e.g. *Oridorsalis umbonatus* – Lear et al., 2000) and offer a means to develop calibrations for coeval extinct species. There is also no consensus as to whether benthic Mg/Ca-temperature relationships are best described by linear or exponential fits (Cramer et al., 2011; Evans and Müller, 2012; Lear et al., 2015); we recommend that calibrations are applied with caution where Mg/Ca ratios are outside the range for which temperatures have been empirically determined.

Present-day benthic foraminifera appear to increase their discrimination against magnesium when calcifying in waters with very low carbonate ion saturation state (ΔCO_3^{2-}); a relationship that has been empirically quantified for some species (Elderfield et al., 2006; Rosenthal et al., 2006). Measurements of benthic foraminiferal B/Ca in tandem with Mg/Ca can be used to identify temporal variations in ΔCO_3^{2-} (Yu and Elderfield, 2007) and may provide a means of correcting for this secondary effect, although it can be difficult to identify the threshold for a ΔCO_3^{2-} influence within downcore records (e.g., Lear et al., 2010). Mg/Li ratios may have a more consistent empirical relationship with temperature than Mg/Ca (Bryan and Marchitto, 2008). However, limited understanding of how the Mg/Li seawater ratio has varied over geological time means that this proxy can only be used as a guide to relative temperature change in deep time studies (Lear et al., 2010). The calcification of infaunal foraminifera species within buffered porewaters may make them relatively insensitive to variations in bottom water ΔCO_3^{2-} (Zeebe, 2007; Elderfield et al., 2010). However, the saturation state of porewaters is dependent on many factors, and likely also varies through time (Weldeab et al., 2016). We recommend that tandem trace metal ratios that are sensitive to

carbonate saturation state (e.g., B/Ca, Li/Ca) are examined to assess downcore ΔCO_3^{2-} variations, even in infaunal records (e.g., Lear et al., 2010; Mawbey and Lear, 2013; Lear et al., 2015).

Evidence from multiple proxies indicates that early Paleogene Mg/Ca_{SW} was significantly lower than the modern value (Horita et al., 2002; Coggon et al., 2010; Lear et al., 2015; Evans et al., 2018a). In addition, the benthic foraminiferal magnesium partition coefficient (D_{Mg} = $Mg/Ca_{CALCITE}$ / Mg/Ca_{SW}) appears to decrease with increasing Mg/Ca_{SW} in some species (Ries, 2004; Hasiuk and Lohmann, 2010; Evans and Müller, 2012; Lear et al., 2015). A similar strategy has been inferred for the infaunal genus, *Uvigerina* (Evans et al., 2016b), whilst a higher sensitivity is thought to characterise the epifaunal genus *Cibicidoides/Cibicides* (Evans et al., 2016b), which is widely used in paleoclimate studies.

***Challenges for planktic foraminifera Mg/Ca*:** The relationship between planktic Mg/Ca ratios and temperature is species- or group-specific (e.g. Regenberg et al., 2009), such that species-specific calibrations should be used whenever possible. Nonetheless, many planktic foraminifera conform to a broader Mg/Ca-temperature relationship (Elderfield and Ganssen 2000; Anand et al., 2003), which is one method by which modern calibrations can be applied to extinct Paleogene taxa. As for benthic foraminifera, when working with pre-Pleistocene samples the control exerted by changes in seawater elemental chemistry over geological time must also be considered. Culture experiments in modified seawater demonstrate not only that Mg/Ca_{sw} impacts planktic foraminifera shell chemistry (Delaney et al., 1985), but also that the slope of the Mg/Ca-temperature relationship may be sensitive to Mg/Ca_{sw} (Evans, et al., 2016b). In addition, several other non-thermal controls on Mg/Ca should be considered when interpreting data from planktic foraminifera. Culture and core-top studies demonstrate a relatively minor salinity effect (Kısakürek et al., 2008; Hönisch et al., 2013) in which, for example, a 2 PSU salinity increase results in a temperature overestimate of ~1°C. In contrast, the carbonate system has been shown to have a large influence on Mg/Ca in several species (Lea et al., 1999; Russell et al., 2004; Evans, et al., 2016a). Lower pH and/or $[CO_3^{2-}]$ results in higher shell Mg/Ca; for example, a 0.1-unit pH decrease results in a temperature overestimate of ~1°C. The effect of the carbonate system on planktic Mg/Ca has been identified in sediment-trap as well as culture studies (Evans et al., 2016a; Gray et al. 2018), with Gray et al. (2018) demonstrating that the widely used Mg/Ca-temperature sensitivity of ~9%°C^{-1} in *Globigerinoides ruber* is an artefact of the covariance of temperature and pH, through the temperature effect on the dissociation constant of water. Specifically, the pH of (sea)water decreases with increasing temperature, resulting in an increase in the incorporation of Mg into planktic foraminiferal calcite due to both processes (see Evans et al., 2018b). The secondary pH effect accounts for around one third of the observed increase in Mg/Ca ratios at higher temperatures, leaving a primary Mg/Ca "temperature only" sensitivity of 6%°C^{-1} (Gray et al., 2018), which is significantly lower than that widely utilized. It is, however, challenging to apply this finding in deep time because high-resolution pH records are scarce (see below for detailed recommendations).

4.2.4 Recommended methodologies for Mg/Ca

Geosci. Model Dev. Discuss., https://doi.org/10.5194/gmd-2018-309
Manuscript under review for journal Geosci. Model Dev.
Discussion started: 17 January 2019

Here we outline our recommendations for generating Mg/Ca data from fossil foraminifera and for converting these data into temperature estimates. We have compiled available planktic Mg/Ca data from five DSDP and ODP sites and six onshore sections and, using the methods outlined below, calculated SSTs and associated uncertainties for the late Paleocene and early Eocene (Supplementary Data File 4).

***Sample preparation*:** Foraminifera need to be thoroughly cleaned prior to analysis. Clay and organic contaminants are removed using a short oxidative procedure, whereas removal of metal oxide contaminants requires a longer procedure including a reductive step (Boyle and Keigwin, 1985). These two procedures result in offsets in Mg/Ca values, which must be corrected when making comparisons to other records (e.g., Barker et al., 2003; Yu et al., 2007). Cleaning efficacy is assessed using Al/Ca, Mn/Ca and Fe/Ca ratios (e.g., Boyle, 1983; Barker et al., 2003). In some cases, a simple threshold value may be used to screen samples, e.g., Al/Ca >80 µmol/mol (Mawbey and Lear, 2013). In many cases, the threshold depends on contaminant composition such that Mn/Mg or Fe/Mg ratios may be a more useful indicator (Barker et al., 2003). Cleaned foraminifera are commonly dissolved in acid and analysed by Inductively Coupled Plasma Mass Spectrometry (ICP-MS), taking into account the dependence of measured Mg/Ca on analyte concentration (the matrix effect – Lear et al., 2002), although other techniques may also be employed (see below). Prior to crushing, several representative specimens should be selected for SEM analysis to record the extent of textural recrystallization on broken chamber walls. Sr/Ca values routinely collected alongside Mg/Ca data can provide one means of monitoring the impact of recrystallization on test geochemistry. Inorganic calcite tends to have lower Sr/Ca and higher Mg/Ca than foraminiferal calcite (Baker et al., 1982), which leads to inverse relationships in diagenetically altered downcore records.

***Recommended steps in converting of planktic Mg/Ca ratios to temperatures*:**

i) The possible presence of dissolution should be determined. In the recent geological past, a dissolution correction can be based on the bottom water saturation state at the sample site (Dekens et al., 2002), but uncertainties in ocean carbonate chemistry currently preclude this approach in deep-time studies. We recommend that planktic foraminiferal test weights are reported along with Mg/Ca data to assess the potential impact of dissolution (e.g., Rosenthal and Lohmann, 2002). Alternatively, chemically resistant domains within individual tests can be selected for analysis (see above).

ii) A salinity correction should be applied if there is independent evidence that the sample site experienced substantial deviations from normal salinity, such as the large changes in the hydrological cycle inferred for the PETM (Zachos et al., 2003). Normalising culture data of three modern species (compiled in Hönisch et al., 2013 and Allen et al., 2016) to the Mg/Ca observed at a salinity of 35 psu for each species results in the following multi-species salinity sensitivity Eq. (2):

$$Mg/Ca_{CORRECTED} = (1 - (salinity - 35) \times 0.042 \pm 0.008) \times Mg/Ca_{MEASURED} \quad (2)$$

Geosci. Model Dev. Discuss., https://doi.org/10.5194/gmd-2018-309
Manuscript under review for journal Geosci. Model Dev.
Discussion started: 17 January 2019

(see the Supplementary Information for further details). This sensitivity of 4.2±0.8% per PSU is in good agreement with global sediment trap and plankton tow data for *G. ruber* (Gray et al., 2018).

iii) A correction for past changes in the carbonate system should be applied. This is complicated, however, because pH and $[CO_3^{2-}]$ are not only driven by long-term changes in the carbon cycle but also by factors such as the temperature effect on the dissociation constant of water (K_W). Therefore, whilst the results of Gray et al. (2018) indicate that the Mg/Ca-temperature sensitivity in the modern ocean is 6%°C^{-1} when the effects of pH and temperature are fully deconvolved, this can only be applied if the control of temperature on K_W (and therefore pH) is accounted for (ideally through δ^{11}B-derived pH reconstructions using the same material). For instance, if the pH reconstruction available for a given interval was determined at a different site, a temperature sensitivity of 6%°C^{-1} should be applied only if the difference in temperature between sites can be estimated, so that the temperature-driven inter-site pH gradient can be accounted for (pH differences between sites may also exist for other reasons). In practice, this requires that the equations for pH and temperature be solved iteratively, given that Mg/Ca is sensitive to both factors. We recommend differing approaches for Mg/Ca data treatment depending on whether a δ^{11}B pH record is available for the same site (see step (v) below).

Where δ^{11}B-based pH reconstructions are available, Mg/Ca ratios should be corrected for pH. However, this correction should be considered with caution until the controlling carbonate system parameter on foraminifera Mg/Ca is identified, particularly given that pH and $[CO_3^{2-}]$ may be decoupled over geological time (Tyrrell and Zeebe 2004). If no pH reconstruction is available for the site of interest, then the temporally and spatially closest data should be used and uncertainties in applying this considered. Based on a linear fit through culture data from three modern species (Evans et al. 2016a), the correction is:

$$Mg/Ca_{CORRECTED} = (1 - (8.05 - pH) \times 0.70\pm0.18) \times Mg/Ca_{MEASURED} \quad (4)$$

Note that Mg/Ca may relate nonlinearly to pH outside the range 7.7-8.4, and more complex relationships have been suggested (Russell et al., 2004; Evans et al., 2016a). This sensitivity of -7.0 ±1.8% per 0.1 pH unit is in agreement with the -8.3±7.7% derived from a global sediment-trap and plankton tow *G. ruber* dataset (Gray et al., 2018), although we recommend applying the culture-derived expression in deep time because it is calibrated over a much wider pH range.

iv) A correction for Mg/Ca_{SW} is usually applied to the pre-exponential component (B) of the relevant Mg/Ca-temperature calibration of the form $Mg/Ca = Bexp^{AT}$ (Hasiuk and Lohmann 2010; Evans and Müller 2012):

$$B_{CORRECTED} = (Mg/Ca_{SW}^{H} / 5.2^{H}) \times B_{MODERN} \quad (3)$$

Geosci. Model Dev. Discuss., https://doi.org/10.5194/gmd-2018-309
Manuscript under review for journal Geosci. Model Dev.
Discussion started: 17 January 2019

where B_{MODERN} is the pre-exponential coefficient derived from modern calibrations, H is the nonlinearity of the relationship between shell and Mg/Ca_{SW}, which may be estimated from culture experiments under variable seawater chemistry (Evans et al., 2016b; Delaney et al., 1985), Mg/Ca_{SW} is that of the time interval of interest, and 5.2 is the modern seawater Mg/Ca ratio in mol mol^{-1}. However, the observation that the slope of this relationship is sensitive to Mg/Ca_{SW} in culture experiments means that equations describing the change in both constants (A and B) have been reported for modern taxa (Evans, et al., 2016b), with the implication that the use of modern calibrations may underestimate relative temperature changes during the early Paleogene. For estimates of early Paleogene Mg/Ca_{SW} we recommend the use of a relatively high-precision, million-year (average) resolution Mg/Ca_{SW} reconstruction from the coupled analysis of Mg/Ca and clumped isotopes in foraminifera (Evans et al. 2018a).

v) Mg/Ca is converted to temperature using an exponential calibration equation:

$$T = \ln (Mg/Ca_{CORRECTED} / B_{CORRECTED}) / A \quad (4)$$

Where A and $B_{CORRECTED}$ are derived from species or group-specific calibrations. The most appropriate calibration for extinct Eocene species should be chosen based on similarities to extant relatives in terms of shell chemistry or, for example, the presence or absence of symbionts. Best practice would report the sensitivity of a reconstruction to the choice of calibration equation. Importantly, the sensitivity factor A should be modified depending on how the carbonate system correction described above is performed. If pH is explicitly accounted for at the site of interest through $\delta^{11}B$ then the 6%°C^{-1} sensitivity of Gray et al. (2018) should be applied. However, if the best available pH reconstruction is from a different site or time interval or derived from a model which represents the global mean (e.g. Tyrell and Zeebe, 2004), then we recommend applying the apparent sensitivity derived from culture (8.5%°C^{-1}) as this indirectly accounts for the effect of temperature on K_W.

These recommendations have been applied to the Mg/Ca analyses included in the DeepMIP database (Supplementary Data File 4). We have compiled Mg/Ca data for planktic foraminifera from five DSDP or ODP sites and six onshore sections. SST has been derived from Mg/Ca ratios as follows: 1000 random draws were performed of salinity (33–37 psu), seawater Mg/Ca (within the 95% CI given by Evans et al. [2018b]), pH (+/-0.2 units), and the Mg/Ca-pH sensitivity (anywhere between 0-8.8% per 0.1 unit, i.e. anywhere between not sensitive at all to the upper confidence interval on the modern culture calibrations) for each data point. Calibration uncertainty was assessed by randomly choosing either the laboratory calibrations of Evans et al. (2016b), which define a Mg/Ca_{SW}-dependent Mg/Ca–T sensitivity, or the modern calibration with an 'H-factor' applied to the pre-exponential constant (Evans and Müller, 2012), which maintains the modern Mg/Ca–T sensitivity in deep time. The uncertainties on each data point are then the 97.5th and 2.5th percentile of these 1000 sets of assumptions. The 'best estimate' SSTs are the 50th percentile of the subset of these 1000 draws that use the calibrations of Evans et al. (2016b), which is preferred because the available evidence suggests that the Mg/Ca-T sensitivity varies as a function of Mg/Ca_{SW}. Note that the

data are subject to revision following replication of that study, and that using the 50th percentile of all estimates including both calibrations would result in overall cooler SST. Analytical uncertainty is not considered significant given the magnitude of these uncertainties.

***Intra-test Mg/Ca analysis by LA-ICP-MS and EPMA*:** In contrast to solution Inductively-Coupled-Plasma Mass Spectrometry (ICPMS), which enables high-throughput of pooled, dissolved foraminifera, highly spatially-resolved techniques such as Laser-Ablation ICPMS facilitate targeted *in-situ* analysis of carbonates (Eggins et al., 2003) and allow intra-specimen preservation to be assessed (e.g. Creech et al., 2010; Evans et al., 2015). Small samples such as foraminifera may be analysed without embedding or sectioning, and high-sample through-put means that the technique is relatively inexpensive. Laser spot sizes are typically 20-80 µm in diameter, with 5 µm possible (Lazartigues et al., 2014), enabling repeat measurements of individual foraminifera chambers or seasonality reconstruction in long-lived organisms with incremental growth layers (Bougeois et al., 2014; Evans et al., 2013). Because each laser pulse removes less than 100 nm of material on carbonates (Griffiths et al., 2013), depth-profiling through the sample has an effective resolution of <0.5 µm when using a fast wash-out ablation cell (Müller et al., 2009). Therefore, element profiles through foraminifera chamber walls not only facilitate the characterization of intra-specimen preservation, which can be assessed by the simultaneous collection of Mg/Ca, Sr/Ca, Mn/Ca, Al/Ca and Fe/Ca ratios, among others, but also allow diagenetically affected areas, such as surface overgrowths, to be excluded from the measurement used to calculate the oceanographic variable of interest (e.g. Hollis et al., 2015; Hines et al., 2017). The disadvantage of LA-ICPMS is that overall data acquisition and reduction is typically more time-consuming compared to solution-based techniques and there is relatively large intra-specimen variability.

Electron Probe Microanalysis (EPMA) is a microanalytical technique based on the detection of element-characteristic x-rays produced by bombarding the sample with an accelerated and focused electron beam. For quantitative analyses, the intensity of the element-specific x-rays is compared against those of the same elements from chemically well-characterized standards. However, the sensitivity of EPMA is limited, and typically only Mg/Ca and Sr/Ca ratios in foraminiferal shells can be quantitatively measured (e.g., Brown and Elderfield, 1996; Anand and Elderfield, 2005). One advantage of this technique is the high spatial resolution; typical beam spot sizes for quantitative analyses in foraminiferal shells is ~2 to 10 µm (e.g., Hathorne et al., 2003). In addition, semi-quantitative elemental distribution maps can be acquired with sub-µm resolution for a larger suite of elements (e.g., Pena et al., 2008) allowing for the identification of diagenetic phases.

Sample preparation for EPMA is time-consuming, as tests need to be embedded in epoxy and polished until suitable cross sections for analysis are exposed. This method is unique in allowing SEM imaging of chamber walls prior to analysis, including an assessment of contaminant and diagenetic phases. The same epoxy mounts can also be used for *in situ* $\delta^{18}O$ analysis by SIMS, so that chemical and isotopic information can be deduced from adjacent domains just microns apart (Kozdon et al. 2013; Wycech et al., 2018). Semi-quantitatively maps of intrashell Mg/Ca variability with sub-µm resolution are possible with

EPMA (e.g., Eggins et al., 2004), but for quantitative Mg/Ca measurements, an electron beam with a diameter of several µm is required, which averages between the high- and low Mg bands or domains observed in many planktic (e.g. Eggins et al., 2004; Spero et al., 2015) and benthic (e.g., de Nooijer et al., 2014) foraminifera. The average of multiple Mg/Ca measurements by EPMA from an individual shell is typically comparable to solution-phase data that consume the whole shell (e.g., Hathorne et al., 2003). A major advantage of this method is that it is non-destructive.

4.3 Clumped isotopes

4.3.1 Theoretical background of clumped isotopes

The carbonate clumped isotope thermometer is based on the temperature-dependent proportion of ^{13}C-^{18}O bonds in carbonate minerals (Ghosh et al., 2006, Eiler, 2007). The proxy has a direct basis in thermodynamics (Schauble et al., 2006; Hill et al., 2014) and has been applied to a wide range of marine and terrestrial samples, from foraminifera to paleosol carbonates (e.g. Tripati et al., 2010; Snell et al., 2013; Douglas et al., 2014). The zero-point energy of atomic bonds decreases with the mass of the atoms involved, favoring bonds between the rare, heavy isotopes. However, this effect decreases with increasing temperature, leading to the theoretical and observed decrease of "clumping" of heavy isotopes with increasing formation temperature of the mineral (Eiler, 2007). Excess abundance of ^{13}C-^{18}O bonds is abbreviated to Δ_{47} and refers to the over-abundance of CO_2 with the composition ^{13}C-^{18}O-^{16}O relative to a stochastic distribution of all isotopes (Eiler and Schauble, 2004). Δ_{47} is measured on an isotope ratio mass spectrometer after acidification of the carbonate, in a very similar way as classical $\delta^{18}O$ measurements. The only difference is that the abundance of mass 47 is recorded in addition to the traditional masses 44-46; $\delta^{18}O$ and $\delta^{13}C$ are obtained as by-products of the measurements and are needed to calculate the expected stochastic abundance of ^{13}C-^{18}O bonds in the respective sample, which is then compared to the observed abundance to calculate Δ_{47}.

4.3.2 Strengths of clumped isotopes

There are three key strengths to this carbonate-based paleothermometer: (1) both theory and empirical studies demonstrate that the isotopic composition of water exerts no measurable control on the clumped isotope signature (Ghosh et al., 2006; Schauble et al., 2006); (2) the technique involves the simultaneous measurement of Δ_{47} and $\delta^{18}O$, enabling the independent and direct calculation of ancient $\delta^{18}O_{sw}$; (3) many biogenic carbonates and inorganic precipitates fall on the same calibration line, suggesting the absence of measurable 'vital effects' (e.g. Ghosh et al., 2006; Zaarur et al., 2013; Tripati et al., 2015). Molluscs and brachiopods (Came et al., 2007; Eagle et al., 2013a; Henkes et al., 2013), foraminifera (Tripati et al., 2010; Grauel et al., 2013; Tripati et al., 2014; Evans et al., 2018a), paleosols (Passey et al., 2010), land snails (Eagle et al., 2013b), and other forms of carbonate (Eiler, 2007) all appear to be reliable archives for the measurement of Δ_{47}. Clumped isotope analysis of speleothems and certain coral species (Ghosh et al., 2006; Tripati et al., 2010; Saenger et al., 2012; Affek and Zaarur, 2014; Tripati et al., 2015; Loyd et al., 2016; Spooner et al., 2016) are more uncertain and require further study.

Geosci. Model Dev. Discuss., https://doi.org/10.5194/gmd-2018-309
Manuscript under review for journal Geosci. Model Dev.
Discussion started: 17 January 2019

4.3.3 Weaknesses of clumped isotopes

Whilst clumped isotope thermometry has been successfully applied to a wide range of sample types, there are several challenges associated with paleoclimate reconstructions. Of these, the most fundamental is the low abundance of doubly substituted ("clumped") carbonate, which typically makes up only ~46 ppm of the total CO_2 produced from a sample. Precision is therefore ultimately limited by our ability to cleanly measure mass 47 CO_2. In practice, this implies relatively large sample masses, typically ~10 mg of material (>500 planktic foraminifera) although recent advances in instrumentation have seen this reduced by a factor of 5-10 in some laboratories (Meckler et al., 2014; Rablen et al., 2015; Müller et al. 2017). Analytical precision for these sample sizes limits the accuracy of the technique to ±2-3°C (1 sigma), which can be improved by performing a greater number of replicate measurements (e.g., Huntington et al., 2009; Thiagarajan et al., 2011; Tripati et al., 2014), with an obvious trade-off between sample size and precision. In addition, the presence of organic carbon, which can contribute to mass 47, can require stringent sample cleaning procedures. In common with many proxies, the potential for seasonal growth of some archives must be considered. In particular, interpretation of isotopic data from molluscs needs to consider seasonal biases and ecology. Careful sample selection and geologic context are of critical importance when designing studies and interpreting clumped isotope data.

As for $\delta^{18}O$ and Mg/Ca, preservation of foraminifera and other carbonates is a key issue that must be addressed. While the impacts of dissolution are not known, recrystallization at different temperatures or the addition of secondary diagenetic calcite precipitated after deposition will bias clumped isotope measurements (Shenton et al., 2015; Stolper et al., 2018). Solid-state reordering within the mineral will alter the isotope ordering, although only in samples that have experienced burial temperatures well above 100-150 °C for over ~10 Ma are thought to be affected by this process (Passey and Henkes, 2012; Henkes et al., 2014; Shenton et al., 2015).

Several empirical calibrations of Δ_{47} to temperature have been developed, with differences partly related to laboratory-specific analytical methodology; these include acid digestion temperature, instrumentation, ion corrections and standards. Some discrepancies observed in earlier studies may be due to the limited temperature range and replication when calibrating biogenic carbonates, whereas calibrations with larger temperature ranges (> 90 °C) across different types of carbonates agree well (Bonifacie et al., 2017; Fernandez et al., 2017; Kelson et al., 2017). Material-specific calibrations have also been suggested, for example, for marine molluscs (Eagle et al., 2013b; Henkes et al., 2013). Accurate absolute temperature reconstructions depend on empirical calibrations being developed (Dennis and Schrag, 2010; Douglas et al., 2014) or checked (Tang et al., 2014) in each laboratory. Differences between laboratories have been attributed to a range of factors (Dennis et al., 2011; Wacker et al., 2014; Defliese et al., 2015; Daëron et al., 2016; Schauer et al., 2016) but are not yet fully resolved. With the use

of rigorous standardization procedures to correct for instrument drift and more consistent methodologies overall, it is hoped that calibrations between instruments and labs will converge (e.g., Bernasconi et al., 2018).

4.3.4 Recommended methodologies for clumped isotopes

Here we outline our recommendations for generating clumped isotope data from fossil shells, and for converting these data into temperature. The current data set for the targeted age range is limited to five early Eocene onshore sections (Supplementary Data File 5). Using the methods outlined below, we have calculated SSTs and error values and compiled a summary of SST estimates for these EECO sites.

We recommend the use of a calibration that covers a wide temperature range with sufficiently replicated analyses that includes calibration samples of the carbonate-type being analyzed. Suitable calibration equations have been published by Tripati et al. (2010, 2015), Kele et al. (2015), Kluge et al. (2015), Bonifacie et al. (2017) and Kelson et al. (2017). As for $\delta^{18}O$ and Mg/Ca, samples need to be carefully screened for diagenetic alteration.

Best practice for measuring, correcting and reporting Δ_{47} includes: (1) measurement of a large number of gas and/or carbonate standards of different compositions; (2) correction for instrumental non-linearities (Huntington et al., 2009; Dennis et al., 2011), such as those which arise from secondary electrons (He et al., 2012; Bernasconi et al., 2013), or use of instruments with electron suppression; (3) reporting of data on an absolute reference frame (Dennis et al., 2011), and; (4) reporting full methodology, including digestion apparatus, digestion temperature, gas cleaning procedure, mass spectrometer and corrections used, working gas composition, constant sets used for calculations, acid digestion fractionation factor, Δ_{47} values and errors, temperature calibration, and estimated temperatures. Ideally, the provision of gas and/or carbonate standard results together with the sample data facilitates the broad use of data and future recalculations. We recommend the open archiving of raw intensity values and datasets, with their own digital object identifiers, to enable the reanalysis of data over the long-term.

Given the required sample amounts and time-intensive measurements, clumped isotope thermometry is most powerful where other proxies are limited by unknown confounding effects. Rather than providing high-resolution reconstructions, clumped isotopes can be used to ground-truth and improve the accuracy of other proxies, including new constraints on seawater compositions (Evans et al. 2018a). Systems allowing the repeated measurement of small (~100 µg) sample aliquots give the required replication rates for Δ_{47}, which are averaged across samples, whilst also providing higher-resolution records of standard $\delta^{18}O$ and $\delta^{13}C$ analyses.

4.4 Isoprenoidal GDGTs (TEX_{86})

4.4.1 Theoretical background of TEX_{86}

The tetraether index of 86 carbons (TEX_{86}) is an organic paleothermometer based upon the distribution in marine or lake sediments of isoprenoidal glycerol dialkyl glycerol tetraethers (GDGTs), which are inferred to be mainly derived from marine Thaumarchaeota (Schouten et al., 2002) and has been widely used to reconstruct SST during the Eocene (Brinkhuis et al., 2006; Pearson et al., 2007; Sangiorgi et al., 2008; Bijl et al., 2009, 2010, 2013; Sluijs et al., 2011; Hollis et al., 2009, 2012; Douglas et al., 2014; Frieling et al., 2014; Inglis et al., 2015; Cramwinckel et al., 2018) and across the PETM (Sluijs et al., 2006, 2007b, 2011, 2014; Zachos et al., 2006; Schoon et al., 2015; Frieling et al., 2017; 2018). The underlying principal of TEX_{86} is that the number of cyclopentane rings (moieties) in GDGTs increases with growth temperature in order to alter the fluidity and permeability of the cell membrane (homeoviscous adaptation). Laboratory culture and mesocosm experiments confirm this response and indicate a linear relationship between TEX_{86} and incubation temperature at least to 40°C (Wuchter et al., 2004, Schouten et al., 2007, Elling et al., 2015), possibly to 50°C (Pitcher et al., 2009; Kim et al., 2010). Marine Thaumarchaeota occupy much of the epipelagic and mesopelagic zone, but cell numbers are highest in the upper few hundreds of meters of the surface ocean (Church et al., 2010), with TEX_{86} correlating most strongly with sea surface (SST) or shallow subsurface (Sub-T, 50-200 m) temperatures (Tierney and Tingley, 2015).

4.4.2 Strengths of TEX_{86}

TEX_{86} has several key advantages over other paleothermometers. Isoprenoidal GDGTs are relatively resistant to thermal degradation and diagenesis (Schouten et al., 2004) and can be used to reconstruct SST in settings where well-preserved foraminiferal calcite is absent (e.g. Bijl et al, 2009; Hollis et al., 2012; Pross et al. 2012) and where alkenones (e.g. the $U^{K'}_{37}$ paleothermometer) are either absent or outside their calibration range (Brassell, 2014). TEX_{86} has become a key proxy for the reconstruction of SSTs in locations where temperatures exceed modern conditions (e.g., Pearson et al., 2007; Frieling et al., 2017, 2018; Cramwinckel et al., 2018). Furthermore, TEX_{86} is not affected by changes in pH and salinity (Wuchter et al., 2004; Elling et al., 2015) and does not require a correction to account for past changes in ocean seawater chemistry (see Sections 5.1.3 and 5.1.4). TEX_{86} values are also not substantially impacted by sediment extraction and processing techniques and interlaboratory variation in TEX_{86} values are comparable to those of other temperature proxies (Schouten et al., 2013a).

4.4.3 Weaknesses of TEX_{86}

The interpretation of TEX_{86} values can be complicated by the input of GDGTs from archaea other than marine Thaumarchaeota. Several indices have been developed to screen for such secondary inputs. The branched-to-isoprenoidal tetraether (BIT) index (Hopmans et al., 2004) is used to assess the impact of terrestrial input upon TEX_{86} values. TEX_{86}-derived SSTs may be warm-biased by 2°C or more when BIT indices exceed 0.4 (Weijers et al., 2006). However, the impact of terrigenous GDGTs is highly variable, being dependent on the nature and temperature of the source catchment (Bijl et al., 2013; Douglas et al., 2014; Inglis et al., 2015). Sedimentary GDGT production can also affect TEX_{86} values. Methanotrophic Euryarchaeota can synthesise GDGTs with up to 3 cyclopentane moieties (Pancost et al. 2001) and may impact TEX_{86} values in settings in which anaerobic oxidation of methane (AOM) has occurred. The Methane Index (MI) can be used to assess

AOM, whereby high MIs (>0.5) reflect high rates of AOM and low values (<0.3) suggest normal sedimentary conditions (Zhang et al., 2011). During the Eocene, MI values rarely exceed 0.5 suggesting that most settings are relatively unaffected by diffusive methane flux and associated AOM. Methanogenic archaea can synthesize GDGT-0 as well as smaller quantities of GDGT-1–3 and may bias TEX_{86} values (Blaga et al., 2009). This can be assessed using the %GDGT-0 index (Inglis et al., 2015). Culturing experiments indicate that a methanogenic source of GDGT-0 is possible when the index is >67%. Methanogenesis appears to have a minor influence on Eocene records as >90% of analyses are below this threshold (Inglis et al., 2015).

One of the major uncertainties in TEX_{86} palaeothermometry is the impact of non-temperature factors upon thaumarchaeotal GDGT distributions, including growth phase (Elling et al., 2014; Hurley et al., 2016) and oxygen concentrations (Qin et al., 2015). Although these factors remain difficult to assess in the geological record, the Ring Index (Zhang et al., 2016) and fCren′:Cren′ + Cren (O'Brien et al., 2017) can potentially help to reveal non-temperature controls, or exclude the influence of such biases. There is also evidence that sedimentary GDGTs are not exported solely from surface waters but also shallow subsurface waters (Taylor et al., 2013) and that their export may be seasonally biased (Herfort et al., 2006; Bijl et al., 2010). These factors may help to explain some apparent SST anomalies (e.g. Taylor et al. 2018) and discrepancies with other proxies (Hollis et al., 2012; Inglis et al., 2015). The suggestion that these discrepancies may be explained by export of GDGTs from the deep ocean (Ho and Laepple, 2016) was refuted by Tierney et al. (2017) who argue that the sedimentary TEX_{86} signal is predominantly derived from the upper water column (50–300 m) and that temperatures through the upper water column are strongly correlated, therefore minimizing any calibration bias. Export from the upper water column rather than sea surface will impart some uncertainty because TEX_{86} is calibrated to climatological ocean temperatures, such that the local dominant depth or season of production and export could introduce bias, particularly in settings with relatively deep, sub-thermocline GDGT production (Taylor et al., 2013). Future calibration studies should provide detailed information about the prevailing oceanographic conditions at each core-top location. In areas with a shallow and steep thermocline, TEX_{86} may be recording thermocline rather than surface variations (e.g., Huguet et al. 2007). To address this, both SST and sub-T calibrations have been developed (e.g. Schouten et al., 2002; Kim et al., 2008; Tierney and Tingley, 2015), and should be applied with knowledge of the oceanographic characteristics of the site in question.

A final weakness is that many early Eocene sites (e.g. Frieling et al., 2017, 2018; Cramwinckel et al., 2018) are characterized by TEX_{86} values that exceed the calibration range in modern oceans (0.3–0.8). Whilst some uncertainty may be alleviated by comparison with associated multi-proxy data (e.g. Frieling et al., 2017; Tierney et al., 2017), TEX_{86} values >0.8 require extrapolation of the relationship between TEX_{86} and temperature beyond the modern calibration dataset or incorporation of limited data from laboratory studies (e.g., Pitcher et al., 2009; Elling et al., 2015). Such high values almost certainly indicate hotter temperatures, but the degree of estimated warming depends on assumptions about the mathematical nature of the temperature-TEX_{86} relationship (see below).

Geosci. Model Dev. Discuss., https://doi.org/10.5194/gmd-2018-309
Manuscript under review for journal Geosci. Model Dev.
Discussion started: 17 January 2019

4.4.4 Recommended methodologies for TEX_{86}

Here we outline our recommendations for generating TEX_{86} data from marine sediments, and for converting these data into temperature. We have compiled available TEX_{86} data from five ODP and IODP sites, five onshore drillholes and nine onshore sections (Supplementary Data File 6). Using the methods outlined below, we have calculated SSTs and associated uncertainties, and compiled a summary of SST estimates for each time slice (LP, PETM, EECO).

Preparation of sediments for TEX_{86} analysis is straightforward, although large sample volumes (100g) may be needed where concentrations of organic matter are low. After extraction and purification, the isoprenoidal GDGTs are analysed by HPLC/MS (see Hopmans et al., 2000). Previously, a Cyano column was used for HPLC separation (Hopmans et al., 2000); however, the use of BEH HILIC UHPLC columns has now been shown to yield better separation while not substantially affecting the TEX_{86} index (Hopmans et al., 2016). The TEX_{86} index is calculated as the ratio between isoprenoidal GDGTs as follows:

$$\text{(GDGT-2 + GDGT-3 + cren')/ (GDGT-1+ GDGT-2 + GDGT-3 + cren')} \quad (5)$$

where GDGT-1, GDGT-2 and -3 are characterized by one, two and three cyclopentane moieties and cren' is the regioisomer of crenarchaeaol.

Several TEX_{86} calibrations have been developed to estimate sea surface or shallow subsurface temperatures. The original TEX_{86} core-top calibration was a linear relationship to SST (Schouten et al., 2002). However, the correlation between TEX_{86} and SST is weak below 5°C and samples from the Red Sea deviate from the wider calibration dataset (Kim et al., 2008). To resolve this, TEX_{86} was recalibrated to exclude samples from the Red Sea and sites where SST < 15 °C (e.g. Kim et al., 2008; Naafs and Pancost, 2016; O'Brien et al., 2017).

Various non-linear relationships have also been proposed (e.g. Liu et al., 2009; Kim et al., 2010). Of these non-linear calibrations, the most commonly-used one is TEX_{86}^{H}, which assumes an exponential relationship between temperature and GDGT distributions. It uses a log transformation of TEX_{86} and excludes core-top data from the Red Sea as well as from sites where SST < 5 °C. SST is derived from TEX_{86}^{H} as follows:

$$TEX_{86}^{H} = \log_{10}\text{(GDGT-2 + GDGT-3 + cren')/ (GDGT-1+ GDGT-2 + GDGT-3 + cren')} \quad (6)$$

$$SST = 68.4 \times TEX_{86}^{H} + 38.6 \text{ (RMSE = 2.5 °C)} \quad (7)$$

However, the TEX_{86}^{H} calibration does not account for observational error and is affected by regression dilution because TEX_{86} is treated as the independent variable and therefore assumed to be error-free. The regression dilution causes it to systematically underestimate warm SSTs in the modern ocean and, by inference, may also underestimate SSTs in ancient greenhouse climates (Tierney and Tingley, 2014; O'Brien et al., 2017).

Kim et al. (2010) also proposed another index, TEX_{86}^{L}, which is also an exponential calibration but uses the entire core-top dataset (with the exception of the Red Sea) and was developed to reconstruct SST across all temperature ranges. However, TEX_{86}^{L} does not strictly reflect the degree of cyclisation in GDGTs and consequently lacks obvious biological rationale. It is also particularly sensitive to contributions from other archaea, especially those living in the subsurface (Kim et al., 2015; Taylor et al., 2013) and its application within the geological record has been questioned (Inglis et al., 2015; Taylor et al., 2018).

Available experimental evidence (Pitcher et al., 2009; Schouten et al., 2013b; Elling et al., 2015) suggests a linear relationship between TEX_{86} and SST, which is consistent with the modern core-top data-set. However, it remains uncertain if TEX86 continues to have a linear relationship with temperature beyond the range of the modern calibration Cramwinckel et al., 2018). The functional form of the calibration has significant consequences for temperature estimation, especially in for values >0.8 (Fig. 4A), which is particularly relevant for the warm Paleogene where such values are common.

The Bayesian regression model (BAYSPAR) of Tierney and Tingley (2014, 2015) applies a linear calibration, but the regression terms can vary spatially to accommodate the modern regional variation in TEX_{86} sensitivity, as in the Mediterranean Sea (Kim et al., 2015). In deep-time settings, BAYSPAR searches the modern core-top dataset for TEX_{86} values that are similar to the measured TEX_{86} value within a user-specified tolerance and draws regression parameters from these modern locations. This assumes that modern TEX_{86} values yield information on the environmental factors that determine the TEX_{86}-SST relationship in the ancient oceans, including factors other than mean annual sea surface temperature that might regionally alter the sensitivity of the proxy. This assumption is difficult to test and has potential to introduce additional uncertainties or bias.

BAYSPAR can be determined without excluding core-tops from the Red Sea or where SSTs < 15 °C. This is likely important as Red Sea-like conditions cannot be precluded for many Eocene sites (Inglis et al., 2015). The Bayesian model can also be used to estimate uncertainty beyond the modern calibration range. BAYSPAR can be used by downloading the publicly-available code in Matlab (https://github.com/jesstierney/BAYSPAR) or Python (https://github.com/brews/baysparpy), or employing the online calculator (http://bayspar.geo.arizona.edu). Both surface ($BAYSPAR_{SST}$) and subsurface ($BAYSPAR_{SubT}$) calibrations are available, the latter being the gamma-weighted average of the temperature range over 0–200 m water depth, with a maximum probability at ~50 m (Tierney and Tingley, 2015).

When applied to TEX_{86} values that exceed the modern calibration range, BAYSPAR typically yields results that lie between the linear and exponential calibrations because it incorporates both "normal tropical marine" and "Red Sea" sensitivities, the latter of which involves a steeper TEX_{86}-SST slope that is closer to the exponential assumption (Fig. 4b). It is thus a good "middle ground" choice for the Paleogene data considered here, and so we have used $BAYSPAR_{SST}$ in our compilations (Fig. 8, Supplementary Data File 6). While an exponential model might be a viable alternative, we do not recommend application of the TEX_{86}^{H} calibration because of the known bias from regression dilution.

Given the ongoing evolution of calibrations, we recommend that researchers include the fractional abundances of all isoprenoidal GDGTs as well as TEX_{86} values in all future publications as these will facilitate easy recalculation if and when the functional form of the calibration becomes better constrained. If BAYSPAR is used, we recommend that researchers report the parameters used (the prior mean and standard deviation, the search tolerance, and the version of the calibration dataset) so that the results are reproducible.

5 Terrestrial proxies for air temperature

Fewer geochemical options are available for reconstructing temperatures on the land (i.e., within the airmass overlying areas of land) than for reconstructing sea temperatures. In this section, we outline the primary geochemical approach, which is based on the distribution of branched tetraethers in sediments, in addition to two fossil-based approaches: physiognomic analysis of leaf fossils (including Leaf Margin Analysis and CLAMP) and paleobiogeographic analysis of pollen assemblages (NLR, Nearest Living Relative approach).

Stable isotopes have also been used to reconstruct early Paleogene terrestrial temperatures, notably $\delta^{18}O$ of pedogenic carbonate (Hyland et al., 2013, 2017; Hyland and Sheldon, 2013) and mammalian teeth (Fricke and Wing, 2004). The clumped isotope method has also been applied to pedogenic carbonate and shows great promise as an effective means to reconstruct seasonal temperatures (Snell et al., 2013). These proxies are not discussed here but the temperature records are included in the DeepMIP database. We adopt the term Land Air Temperature (LAT) for what is otherwise referred to as Mean Air Temperature (MAT) or Mean Annual Air Temperature (MAAT).

We have compiled terrestrial proxy data from 80 sites, which include four ODP or IODP sites and 76 onshore localities (Supplementary Data File 7). These data comprise 129 LAT estimates from a considerable range of proxies. Only the most widely used of these are described below.

5.1 Branched tetraether (brGDGT) paleothermometry

5.1.1 Theoretical background of branched tetraether (brGDGT) paleothermometry and early work

Geosci. Model Dev. Discuss., https://doi.org/10.5194/gmd-2018-309
Manuscript under review for journal Geosci. Model Dev.
Discussion started: 17 January 2019

Branched glycerol dialkyl glycerol tetraethers (brGDGTs) are membrane-spanning lipids produced by bacteria, probably acidobacteria (Sinninghe Damsté et al., 2011; Weijers et al., 2009). First discovered in a Dutch peat deposit (Sinninghe Damsté et al., 2000), brGDGTs are ubiquitous in terrestrial settings (see review in Schouten et al., 2013b). These compounds have been used increasingly as paleothermometers since a study of a global suite of mineral soil samples (Weijers et al., 2007) found that the degree of methylation in brGDGTs (MBT index) is correlated to LAT and pH, and that the number of cyclopentane rings in the same brGDGTs (CBT index) is related to soil pH, resulting in the MBT–CBT paleotemperature proxy. The proxy has been subsequently revised and recalibrated as MBT'–CBT (Peterse et al., 2012). The following three equations are used to derive LAT from the MBT'–CBT proxy [Eqs. 8–10].

$$MBT' = \frac{Ia+Ib+Ic}{Ia+Ib+Ic+IIa+IIa'+IIb+IIb'+IIc+IIc'+IIIa+IIIa'} \quad (8)$$

$$CBT = -\log\left(\frac{Ib+IIb+IIb'}{Ia+IIa+IIa'}\right) \quad (9)$$

$$MAT\ (°C) = 0.81 - 5.67 \times CBT + 31.0 \times MBT' \quad (n = 176, R^2 = 0.59, RSME = 5.0\ °C) \quad (10)$$

The MBT'–CBT proxy has been used to reconstruct early Paleogene terrestrial temperatures from continental margin marine records from the Southern Hemisphere (Bijl et al., 2013; Pancost et al., 2013; Pross et al., 2012) and the PETM in the Northern Hemisphere (Schoon et al., 2015; Weijers et al., 2007). These studies explicitly assumed that the majority of brGDGTs in marine sediment cores are produced within mineral soils at around sea level close to the core site and transported without alteration into marine sediments of similar age. The resulting LATs are significantly higher than present day. However, despite being in good agreement with other terrestrial proxies for LAT as well as with modelled LAT (Huber and Cabellero, 2011), they are ~5–10 °C lower than SST estimates derived from the same samples. This anomaly is discussed further below.

5.1.2 Strengths of brGDGT paleothermometry

Terrestrial temperatures are a crucial climatic variable, but most of our temperature records during the geological past are from the marine realm. The main strength of the MBT'–CBT terrestrial temperature pSchouteroxy is that it is one of the few proxies currently available that can provide high-resolution quantitative estimates of terrestrial temperatures during the Cenozoic. In addition, brGDGTs are ubiquitous in ancient soils (e.g. Chinese loess), peats and lignites from across the Cenozoic (Peterse et al., 2012; Naafs et al., 2018a), making it possible to apply this proxy across a range of archives and depositional environments.

5.1.3 New developments in brGDGT paleothermometry

Studies over the past few years suggest that caution should be applied to the interpretation of existing MBT'–CBT data. De Jonge et al., (2013; 2014) used refined analytical techniques to show that the 5-methyl penta- and hexamethylated brGDGTs, which were used to calculate the original CBT and MBT' indices, coelute with newly identified 6-methyl brGDGTs

that have a strong pH dependence. Re-evaluation of the global mineral soil dataset has led to new indices and calibrations based on 5-methyl brGDGTs, which are dependent on temperature alone (De Jonge et al., 2014).

$$MBT'_{5ME} = \frac{(Ia+Ib+Ic)}{(Ia+Ib+Ic+IIa+IIb+IIc+IIIa)} \quad (11)$$

$$MAT = -8.57 + 31.45 \times MBT'_{5ME} \quad (n = 231, R^2 = 0.64, RMSE = 4.9\ ^oC) \quad (12)$$

As well as a multiple linear regression (MAT_{mr}) calibration:

$$MAT_{mr} = 7.17 + 17.1 \times \{Ia\} + 25.9 \times \{Ib\} + 34.4 \times \{Ic\} - 28.6 \times \{IIa\} \quad (13)$$
$$(n = 231, R\text{^}2 = 0.67, RMSE = 4.7°C)$$

Naafs et al. (2017a) extended the calibration dataset and developed a new calibration for LAT as well as one to reconstruct Growing Degree Days above freezing (GDD_0), a measure of cumulative temperature over the growing season. GDD_0 is a guide to warm season temperatures and helps to constrain seasonal temperature variations, which is particularly important in high latitudes with high seasonality.

$$MAAT_{soil}\ (^oC) = 40.01 \times MBT'_{5me} - 15.25\ (n = 350, R^2 = 0.60, RMSE = 5.3\ ^oC) \quad (14)$$

$$GDD_{0\ soil} = 14344.3 \times MBT'_{5me} - 4997.5\ (n = 350, R^2 = 0.63, RMSE = 1779) \quad (15)$$

5.1.4 Weaknesses of brGDGT paleothermometry

Due to the potential for co-elution of newly identified 6-methyl brGDGTs that may compromise MBT'–CBT estimates for LAT, earlier datasets should be re-analyzed using the latest analytical methods and calibrations. This problem may not be widespread because the brGDGT distributions reported in several Paleogene studies (e.g. Bijl et al., 2013) are dominated by tetramethylated brGDGTs, which have no 6-methyl homologues. Consequently, the effect of co-eluting 6-methyl brGDGTs on the MBT'/CBT proxy might be small but warrants testing in future studies.

Recent studies have highlighted additional challenges in applying brGDGT paleothermometry in marine settings. The assumption that brGDGTs in marine sediments are mainly derived from mineral soils formed at sea level may not be valid in some cases. Recent work has shown that brGDGTs are also produced *in situ* in the marine water column and in the hosting marine sediments (Sinninghe Damsté, 2016; Weijers et al., 2014), in rivers (Zell et al., 2014), and in lakes (Naeher et al., 2014; Weber et al., 2015). To illustrate this, we plot the relative abundance of the tetra-, penta-, and hexamethylated brGDGTs of the published early Paleogene data from five sites together with the modern mineral soil and peat data (Naafs et al., 2017a, 2017b) early Paleogene data from lignites (Naafs et al., 2018a), following the approach of (Sinninghe Damsté, 2016) (Fig. 5a).

The result demonstrates that most of the marine samples analyzed have brGDGT distributions that are different from that found in any modern mineral soil or peat with a higher relative contribution of hexamethylated brGDGTs. This difference in brGDGT distribution suggests that these brGDGTs may not originate exclusively from mineral soils or peat. However, it is worth noting that the LATs derived from MBT'/CBT from some of these sites are in close agreement with LATs derived from pollen assemblages using the Nearest Living Relative methods (Pross et al, 2012; Pancost et al., 2013).

Even when derived from mineral soils, the brGDGT assemblage in marine sediment will reflect varying combinations of settings across an entire terrestrial catchment, including different elevations and microclimates (Bendle et al., 2010). Moreover, brGDGT distributions have also been found to be influenced by soil moisture content in some settings, which needs to be considered in paleoclimate reconstruction, especially in arid regions (Dang et al., 2016; Menges et al., 2014).

Although brGDGTs appear resistant to initial degradation in the water column, thermal maturation of brGDGTs on geological time scales does influence the proxy. Schouten et al. (2013b) used artificial maturation experiments to demonstrate that the degree of cyclization of brGDGTs (e.g. CBT-indices) changes at temperatures above 240 °C and brGDGTs are completed degraded at 300 °C. However, the influence of thermal maturity on the degree of methylation (MBT indices) appears to be limited as long as brGDGTs are not fully degraded.

Perhaps the greatest weakness of this proxy is that it fails to capture the super-warm temperatures of the early Paleogene because the calibrations saturate at ~25°C (e.g., Peterse et al., 2012; Naafs et al., 2017a). Many of the proxies for terrestrial temperature discussed here suffer from this problem because the modern environments that form the analogues for the calibration do not extend into tropical settings >25°C. For this reason, data sets should be scrutinized for evidence of LAT plateaus, which suggest the calibration has saturated.

5.1.5 Recommended methodology for brGDGTs

If the brGDGT-proxy is to be applied to reconstruct terrestrial temperatures during the Paleogene the latest set of calibrations (De Jonge et al., 2014; Naafs et al., 2017a) and analytical techniques that separate the 5- and 6-methyl brGDGTs should be used (e.g., Hopmans et al., 2016). In addition, if applied to marine sediments to reconstruct terrestrial temperatures, supporting evidence should be provided (Fig. 5) to demonstrate a dominant input of brGDGTs from mineral soils or peat.

Another option is to avoid the source uncertainty associated with analyses from marine sediments by directly analyzing terrestrial sediments. For example, Inglis et al. (2017) used the latest analytical techniques and mineral soil calibrations to reconstruct early Eocene terrestrial temperatures from lignites in northern Germany. Although determining accurate ages for lignites can be challenging, these systems are dominated by *in situ* production of brGDGTs, resulting in reconstructed temperatures with a higher fidelity to local LAT.

Geosci. Model Dev. Discuss., https://doi.org/10.5194/gmd-2018-309
Manuscript under review for journal Geosci. Model Dev.
Discussion started: 17 January 2019

Some studies have questioned whether soil-based calibrations should be applied to peat and lignite (Huguet et al., 2013, 2014; Weijers et al., 2011). Consequently, Naafs et al. (2017b) recently developed new peat-specific brGDGT-based temperature and pH calibrations, following Eqs. (16–19)

$$MBT'_{5ME} = \frac{(Ia+Ib+Ic)}{(Ia+Ib+Ic+IIa+IIb+IIc+IIIa)} \quad (16)$$

$$LAT_{peat}\ (℃) = 52.18 \times MBT'_{5me} - 23.05 \qquad (\mathrm{RMSE} = 4.7\ ℃) \quad (17)$$

$$CBT_{peat} = \log\left(\frac{Ib+IIa'+IIb+IIb'+IIIa'}{Ia+IIa+IIIa}\right) \quad (18)$$

$$pH = 2.49 \times CBT_{peat} + 8.07 \qquad (\mathrm{RMSE} = 0.8) \quad (19)$$

In addition, the relative abundance of H-brGDGTs (brGDGTs with an extra covalent bond between the two alkyl chains) and the degree of methylation of H-brGDGTs is also correlated with LAT (Naafs et al., 2018a). Although the correlation is not strong enough to provide quantitative temperature estimates, a high abundance of H-GDGTs in ancient lignites could provide additional evidence for elevated terrestrial temperatures. Applying the peat-specific brGDGT temperature calibration to the lignite record from North Germany confirms that LAT was significantly higher than present day, and 2-3 °C higher than those obtained with the mineral soil calibrations (Naafs et al., 2018b). These peat-specific calibrations were recently applied to a range of early Paleogene lignites from across the globe and indicate that LAT were significantly higher than previously thought and are more consistent with the marine-based temperature estimates (Naafs et al., 2018b).

In summary, the application of peat-specific brGDGT-based temperature calibrations to early Paleogene lignites is in the early stages of development but holds great potential to provide new insights into terrestrial temperatures during this key period of the Cenozoic (Naafs et al., 2018b). MBT-based approaches are still judged useful to provide temperature constraints, especially for multi-proxy comparisons in well-dated marine sediments, but must be carefully assessed for calibration saturation at high temperatures, sampling of wide catchment areas, and inputs of brGDGTs that are not sourced from non-mineral soils or peat.

5.2 Leaf morphology-based approaches

5.2.1 Theoretical background of leaf morphology-based approaches

Methods of estimating paleotemperatures and other climate parameters from the physiognomy of fossil leaves have been explored since the early 1900s (Bailey and Sinnott, 1915, 1916). They are based on the general premise that plants adapt their physical features to tolerate the climate in which they germinate due to their immobility. Early observations of Southeast Asian floras identified a positive correlation between temperature and the percentage of woody dicotyledonous (dicot) species that had smooth-margined leaves (Bailey and Sinnott, 1915). This correlation was later developed into the widely-applied method,

Leaf Margin Analysis (LMA; Wolfe 1979; Wing and Greenwood, 1993). Numerous modifications, different calibration data sets and measures of uncertainty related to LMA have since been explored (e.g. Wilf, 1997; Greenwood et al., 2003; Kowalski and Dilcher, 2003; Greenwood et al., 2004; Hinojosa and Villagran, 2005; Miller et al., 2006; Spicer et al., 2011). Essentially, LMA involves assessment of the margin character (whether smooth [entire] or toothed [non-entire]) of all dicot leaf morphotypes in a fossil assemblage. The percentage of entire margins is calculated, and temperature determined using an LMA calibration equation.

Several shortcomings were recognized quite early in the development of the LMA method. For example, the relationship between the percentage of entire margins and temperature was found to vary between geographic regions with no robust means of ascertaining which modern calibration should be used for a fossil leaf flora. In response to these shortcomings and in recognition that other leaf characters may be correlated with climate variables, multivariate methods were explored. CLAMP (Climate Leaf Analysis Multivariate Program; Wolfe, 1993; Spicer et al., 2009; Yang et al., 2011, 2015) is the most widely used of these methods. In this method, 31 leaf character variables are measured for each fossil leaf morphotype and multiple climate proxies are produced. CLAMP relies on comparison of fossil leaf data with large calibration datasets of modern dicot leaf morphology data collected using rigid protocols. The initial calibration dataset (Wolfe, 1993) was dominated by Northern Hemisphere assemblages. Subsequently, calibrations from other geographic areas have been developed (Steart et al., 2010; Jacques et al., 2011; Kennedy et al., 2014; Khan et al., 2014; Yang et al., 2015). Corresponding climate data sets are either based on the closest available long-term climate station measured data, or model-generated gridded data sets (Spicer et al., 2009). More information on calibration and an online analysis are available on the CLAMP website (http://clamp.ibcas.ac.cn/).

Although LMA and CLAMP are the most widely applied of the leaf morphology-based methods, leaf size has also been used as a univariate climate proxy (Dolph and Dilcher, 1980; Wilf et al., 1998; Wiemann et al., 1998; Carpenter et al., 2012) and other multivariate methods have been investigated, such as the Nearest Neighbor Approach (Stranks and England, 1997) and Canonical Correspondence Analysis (Hinojosa et al., 2005, 2006), both using the CLAMP dataset, and digital leaf physiognomy (Huff et al., 2003; Royer et al., 2005; Peppe et al., 2011).

5.2.2 Strengths of leaf morphology-based approaches

The strengths and weaknesses of leaf morphology-based approaches to paleoclimate analysis have been discussed extensively (e.g. Wolfe, 1993; Wilf, 1997; Uhl et al., 2003; Spicer et al., 2004; Traiser et al., 2005; Spicer et al., 2005; Green, 2006; Greenwood, 2007; Yang et al., 2007; Spicer and Yang, 2010; Peppe et al., 2011; Spicer et al., 2011; Yang et al., 2015). A key strength is that they provide quantitative estimates of climate variables that do not depend on correct assignment of fossil leaf forms to modern taxa and their current climate affiliations (e.g. Uhl et al. 2003). Each leaf morphology-based method also has its own particular strengths. Univariate methods such as LMA are relatively easy to apply (e.g. Yang et al., 2015) whilst the

inclusion of several leaf morphology characters within the multivariate method CLAMP is that the inclusion of several leaf morphology characters alleviates some of the problems associated with taphonomic loss of character information in fossils.

5.2.3 Weaknesses of leaf morphology-based approaches

A number of assumptions are made when applying leaf morphology-based paleoclimate methods, including that calibrations between leaf morphology and climate parameters are stable back through time and that fossil leaf collections are sufficiently representative of the source vegetation. Each method has its own set of weaknesses, many of which are discussed in the references given in section 5.2.2. Univariate methods such as LMA are potentially strongly affected by taphonomic biases because they are reliant on the representative preservation of a single leaf character. LMA is also strongly influenced by geographic variability, with vegetation from different parts of the world yielding significantly different LMA calibrations. CLAMP is less influenced by these weaknesses but is more complicated and time-consuming to apply. As with the MBT'–CBT proxy, the calibration for leaf morphology proxies saturates at ~25°C for most calibrations, perhaps at ~28C for CLAMP (Utescher et al., 2014). An exception is LMA using the Kowalski and Dilcher (2003) calibration, where LATs approach 30°C. This calibration endeavours to account for a cool bias in many other approaches, which is inferred to be due to the over-representation of toothed leaves in the wet environments that typify most settings where fossil leaves are preserved. However, this is still considered a provisional calibration dataset because it includes only ten sites from a restricted geographic area (Spicer et al., 2011).

5.2.4 Recommended methodology for leaf morphology-based approaches

A multi-proxy approach to reconstruction of land-based climate parameters is advocated where possible, including alternative leaf morphology-based methods, taxonomic (Nearest Living Relative) and geochemical approaches. Choice of univariate or multivariate methods (i.e., LMA versus CLAMP) depends on the quality of available material and the required output. Both LMA and CLAMP provide temperature estimates, but only CLAMP will produce estimates of both temperature and precipitation. For LMA, careful consideration should be given to the choice of calibration dataset, which have significant geographic variation. For CLAMP, the collecting and scoring protocols outlined on the CLAMP website should be followed to ensure the most robust estimates are produced. Updates to the calibration datasets and CLAMP methodology are also available through the CLAMP website (http://clamp.ibcas.ac.cn/). Both LMA and CLAMP are only applicable to leaf assemblages of woody dicot species and should ideally be applied to fossil assemblages with at least 20 morphotypes (e.g. Wolfe, 1979; Povey et al., 1994; Spicer et al., 2004, 2005).

5.3 Nearest Living Relative Analysis

5.3.1 Theoretical background of the Nearest Living Relative (NLR) approaches

The Nearest Living Relative (NLR) approach is the most widely used technique to derive quantitative climate parameters from pre-Quaternary fossil pollen assemblages. In contrast to leaf morphology-based methods that relate physical attributes of plants to climate, NLR uses a taxonomic approach to derive climate parameters from fossil pollen assemblages based on the climatic ranges of their present-day nearest living relatives. The NLR approach includes several different methods such as the Mutual Climate Range technique (e.g. Pross et al., 2000; Thompson et al., 2012), Bioclimatic Analysis (e.g. Kershaw and Nix, 1988; Greenwood at al., 2005; Eldrett et al., 2009; Pross et al., 2012; Pancost et al., 2013), Climatic Amplitude Method (e.g. Suan et al. 2017) and the Coexistence Approach (Mosbrugger and Utescher, 1997; Carpenter et al., 2012; Pross et al, 2012; Pancost et al., 2013; Utescher et al., 2014). All these methods apply similar principles. Here we focus on the most widely used method, the Coexistence Approach (CA). The method utilizes "*Palaeoflora*", an extensive database on the climate requirements of fossil taxa derived from the modern distribution of their NLR (Utescher and Mosbrugger, 2015). Although "*Palaeoflora*" is a global database, there is a focus on Eurasia, but additional information on climate requirements of NLRs is available through online botanical databases, such as the Australia's Virtual Herbarium (http://avh.chah.org.au) or the atlas of North American trees and shrubs (Thompson et al., 2015; https://pubs.usgs.gov/pp/p1650-g). Paleoclimate estimates derived from the CA usually include mean annual air temperature (MAAT or LAT as used here), coldest/warmest month mean temperature and the mean annual precipitation range. To generate a paleoclimate estimate, the climate ranges in which a maximum number of NLRs of a given fossil assemblage can coexist must be defined for each parameter (Utescher et al., 2014).

5.3.2 Strengths of the Coexistence Approach

The NLR approach uses the presence or absence of individual taxa in fossil assemblage rather than relative abundance, which reduces the likelihood of taphonomic biases. This facilitates, to some extent, the reconstruction of past non-modern analogue climates and environments (Pross et al., 2000; Utescher et al., 2014). Due to the use of presence-absence data, the method does also not require a calibration dataset using modern plant communities. Other methods that assess the direct relationship between pollen abundance and climate (e.g. transfer function techniques), require large calibration datasets from modern environments and their use for deep-time climate reconstruction is therefore very limited (e.g. Bartlein et al., 2011; Garreta et al., 2012). The CA can be applied to a wide range of plant fossils, including seeds, woods, pollen/spores and leaves. Comparisons of CA-based estimates with other biogeochemical and paleobotanical methods, including CLAMP and LMA, show generally good agreement for the early Cenozoic (e.g. Uhl et al., 2003; Roth-Nebelsick et al., 2004; Pound and Salzmann, 2017; Pross et al., 2012), providing some confidence in the utility of the method for the reconstruction of "deep-time" climates.

5.3.3 Weaknesses of the Coexistence Approach

Quantitative climate estimates from the fossil plant record of "deep-time" geological intervals are always accompanied by large uncertainties. The accuracy of a coexistence range depends strongly on the quality of the modern climate and plant distribution database, uncertainties in the identification of a fossil taxa and their nearest living relatives, as well as on the total number of taxa within a fossil assemblage (Utescher et al., 2014). The CA also does not account for relative changes in fossil

taxa percentages or long-distance transport of palynomorphs resulting in "mixed" assemblages from different habitats or vegetation zones. This places an important caveat on use of the CA for terrestrial assemblages from marine records or relatively open vegetation communities with low plant diversity (such as semi-deserts). Whereas low taxon numbers and large catchment areas results in unusual large coexistence intervals, inaccuracies of the CA have been also described for estimates from higher elevations (Grimm and Denk 2012). One of the greatest weaknesses that affects all NLR approaches is the assumption of uniformitarianism, namely that the climate tolerances of modern species can be extended into the past. This assumption inevitably introduces uncertainty that increases with the age of the geological record. Grimm et al. (2016) demonstrated how the incorrect use of outliers and fossil taxa with ambiguous affinity, as well as insufficient documentation of modern distribution of the NLR, can result in erroneous climate estimates from the CA. By its nature, the NLR approach cannot accurately predict environmental conditions beyond the present-day range. For instance, maximum LAT estimates plateau at ~25 for CA (Utescher et al., 2014).

5.3.4 Recommended methodology for applying the Coexistence Approach

A detailed methodological description including recommendations of how to treat outliers and relict taxa in the CA have been provided by Utescher et al. (2014). It is important to note that the CA generates ranges of equally possible values within which a fossil plant community could have co-existed. CA-derived estimates should therefore not be used as absolute or mid-point values. This is particularly important for data-model comparison studies. The accuracy of CA-based climate estimates is greatly reduced in sites with low taxa diversity (such as semi-deserts), large catchments (such as marine records), or non-modern analogue vegetation (such as the Arcto-Tertiary relict flora). Whenever possible, CA-derived climate estimates should be presented with confidence ranges including the uncertainty associated with the estimate of climate tolerances (Grimm et al., 2016). For comparisons using larger datasets, each climate estimate should be rated using a qualitative ranking system (i.e. confidence assessment) that addresses major influencing factors, such as taphonomy, diversity and age control (Salzmann et al., 2013). The confidence level should be used in addition to the indicated temperature range as a guide to assess the robustness of a temperature estimate. Finally, we recommend combing CA with other pollen-based methods and other proxies to facilitate a systematic comparison of climate estimates and possible sources of bias (e.g. Pross et al., 2012).

6 Proxies for atmospheric CO_2

In this section, we outline the four main approaches for reconstructing atmospheric CO_2 concentrations: the boron isotopic composition of marine carbonate, the carbon isotopic composition of marine phytoplankton, stomatal morphology and the carbon isotopic composition of land plants, and the carbon isotopic composition of pedogenic carbonates. We also include in our CO_2 compilation (Fig. 6) one estimate from the nahcolite proxy, which is based on mineral phase equilibria (Lowenstein and Demicco, 2006; Jagniecki et al., 2015).

6.1 Boron-based CO_2 reconstructions

Geosci. Model Dev. Discuss., https://doi.org/10.5194/gmd-2018-309
Manuscript under review for journal Geosci. Model Dev.
Discussion started: 17 January 2019

6.1.1 Theoretical background of boron-based CO_2 reconstructions

Boron isotopes within foraminiferal calcite ($\delta^{11}B_c$) have been used extensively to reconstruct atmospheric CO_2 concentrations on a variety of different timescales (Foster, 2008; Hönisch et al., 2009, 2012; Pearson et al., 2009; Seki et al., 2010; Anagnostou et al., 2016; Gutjahr et al., 2017). The $\delta^{11}B$-pH proxy has a strong grounding in theory (Hönisch et al., 2009; Foster and Rae, 2016) and is based on several foraminiferal calibration studies (e.g. Sanyal et al., 2001; Henehan et al., 2013; Foster and Rae, 2016).

6.1.2 Strengths of boron-based CO_2 reconstructions

Boron-based CO_2 reconstructions spanning the last ~800,000 years show excellent agreement with ice core CO_2 estimates (Hönisch et al., 2009). The results of boron isotope studies have also been found to be highly reproducible between different laboratories (Foster et al., 2017; Gutjahr et al., 2017), allowing the integration of multiple datasets and providing high confidence in the fundamental measurement of boron isotopes in biogenic carbonates. In common with other marine CO_2 proxies (e.g., alkenones below), age constraints are also typically strong for $\delta^{11}B_c$ and it is easy to correlate the resultant CO_2 estimates with marine-based climate proxies, some of which can be measured on the same material (e.g. $\delta^{18}O$, Δ_{47} and Mg/Ca in planktic foraminifera). Finally, detailed studies comparing $\delta^{11}B_c$ from contemporaneous diagenetically recrystallized foraminifera and "pristine" glassy foraminifera show no influence of diagenesis on the recorded values (Edgar et al. 2015), indicating that $\delta^{11}B$ is more diagenetically robust than $\delta^{18}O$; the reasons for this are not yet understood (Edgar et al. 2015).

6.1.3 Weaknesses of boron-based CO_2 reconstructions

The complications of the boron isotope proxy can be separated in two categories, based on the two main steps required to estimate CO_2 from $\delta^{11}B_C$ values: (i) the calculation of pH from measured $\delta^{11}Bc$ values that requires additional constraints on seawater $\delta^{11}B$ ($\delta^{11}B_{SW}$), the vital effects in extinct species, the calcification temperature, the relative depth habitat of foraminifera and the extent of any diagenetic overprint on primary $\delta^{11}B_C$ values, and (ii) the translation of the pH estimate into one of atmospheric CO_2, which first requires an estimate of a second carbonate system parameter to infer aqueous CO_2 concentrations at specific seawater concentrations for Mg and Ca, and determination of CO_2 disequilibrium between surface waters and the atmosphere at the study site. The influence of the latter can be reduced by careful site selection targeting oligotrophic settings.

Offsets between the boron isotopic composition of ambient seawater borate ion ($\delta^{11}B_{borate}$) and that of foraminiferal calcite are generally known as 'vital effects' following the usage of Urey et al. (1951) for oxygen isotopes. Many different processes could, in principle, be responsible for such offsets which could also differ between species. Of particular concern is the modification of pH in the diffusive boundary layer around foraminfiera by the photsynthesis of algal symbionts in some foraminifera (Hönisch et al., 2003). Other possibilities include physiological controls of the local pH during calcification (Rollion-Bard and Erez, 2010) and the incorporation of boron from aqueous boric acid (Vengosh et al., 1991).

Geosci. Model Dev. Discuss., https://doi.org/10.5194/gmd-2018-309
Manuscript under review for journal Geosci. Model Dev.
Discussion started: 17 January 2019

6.1.4 Recommended methodology for boron-based CO_2 reconstructions

The recommended procedure for boron isotope reconstructions of atmospheric CO_2 is designed to constrain unknowns and limit uncertainties associated with the proxy method. First, $\delta^{11}B_{sw}$ can be constrained in a number of ways: (i) by modelling the pH profile of the water column using multiple species (Pearson and Palmer, 1999, 2000; Anagnostou et al., 2016); (ii) using pairs of planktic/benthic foraminiferal $\delta\ ^{11}B_c$ (Greenop et al., 2017); (iii) utilizing existing records of benthic foraminiferal $\delta\ ^{11}B_c$ coupled with assumptions regarding deep water pH evolution (Raitzsch and Hönisch, 2013); (iv) using geochemical box models of the boron cycle (Lemarchand et al., 2000). All of these approaches indicate that the maximum rate of $\delta^{11}B_{sw}$ change is most likely ~0.1 ‰/Ma, which is consistent with the long residence time of boron in the ocean (10–20 Ma), its relatively large oceanic budget and the modern fluxes of boron in and out of the ocean (Lemarchand et al., 2002). Future studies should reconstruct surface ocean pH depth profiles using foraminiferal $\delta^{11}B_c$ to constrain changes in $\delta^{11}B_{sw}$ on shorter time scales, especially during periods when abrupt changes in weathering inputs of boron are possible. It is unlikely that these would be the main control on the evolution of $\delta^{11}B_{SW}$ over longer time scales (e.g. Lemarchand et al., 2002). Alternatively, carefully spaced, short (< 1Ma) time series of relative changes in pH, and hence CO_2 (Foster and Rae 2016), could bypass the need of accurate $\delta^{11}B_{sw}$ constrains, as they will encompass minimal change in seawater boron composition, typically of a magnitude less than analytical precision (i.e. <0.2 ‰).

Second, the issue of vital effects can be directly investigated within modern species by controlled culturing experiments (Sanyal et al., 1996, 2001; Foster, 2008; Henehan et al., 2013, 2016). For extinct species, vital effects can only be assessed indirectly. Recent work suggests that vital effects of Paleogene foraminifera play a less significant role in determining $\delta^{11}B_{borate}$ than in more recent times (Penman et al., 2014; Anagnostou et al., 2016). Nevertheless, foraminifera from smaller size fractions (150–250 µm) should be used to minimize the likelihood of unaccounted vital effects (Birch et al., 2013), and analysis of monospecific (or similarly behaving) foraminiferal species in terms of $\delta^{18}O$, $\delta^{13}C$ and $\delta^{11}B_c$ – will reduce uncertainties in pH and CO_2 reconstructions.

Third, estimates of salinity and temperature exert a relatively minor influence on estimates of pH (0.005 pH per psu change and 0.01 pH per ºC) in carbonate system calculations. Seawater temperature estimates are commonly derived from paired analyses of $\delta^{18}O_c$ (Pearson et al., 2007; John et al., 2013; Anagnostou et al., 2016) or Mg/Ca (Pearson et al., 2009; Foster et al., 2012; Martinez-Boti et al., 2015.

Finally, an additional carbonate parameter is required to calculate CO_2 concentrations at any given seawater salinity and temperature. For pre-Quaternary applications, this is typically provided by assumptions regarding the saturation state of calcium carbonate or alkalinity estimates constrained using geochemical models (Ridgwell, 2005; Pälike et al., 2012; Anagnostou et al., 2016; Gutjahr et al., 2017). Modelling studies indicate that the saturation state of calcium carbonate in

surface waters (surface $\Omega_{calc} = [Ca]_{sw} * [CO_3^{2-}]/K_{sp}$) remains essentially constant through the Cenozoic, independent of model boundary conditions (Tyrrell and Zeebe, 2004; Ridgwell and Zeebe, 2005; Hönisch et al., 2012; Pälike et al., 2012). This has recently been confirmed empirically, at least for the last 20 Myrs (Sosdian et al., 2018). Estimates of $[Ca]_{sw}$ are, however, required to derive carbonate ion concentration ($[CO_3^{2-}]$), which is used as the second carbonate system parameter, and these estimates are typically derived from fluid inclusion analysis (e.g. Horita et al. 2002).

At this stage, mean, upper and lower bounds of atmospheric CO_2 are calculated using a Monte Carlo approach to solve the relevant carbonate system equations. All simulations are iterated assuming Gaussian distribution of these parameters within the 2σ. For pre-Quaternary time scales, propagated estimates of CO_2 carry an uncertainty of ~25% (95% confidence intervals). Relative CO_2 estimates, however, carry a much-reduced uncertainty of 2-10% (Foster and Rae, 2016).

6.2 Carbon isotopic composition of marine phytoplankton

The carbon isotopic composition of marine phytoplankton, as recorded by bulk organic matter, chlorophyll-related compounds (porphyrins, pristane and phytane) or organism-specific biomarkers, has long been used to reconstruct changes in atmospheric CO_2 (i.e. Freeman and Hayes, 1992). This method relies on the concentration of CO_2 in seawater being the primary influence on the magnitude of carbon isotopic fractionation between dissolved inorganic carbon in the growth medium and the primary photosynthate of the algal cell (Rau et al., 1989). The fractionation factor, εp, is also influenced by algal cell geometry (Popp et al, 1998) and physiology, including specific growth rates (Laws et al., 1995; Bidigare et al., 1997) and the type of carbon acquired and lost from the cells (Sharkey and Berry, 1985). The most widely applied proxy of this type is based on the $\delta^{13}C$ composition of haptophyte algal alkenone biomarkers (Freeman and Pagani, 2005; Pagani, 2014), which have been used to reconstruct atmospheric CO_2 from the middle Eocene to modern (Pagani et al., 2005; Bijl et al., 2010; Zhang et al., 2013). Alkenones are typically scarce in sediments older than ~40 Ma (Brassell, 2014), which has encouraged the development of proxies based on similar principles using dinoflagellate cysts (Hoins et al., 2015; Wilkes et al., 2017) and other types of primary photosynthetic biomarkers with longer geological ranges (Freeman and Hayes, 1992; Naafs et al. 2016).

6.2.1 Theoretical background of alkenone-based CO_2 reconstruction

The saturation state and isotopic composition of alkenone biomarkers, unsaturated ethyl and methyl ketones with carbon chain lengths of C37–C39, are the basis for SST (Brassell et al., 1986; Conte and Eglinton, 1993; Conte et al., 2006) and salinity proxies (e.g., van der Meer et al., 2007; Warden et al., 2016), as well as CO_2 estimation (e.g., Pagani, 2002; Zhang et al., 2013). In the modern oceans, alkenones are produced by a relatively limited number of calcifying haptophyte algae ("coccolithophores"), all within the family Noelaerhabdaceae and including *Emiliania huxleyi* and *Gephyrocapsa* species (Volkman et al., 1980; Conte et al., 1998; Pagani, 2014). Where alkenone-bearing sediments predate the first appearance of the modern alkenone-producing species, it is assumed that ancient relatives within the Noelaerhabdaceae, such as the early Eocene to modern genus *Reticulofenestra*, are the primary alkenone-producers (Pagani, 2014). Alkenone-based estimates of

Geosci. Model Dev. Discuss., https://doi.org/10.5194/gmd-2018-309
Manuscript under review for journal Geosci. Model Dev.
Discussion started: 17 January 2019

CO_2 rely on the relationship between ε_p and $[CO_{2(aq)}]$ in the surrounding growth medium, which is related to atmospheric CO_2 via Henry's Law (Freeman and Hayes, 1992; Pagani, 2014). Calculation of ε_p requires determination of the difference between the $\delta^{13}C$ of $CO_{2(aq)}$ in the growth medium ($\delta^{13}C_{CO2(aq)}$) and the $\delta^{13}C$ of biosynthesised cellular organic matter ($\delta^{13}C_{org}$). The latter is measured on the haptophyte-specific C37:2 alkenone ($\delta^{13}C_{37:2}$) (Pagani, 2014; Zhang et al., 2013) as follows:

$$\varepsilon p37{:}2 = [(\delta 13\ \mathrm{C}[CO2(aq]) + 1000)/\ ((\delta 13\mathrm{C}[org] + 1000 - 1)] * 1000 \quad (20)$$

As lipids are depleted in ^{13}C relative to the carbon isotope composition of the whole cell a correction of +4.2‰ is applied when calculating $\delta^{13}C_{org}$ from $\delta^{13}C_{C37:2}$ (Schouten et al., 1998; Pagani, 2014). Alkenone-based estimates of ancient CO_2 assume diffusive transport of inorganic carbon across algal cell membranes (discussed below), with the total carbon isotope fractionation associated with marine photosynthetic activity (Zhang et al., 2013; Pagani, 2014) being described by:

$$〚\varepsilon〛\_(p37{:}2) = \varepsilon\_t + (\varepsilon\_f - \varepsilon\_t)(C\_i/C\_e) \quad (21)$$

where the total carbon isotope fractionation associated with photosynthesis and carbon transport is denoted by ε_f – typically ~25 to 28 ‰ (Goericke et al., 1994; Farquhar and Richards, 1984) - and ε_t respectively. C_e is the ambient, and C_i the intracellular, concentrations of aqueous CO_2. The physiological factors that control the C_i term are complex and poorly known, and so a simplified version of this relationship is typically used (Jasper et al., 1994; Rau et al. 1996):

$$\varepsilon_{p37:2} = \varepsilon_f - \left(\frac{b}{[CO_{2(aq)}]}\right) \quad (22)$$

where the *b* term integrates a suite of physiological variables, including cellular growth rate and cell geometry, that can influence photosynthetic carbon isotope fractionation (Pagani, 2014 and references therein). Studies reconstructing ancient CO_2 typically assume that the *b* term is correlated to nutrient levels, represented by phosphate concentrations, as follows (Pagani et al., 2005):

$$[CO_{2(aq)}] = \frac{118.52*[PO_4^{3-}]+84.07}{\varepsilon_f - \varepsilon_{p37:2}} \quad (23)$$

Ultimately, CO_2 is calculated from $[CO_{2(aq)}]$ by applying Henry's Law:

$$CO_2 = [CO_{2(aq)}]/k_H \quad (24)$$

k_H is defined as:

$$k\_(H\ ) = (-0.00004 * T\hat{}3 + 0.0048 * T\hat{}2 - 0.2313 * T + 6.2665)/100 \quad (25)$$

Where 'T' is an independently derived estimate of sea surface temperature.

6.2.2 Strengths of the alkenone CO_2 method

The relatively high abundance of alkenone biomarkers throughout the Neogene, and the relative ease of analysis of $\delta^{13}C_{37:2}$, makes alkenone CO_2 estimation suitable for high temporal-resolution studies of CO_2 dynamics. The alkenone CO_2 method is advantageous over other estimates of ε_p, such as the use of bulk organic carbon or other less specific biomarkers, because of the high specificity of marine alkenone production to one family within the haptophyte algae (Volkman et al., 1980; Conte and Eglinton, 1993). This source-specificity also allows for independent constraints on other factors that influence ε_p including cell geometry and physiology, based on the coccolithophore fossil record (Henderiks and Pagani, 2007; Pagani, 2014; Bolton et al. 2016). Finally, as the distribution ratio of alkenones produced by haptophyte algae is closely related to sea surface temperature (SSTs) (U_K^{37} index; applicable below ~28ºC) (Conte et al., 2006), similar to $\delta^{11}B$ methods, it is possible to directly generate parallel records of two key parameters for CO_2 estimation - SSTs and $\varepsilon_{p37:2}$.

6.2.3 Weaknesses of the alkenone CO_2 method

There are several uncertainties and assumptions in translating measured $\delta^{13}C_{37:2}$ first into a value for $\varepsilon_{p37:2}$, and then into an estimate of $[CO_{2(aq)}]$ and CO_2. In particular, robust proxy estimates of $\delta^{13}C_{CO2(aq)}$ and SST are required. These have not always been available in previous alkenone-based estimates of Paleogene CO_2 (Pagani et al., 2005). Inaccurate estimates of SST can cause substantial error in alkenone-based CO_2 estimates (Super et al., 2018), especially at high CO_2 where ε_p approaches the assumed value for ε_f (Bidigare et al., 1997; Riebesell et al., 2000; Pagani et al., 2011; Pagani, 2014). Although the '*b*' term integrates the effects of a number of physiological variables (e.g., specific growth rate, cell geometry) on net carbon isotope fractionation during photosynthesis (Bidigare et al., 1997; Riebesell et al., 2000; Pagani et al., 2011; Pagani, 2014) it is typically derived from the strong empirical relationship with surface ocean phosphate concentrations $[PO_4^{3-}]$ in the modern oceans (Bidigare et al., 1997). Although there have been attempts to disaggregate cell geometry effects (e.g. Henderiks and Pagani 2007), most existing records of ancient CO_2 rely on assumed ranges of the *b* term based on estimates of ancient $[PO_4^{3-}]$ (Pagani, 2014).

Alkenone-based CO_2 estimates also assume the dominance of diffusive CO_2 transport across the algal cell membrane (Zhang et al., 2013). Some studies have shown the operation of carbon concentrating mechanisms (CCMs), including the potential use of bicarbonate carbon (Holtz et al., 2015, 2017), under conditions of CO_2 limitation, resulting in non-linear relationship between ε_p, growth rate and CO_{2aq} (Riebesell et al., 2000; Zhang et al., 2013). Such CCM activity could impact the value of ε_p

through active transportation of carbon species with varied isotope compositions (Zhang et al., 2013). Ongoing empirical and modelling studies of carbon uptake and partitioning (Bolton and Stoll, 2013; Holtz et al., 2017, 2015; McClelland et al., 2017), and those examining the role of environmental conditions on CCM behaviour (Raven and Beardall, 2014; Raven and Hurd, 2012) will hopefully provide constraints on the ubiquity, importance and impact of these mechanisms within the alkenone-producing haptophytes. Finally, changes in growth rate can impact the isotopic offset (Δδ) between alkenone $\delta^{13}C_{C37:2}$ and the $\delta^{13}C_{org}$ of the whole cell. Δδ is commonly set at 4.2‰, although culture study estimates typically range from 3.1 to 5.9‰ (Pagani, 2014 and references therein), up to a reported maximum of 7-12‰ (Benthien et al., 2007). Where ε_p is high, changes of this order in Δδ can exert a significant impact on reconstructed CO_2 values (Pagani, 2014).

6.2.4 Recommended methodologies for the alkenone CO_2 method

The alkenone CO_2 method requires estimation of several physiological (εf, cell size, 'b') and environmental ($[PO_4^{3-}]$, SST, $\delta^{13}C_{CO2(aq)}$) parameters. Reconstruction of SSTs should follow best practice from one of the established proxies outlined in Section 4 and, where possible, SST uncertainty should be propagated through to final estimates of CO_2. The most reliable estimates of $\delta^{13}C_{CO2(aq)}$ are derived from the measurement of test $\delta^{13}C$ compositions of well-preserved, mixed-layer dwelling foraminifera, within the narrow 250 – 300µm size window, which are closest to equilibrium with $\delta^{13}C_{DIC}$ (Birch et al. 2013). Although very low ε_f values for *Emilliania huxleyi* of ~11‰ have been published (Boller et al., 2011), these results are yet to be replicated, and we recommend the existing approach of providing propagated CO_2 uncertainty based on a 25-28‰ range of ε_f for algae using C3 pathways (Pagani, 2014).

As with ε_f, establishing robust estimates for the *b* factor in ancient communities is non-trivial, and we recommend a similar propagation of uncertainty based on a range of *b* factors drawn from surface water $[PO_4^{3-}]$ measurements in analogous modern environments (Zhang et al., 2013). Given the potential importance of cell size within the physiological factors that make up the *b* term, some studies have sought to use an explicit cell-size 'correction' to alkenone CO_2 reconstructions (Bolton et al., 2016). However, the precise application of a cell size correction and its relation to the standard *b* term remains unclear. Here, we recommend that reticulofenestrid coccolith size is measured along with the determination of $\delta^{13}C_{37:2}$, at least for the purposes of screening out the impact of major shifts in cell-size on CO_2 records (Pagani, 2014), and for potential future use to improve quantitative estimates of the *b* factor.

6.2.5 Other algal substrates for CO_2 estimation

Dinoflagellates: Significant progress has been made towards a CO_2 proxy based on the carbon isotope fractionation of phototrophic dinoflagellates and their preservable cysts (dinocysts) (Hoins et al., 2015, 2016a, b, Wilkes et al. 2017). A strong correlation between ε_{pDINO} and CO_2 was found in four cultured dinoflagellate species (Hoins et al., 2015). Importantly, there appears to be species-specific effects on ε_{pDINO} based on uptake and leakage of different carbon species (HCO_3^- and $CO_{2(aq)}$) and light intensity, making single-species records preferable (Hoins et al. 2016a, b). Dinocysts are found in the geological

record from the Triassic onwards (MacRae et al., 1996) and several extant species are remarkably long ranging (e.g. Williams et al. 2004). This includes two species used in culture experiments (Hoins et al., 2015), *Protoceratium reticulatum* and *Gonyaulax spinifera*, which are preserved in the fossil record as dinocyst species *Operculodinium centrocarpum* and *Spiniferites* ramosus, respectively. The geological record for *O. centrocarpum* and *S. ramosus* spans the last 60 my and 130 my, respectively (e.g. Williams et al., 2004). The morphology and ecological affinity of these ubiquitous species is well known and apparently unchanged since the early Paleogene (Zonneveld et al., 2013, Sluijs et al., 2005, Frieling and Sluijs, 2018).

Unlike biomarker-based CO_2 proxies, individual dinocysts of a single species are selected based on morphological characteristics prior to analysis to maximize the similarity in size and shape between analysed individuals, both within and between samples. A recently developed laser-ablation nano-combustion isotope ratio mass spectrometry (LA-nC-IRMS) method (van Roij et al., 2017) allows for accurate analyses of the carbon isotope composition of single dinocysts (Sluijs et al. 2017).

While results from culture experiments are promising, it should be noted that several, potentially important, factors should be constrained before ε_{pDINO} can be widely applied as a CO_2 proxy. For example, current efforts aim to resolve the potential offset between the cultured motile cell and the preservable cyst as well as the relation of ε_{pDINO} to parameters other than CO_2, both in culture and in their natural environment. Although these and perhaps other issues still need to be addressed, the CO_2 dependent ε_{pDINO} in several dinocyst species may represent an opportunity to reconstruct CO_2 in geological deep time, excluding any morphology, species or genus-related factors in CO_2-dependency that may cause significant uncertainty in CO_2 estimates based on less specific algal compounds.

Phytane and general biomarkers: The carbon isotopic composition of phytoplankton has also been tested in a variety of general biomarkers, compounds which are representative of overall phytoplankton community. Chlorophyll, the primary pigment in all photoautotrophs, is of particular interest for reconstructing secular trends given its spatially and temporally ubiquitous presence in the geologic record. For this reason, studies on both its porphyrin head (Popp et al., 1989) and its side-chain phytol preserved as the diagenetic product phytane (Freeman and Hayes, 1992) are some of the earliest uses of ε_p for CO_2 reconstruction. Here, we will discuss phytane as an example of using general biomarkers for estimating past CO_2.

The overall theoretical background for using general biomarkers, such as phytane, are the same as the alkenone-based reconstructions. Like other lipids, phytane is depleted in ^{13}C relative to the carbon isotopic composition of the whole cell; a correction of 3.3 ± 1.3‰ standard deviation is applied when calculating $\delta^{13}C_{org}$ from phytane, based on the average of twenty-two cultured species (Witkowski et al., 2018). As seen with the other ε_p-based proxies, the physiological variable *b* (Eq. 24) is difficult to constrain. Studies for phytane have used a constant b = 170‰ kg μM^{-1} (Bice et al., 2006; Damsté et al., 2008; Naafs et al., 2016), consistent with average *b* found in modern marine sediments for total organic matter at 168 ± 43 ‰ kg

μM^{-1} (Witkowski et al., 2018) and for alkenone at 165 ± 53 ‰ kg μM^{-1} (Pagani, 2014). All other parameters are treated as seen in the alkenone-based reconstructions.

Based on these assumptions, a recent study shows that phytane yields a robust and consistent trend over the Phanerozoic, the longest record for CO_2 from a single proxy (Witkowski et al., 2018). This record has the potential to span even further in time given that the $\delta^{13}C$ of phytane has been measured in 1.73 Ga sediments (Li et al., 2003). This opportunity to observe changes in CO_2 from a single proxy is beneficial to understanding secular trends. In addition to its span in preservation, phytane is one of the most abundant biomarkers in both marine sediments and oils. This availability of phytane is critical during periods where other proxies are rare, extending beyond the alkenone and boron records, most notably used for reconstructing Cretaceous CO_2 (Bice et al., 2006; Damsté et al., 2008; Naafs et al., 2016). The ubiquity of phytane throughout time, location, and sample type lends to the possibility for amassing large data sets which can be used for developing robust average estimations for CO_2.

Although the phytane-based reconstructions show remarkably similar trends to other CO_2 proxies over the Phanerozoic, this biomarker requires more investigation. Nearly all studies regarding the mechanisms behind ε_p for CO_2 reconstructions have been species-specific and almost exclusively for alkenone-producing Haptophytes. It is unknown whether integrating the entire phytoplankton community, as opposed to several species, has an effect on the observed signal. Studies testing the different parameters and other potential effects on fractionation are still needed in order to properly constrain the uncertainties on using phytane.

6.3 Leaf stomatal and gas-exchange proxies

6.3.1 Theoretical background, strengths, and weaknesses of leaf stomatal and gas-exchange proxies

Plants interact directly with the atmosphere, making them well suited as climate proxies. Woodward (1987) and subsequent work (e.g., compilation in Royer, 2001) demonstrated that the stomatal density and stomatal index (stomatal density / stomatal + epidermal cell density) in many plant species respond inversely to the partial pressure of atmospheric CO_2; these responses are usually species-specific. If the stomatal response to CO_2 is known (usually from herbaria specimens and elevated CO_2 experiments), it can be applied to fossils of the same species to reconstruct paleo-CO_2. The genetic (Casson and Gray, 2008), signaling (Lake et al., 2002), and functional bases of the stomatal-CO_2 response are known reasonably well: theoretical considerations of the latter predict an inverse power law between stomatal density and CO_2 (Wynn, 2003; Franks et al., 2014; Konrad et al., 2017). The stomatal proxy is popular, having been applied in dozens of studies to produce over 300 estimates of paleo-CO_2 across the Phanerozoic, including the early Paleogene (Royer, 2014). A related proxy called the stomatal ratio relates the ratio of paleo-atmospheric CO_2 to present-day CO_2 to the ratio of stomatal density in a fossil to that in its nearest living equivalent (i.e., not necessarily the same species) via a one-point calibration and an assumed exponent of -1 for the power law. Because of these features, the stomatal ratio is best used for tracking relative (not absolute) changes in CO_2 (McElwain and Chaloner, 1995).

Some limitations of the stomatal proxy are: 1) only species whose stomatal density responds to CO_2 can be used; 2) extant calibrations are laborious to construct, and most fossil plant species are not alive today; 3) the method is empirical, not explicitly mechanistic, meaning that it is difficult to exclude the possibility that the extant relationships differed in the geologic past; and 4) in many species the upper error limit on the CO_2 estimate becomes very large or unbounded when the estimated CO_2 is moderately high or higher. An alternative approach that partly addresses these limitations is a mechanistic model based on the fundamentals of leaf gas-exchange (Konrad et al., 2008, 2017; Franks et al., 2014). The core of these models is the well-known relationship between leaf assimilation rate and the product between total leaf conductance (which partly reflects the "supply" side of assimilation) and the CO_2 gradient between the atmosphere and intercellular spaces (the "demand" side) (Farquhar and Sharkey, 1982). The critical measurements needed to estimate atmospheric CO_2 are the leaf $\delta^{13}C$, stomatal size and density, and an estimate of assimilation rate from a nearest living relative. The gas-exchange proxy of Franks et al. (2014) typically has 95% confidence intervals within -25% to +35% of the median CO_2 estimate, on par with other popular paleo-CO_2 proxies.

6.3.2 Recommended methodology of leaf stomatal and gas-exchange proxies

Both the stomatal ratio and leaf-gas-exchange proxies can be applied to most fossil leaves, even if the taxa are extinct today. Because the CO_2 estimates from stomatal ratios are "semi-quantitative" (McElwain and Chaloner, 1995), they are best used when complementary CO_2 information is present (e.g., Montañez et al., 2016). The stomatal density and stomatal index proxies work well when calibrated taxa are present as fossils and when estimated CO_2 is low to moderate. At higher CO_2 (above ~500 ppm for many species; e.g., Smith et al., 2010; Doria et al., 2011), the upper error limit can be unbounded, meaning that only minima can be quantified. One challenge with this proxy is the construction of robust calibrations, especially at the high end of the calibrations, because plants may need multiple growing seasons in experimentally elevated CO_2 concentrations before their stomatal densities and indices fully equilibrate (Royer, 2003; Hincke et al., 2016). The leaf-gas-exchange proxies are comparatively more recent, and so have been tested less. We encourage rigorous testing in nearest living relatives, especially for sensitive model inputs that cannot be measured directly in fossils, for example the assimilation rate at a known CO_2 concentration and the scaling between maximum and operational stomatal conductance to CO_2 (Maxbauer et al., 2014; McElwain et al., 2016a, 2016b, 2017; Franks and Royer, 2017).

In cases where multiple stomatal proxies have been applied to the same fossils, the corresponding CO_2 estimates are broadly similar (e.g., Maxbauer et al., 2014; Montañez et al., 2016; Richey et al., 2018), conferring mutual support for the methods. Generating CO_2 estimates from multiple taxa from a single typically leads to a more accurate consensus estimate outcrop (e.g., Montañez et al., 2016; Kowalczyk et al., 2018; Richey et al., 2018; Steinthorsdottir et al., 2018). Routines for propagating all known uncertainties associated with the leaf-gas-exchange and stomatal density / index proxies have been developed (Beerling et al., 2009; Franks et al., 2014) and should be used.

Geosci. Model Dev. Discuss., https://doi.org/10.5194/gmd-2018-309
Manuscript under review for journal Geosci. Model Dev.
Discussion started: 17 January 2019

6.4 Pedogenic carbonate proxy for atmospheric CO_2

For soils developing on carbonate-free bedrock, soil CO_2 is a mixture between two sources: atmospheric CO_2 that has diffused into the soil and CO_2 produced in-situ via biological respiration. In arid and semi-arid climates, carbonate commonly precipitates in soils and its $\delta^{13}C$ value reflects that of the mixed soil CO_2. Because the $\delta^{13}C$ of the two sources is different, the concentration of atmospheric CO_2 can be calculated with a two-end-member mixing model if the atmospheric $\delta^{13}C$, pedogenic carbonate $\delta^{13}C$, and concentration and $\delta^{13}C$ of biological CO_2 is known (Cerling, 1991, 1999). This pedogenic carbonate proxy has been widely applied across the Phanerozoic: over 500 estimates from dozens of studies (Royer, 2014). One difficulty has been the estimation of the biological CO_2 concentration, S(z). It is clear now that S(z) was overestimated in most early studies because pedogenic carbonate mostly forms during the dry season, when biological productivity is lowest (Breecker et al., 2009, 2010). Several promising quantitative proxies for S(z) have been proposed in recent years (Cotton and Sheldon, 2012; Montañez, 2013; Breecker and Retallack, 2014). The 95% confidence intervals typically range from -30/+40% to -50/+100% of the median estimate, depending on the characteristics of the paleosol in question (Breecker, 2013).

6.5 C_3 land plant carbon isotope proxy for atmospheric CO_2

6.5.1 Theoretical background of C3 land plant proxy method

Controlled growth chamber experiments conducted across a wide range of CO_2 show that carbon isotope discrimination between the $\delta^{13}C$ value of the atmosphere ($\delta^{13}C_{CO2}$) and the resulting plant tissue ($\delta^{13}C_{org}$) [$\Delta^{13}C = (\delta^{13}C_{atm} - \delta^{13}C_{org})/(1 + \delta^{13}C_{org}/1000)$] increases with increasing CO_2 (Schubert and Jahren, 2012). These data were consistent with other field and chamber experiments measured across smaller changes in CO_2 and revealed a unifying hyperbolic relationship between CO_2 and $\Delta^{13}C$ value (Schubert and Jahren, 2012). Using a large data compilation of terrestrial organic matter spanning the Pleistocene-Holocene transition, Schubert and Jahren (2015) showed how this relationship could be used to reconstruct CO_2 within the fossil record by relating changes in CO_2 to changes in $\Delta^{13}C$ value [i.e., $\Delta(\Delta^{13}C) = \Delta^{13}C_{(t)} - \Delta^{13}C_{(t=0)}$] between a time of interest (t) and a reference time ($t = 0$), through the following equation:

$$\Delta(\Delta^{13}C) = [(A)(B)(CO_{2(t)} + C)]/[(A + (B)(CO_{2(t)} + C)) - [(A)(B)(CO_{2(t\ =0)} + C)]/[(A + (B)(CO_{2(t=0)} + C) \quad (26)$$

where values for A, B and C are curve fitting parameters (Cui and Schubert, 2016; Schubert and Jahren, 2012). By rearranging Eqn. (27), one can therefore quantify $CO_{2(t)}$ using the following equation:

$$pCO_{2(t)} = \frac{\Delta(\Delta^{13}C)\times A^2 + \Delta(\Delta^{13}C)\times A\times B\times pCO_{2(t=0)} + 2\times\Delta(\Delta^{13}C)\times A\times B\times C + \Delta(\Delta^{13}C)\times B^2\times C\times pCO_{2(t=0)} + \Delta(\Delta^{13}C)\times B^2\times C^2 + A^2\times B\times pCO_{2(t=0)}}{A^2\times B - \Delta(\Delta^{13}C)\times A\times B - \Delta(\Delta^{13}C)\times B^2\times pCO_{2(t=0)} - \Delta(\Delta^{13}C)\times B^2\times C} \quad (27)$$

Excellent agreement between the proxy results and ice core data validated changes in $\Delta^{13}C$ value as an accurate proxy for CO_2 in the fossil record (Schubert and Jahren, 2015). Much of the application of this work has focused on the early Paleogene greenhouse and accompanying hyperthermals (Schubert and Jahren, 2013; Cui and Schubert, 2016, 2017, 2018). These studies have all revealed background CO_2 across the late Paleocene and early Eocene (prior to the EECO) less than ~3.5 times preindustrial levels (<1000 ppm), but with significantly higher levels at the hyperthermals.

6.5.2. Strengths of C3 land plant proxy

The C3 land plant proxy has the potential for wide applicability in the fossil record because it relies on measurements of the $\delta^{13}C$ value of terrestrial organic matter, an abundant and widely measured substrate that can integrate carbon contributions across a large number of plants. Notably, the proxy: (i) has been validated through comparison with ice core data (Schubert and Jahren, 2015); (ii) includes a robust uncertainty analysis for all input parameters and accounts for potential contemporaneous environmental change (Cui and Schubert, 2016); (iii) can resolve differences in carbon isotope excursion magnitude between terrestrial and marine substrates (Schubert and Jahren, 2013); (iv) provides a method for producing nearly continuous records of CO_2 at resolution sufficient for resolving early Paleogene CIEs, such as the PETM (Cui and Schubert, 2017); (v) can help identify potential sources of the CIEs (Cui and Schubert, 2018); (vi) is applicable across the entire range of Cenozoic CO_2, including the early Paleogene greenhouse (Cui and Schubert, 2016), and (vii) includes an understanding of the mechanism driving the observed increase in discrimination with increasing CO_2 that fits within the framework for carbon isotope discrimination developed by Farquhar et al. (1982; Schubert and Jahren, 2018).

6.5.3 Weakness of C3 land plant proxy

Weaknesses include: (i) potential for different responses among different plant groups (Hare et al. 2018; Porter et al., 2017); (ii) the effect of O_2 on $\Delta^{13}C$ is poorly constrained (Beerling et al., 2002; Berner et al., 2000; Porter et al., 2017), and (iii) the proxy saturates at very high CO_2, yielding positive uncertainties of >120% above 1000 ppmv (Cui and Schubert, 2016). Large uncertainties in CO_2 can be reduced if changes in other environmental parameters that are known to affect $\Delta^{13}C$ value (e.g., water availability, plant community shifts) are constrained (Cui and Schubert, 2016). The proxy also requires estimates of $\delta^{13}C_{CO2}$, which for the Paleocene and Eocene, can be calculated from the $\delta^{13}C$ value of benthic foraminifera (Tipple et al., 2010). Because the proxy is based on relative changes in $\Delta^{13}C$ value, quantitative estimates of CO_2 require either: (i) knowledge of $\Delta^{13}C$ value at a known CO_2 level (Schubert and Jahren, 2015), or (ii) independent estimates of the change in CO_2 across the two time periods of interest (i.e., $\Delta CO_2 = CO_{2(t)} - CO_{2(t=0)}$; Schubert and Jahren, 2013).

6.5.4 Recommended methodology of C3 land plant proxy

This proxy is ideal for reconstructing the wide range of CO_2 characteristic for the early Eocene and associated hyperthermals. Like many other CO_2 proxies, uncertainties increase with increasing CO_2; positive and negative errors, however, are less than ~120% and 40%, respectively, at the CO_2 levels predicted for the late Paleocene and early Eocene (Cui and Schubert, 2016).

Geosci. Model Dev. Discuss., https://doi.org/10.5194/gmd-2018-309
Manuscript under review for journal Geosci. Model Dev.
Discussion started: 17 January 2019

Choice of record is important for producing robust median CO_2 estimates because there is potential for systematic bias in the median CO_2 estimate resulting from: (i) sampling resolution, (ii) substrate type, (iii) diagenesis, and (iv) environmental change (Cui and Schubert, 2017). For example, working in sites with high mean annual precipitation may help to reduce variability in median CO_2 esitmates, as $\Delta^{13}C$ value is less responsive to changes in MAP in ever-wet sites (e.g., Diefendorf et al., 2010). Marine carbonate records, which can be used to quantify ΔCO_2, might be affected by dissolution (Cui and Schubert, 2017); changes in the $\Delta^{13}C$ value of paleosol carbonate mimic changes in the $\Delta^{13}C$ value of terrestrial organic matter, but might also be affected by diffusion of increased CO_2 into the soil and increased productivity (Schubert and Jahren, 2013). Therefore, careful consideration of the selected substrate and site is required; when information on environmental change is not available, use of multiple records might lead to better CO_2 estimates (Cui and Schubert, 2017). R code is available for calculating CO_2 using paired marine and terrestrial records across geologically brief CIEs (Cui and Schubert, 2016) and for generating high-resolution CO_2 records via Eq. (28) (Cui and Schubert, 2018).

7 DeepMIP data compilation

We have compiled data files for sea surface and land air temperatures (SST and LAT) through the late Paleocene and early Eocene (Supplementary Data Files 3–7) as the first stage of creating a DeepMIP database and to show how the methodologies outlined above can be applied to the three time slices. Once the online platform has been completed, we encourage others to add to the database, such that it becomes an indispensinble tool for Deep-time model-data comparisons and to better characterize and understand the climate of this warm, high-CO_2 time in earth history. The geographic coverage of sites with marine and terrestrial paleotemperature data is shown on early Eocene (52 Ma) paleogeographic maps (Fig. 7a, 7b). Fig. 7c illustrates how choice of plate tectonic reference frame has a significant effect on paleogeographic locations of the sites from which climate proxy data are derived (Matthews et al., 2016). Offsets in paleolatitude approach 10° in some regions. As noted previously (Lunt et al., 2017), we endorse the recommendation of van Hinsbergen et al. (2015) to use a paleomagnetic reference frame based on reconstructed polar wander paths because it can be directly related to the Earth's spin axis in preference to a mantle-based reference frame. In general, the paleomagnetic reference frame shifts Pacific sites northward and Atlantic sites southward. Because some models have already adopted a mantle-based reference frame (e.g. Herold et al., 2014), we include paleolocations derived from both reference frames in Supplementary Data File 2.

Although the number of sites for which robust proxy climate reconstructions are available continues to increase through the concerted efforts of paleoclimate research teams, the global coverage remains restricted, especially for marine proxy records of the EECO and terrestrial proxy records for the PETM and LP. For marine sites, we have compiled data for 24 LP, 27 PETM and 16 EECO sites (Fig. 7a). Best coverage is in the Atlantic but there are large tracts in the Pacific Ocean that lack data, especially in the central and northern West Pacific and the central and southern East Pacific. The Arctic Ocean remains represented by a single site. Our LAT data are mainly from terrestrial sites although several data sets are derived from marine sites, which have the added value of good chronology and accompanying data from marine proxies. Otherwise our data

compilation is hampered by poor age control for many terrestrial sites, with numerous proxy records excluded because they have a broadly defined late Paleocene-early Eocene age range. For this reason, our compilation is dominated by later early Eocene records, which we include in a broadly defined EECO time-slice comprising 41 sites, with only five PETM and nine LP sites. There are vast tracts of the planet that remain poorly represented by terrestrial proxies, especially Asia, Africa, South America and Antarctica.

Once model-data comparisons are carried out with this new dataset, we anticipate that new regions and environmental settings will be identified for new data acquisition. These will include regions where there is disagreement between models and data, between different models, or between different proxies. A particular focus may be regions where significant climate gradients are suggested either by models or data, such as the Sothern Ocean (Douglas et al., 2014). We also anticipate ongoing focus on those environmental settings judged to have greatest potential for yielding robust temperature reconstructions, such as clay-rich marine settings (e.g., Pearson et al., 2007; Frieling et al., 2017, 2018) and ancient terrestrial peat deposits (Naafs et al., 2017b).

7.1 Data organization and management

At present, we include this version 0.1 of the DeepMIP database as supplementary files to this paper (Supplementary Data Files 1 to 8), but we intend to import these and other datasets into a bespoke online database. A comprehensive data-model and data-data comparison effort requires new tooling for data organization, manipulation and management. It is critically important to provide full traceability of data sources and reproducibility of methods to produce derived data sets, both in terms of stratigraphic correlations, age-model development, and calculation of derived values from raw measurements. This effort has two main components: data organization and scientific workflow management.

We will organize data in a publicly accessible database that has a common format allowing easy data retrieval and manipulation. This database is part of the EARTHSEQUENCING project and is currently in the process of incorporating primarily data from the various ocean drilling efforts (DSDP, ODP, IODP). The specific database system chosen allows much faster access than traditional relational databases while still preserving the typical cross-table relationships that allow relating parameters, e.g., core-depths and sample identifiers to derived properties like age models. This backend system stores the relevant data and meta-data and allows programmatic and external access to data and derived properties. In order to avoid the slow-access and cumbersome retrieval of data from existing systems, where each individual measurement is stored in its own row, the EARTHSEQUENCING database stores data aggregated on a *per-Location* and *per-Analysis/Datatype* basis, with supporting structural meta-data, consistently formatted and heavily compressed. Overall this approach results in access times per hole and analysis on the order of seconds, thus allowing near real-time data retrieval and analysis. The actual data tables are flexible and can be imported from traditional text files that can be exported from all major spreadsheet applications. Where necessary, existing stacks and compilations can be imported (e.g., Zachos et al., 2008).

Whilst the database system was primarily designed for IODP data sets, it is flexible enough to incorporate data and measurements from land-based sections. The primary requirement for data input and traceability are unique measurements and sample identifiers, following existing IODP standards, i.e. each measurement requires complete information about sample depths and offsets, measurement units, and related meta-information such as site location, and publication reference where applicable. The database can also store additional information, such as biostratigraphic or paleomagnetic age constraints to facilitate easy and reproducible age model development, assigning of ages to measurements, and re-mapping between different age models. We also strongly encourage a full documentation of uncertainties in proxy records. As such, for all climate estimates in the DeepMIP database, the following will be recorded: (a) analytical uncertainty, (b) calibration uncertainty, and (c) uncertainties associated with generating mean or median values for data records within time slices. This should include separate estimates for effects such as diagenesis, dating uncertainty, the use of extinct species, seasonality effects, etc. We recognize that these additional uncertainties are subjective and hard to quantify, but they are crucially important for giving context to model-data comparisons. Calibration uncertainty includes estimation of poorly constrained parameters, especially the chemical composition ($\delta^{18}O$, Mg/Ca) of ancient seawater. New approaches are moving towards a more comprehensive treatment of uncertainty on these parameters, including Monte Carlo methods. Further work on the best practice in this area would be strongly supported within or outside of the current DeepMIP working group. Where data already exist in other databases, a URL or DOI should be provided (e.g. to data in PANGAEA). A current (but incomplete) overview of datasets already imported is available at https://paloz.marum.de.

7.2 Data management, and scientific workflow development

In addition to the database system described above, we have also designed a scientific workflow system, which allows for full reproducibility of all data manipulation steps and to allow for repeated re-analysis of derived data, such as applying alternative age models or computational steps for calculations as described earlier. Specifically, the chosen system is based on an existing open-source system (https://kepler-project.org). In this system, individual parts of a complete scientific workflow are connected through so-called Actors, where each actor performs a specific task in a sequence of steps, connected through inputs and outputs. We have augmented the Kepler system with specific Actors that implement, for example, data splicing, data correlation, data visualization, and the ability to apply domain-specific tools such as Astrochron, Meyers, 2014) or the running of arbitrary scripts in Matlab, R, Python or other scripting tools. Individual data analysis steps can then be saved as a project and re-applied by the scientific community while easily changing specific analysis parameters. These project files will be separately archived and curated, providing an easily accessible archive of DeepMIP data analysis efforts, ideally with a citable and versioned DOI reference.

8 Preliminary synthesis

Geosci. Model Dev. Discuss., https://doi.org/10.5194/gmd-2018-309
Manuscript under review for journal Geosci. Model Dev.
Discussion started: 17 January 2019

8.1 Comparisons between climate proxies and time slices

The proxies for atmospheric CO_2 exhibit considerable variability through the early Cenozoic and uncertainty is high for individual measurements, well above 100-200 ppm in most cases (Fig. 6). However, LOESS smoothing by Foster et al. (2017) produced a long-term trend that is broadly consistent with the temperature trend recorded in benthic $\delta^{18}O$, with marine-based CO_2 proxies generally above the LOESS curve and the terrestrial proxies on or below the curve. Taken together it appears that background CO_2 levels are ~500 ppm in the latest Paleocene and rise to ~1000 ppm during the EECO whereas the PETM is associated with a short-lived rise in CO_2 to ~2000–3000 ppm. Thus, we can have some confidence that our three time slices allow us to investigate two types of CO_2-modulated global warming scenarios: rapid warming associated with the PETM and longer term warming associated with the EECO. A finer determination of CO_2 during our time slices is however clearly desirable and a number of community efforts are underway to achieve this (e.g. www.p-CO2.org), including a number of new data generation efforts (www.deepmip.org/sweet/).

Preliminary illustrations of the distribution of SST and LAT data by latitude are shown in Figs. 8 and 9. These figures serve to represent the overall data coverage and the level of agreement between proxies. The data points plotted are mean or median values for samples that span the three time slices. Error bars are 95% confidence intervals unless noted otherwise. Full sample suites, analytical results, temperature determinations and summary metrics are provided in Supplementary Data Files 3–7. More detailed data-model comparisons and interrogation of sources of error and uncertainties will be the focus of future work.

As expected, the SST compilation shows that temperature estimates derived from the $\delta^{18}O$ values of recrystallized foraminifera are significantly cooler than estimates derived from the $\delta^{18}O$ of well-preserved foraminifera, foraminiferal Mg/Ca ratios, and clumped isotope values from larger benthic foraminifera (Fig. 8a). This is considered to reflect diagenetic modification of foraminiferal calcite. Estimates derived by SIMS measurements of foraminiferal $\delta^{18}O$ at central Pacific ODP Site 865 (Kozdon et al., 2011, 2013) are more in line with other proxies for the LP and PETM time slices. However, a large offset between SSTs derived from SIMS and Mg/Ca for the EECO suggests that the SIMS approach cannot always counter the effects of recrystallisation. Another large offset between SSTs derived from the $\delta^{18}O$ values in well preserved foraminifera in the New Zealand Hampden section and those derived from Mg/Ca at the same section, as well as other New Zealand sections, is harder to explain (Hollis et al., 2012; Hines et al., 2017). The sample from which the $\delta^{18}O$ measurements were obtained is slightly younger (lower Heretaungan New Zealand Stage ~49 Ma) than the other samples (upper Mangaorapan, ~50 Ma) and possibly records post-EECO cooling at this site or, alternatively, local hydrological factors at this coastal site may have affected the $\delta^{18}O$ values. A similarly large offset between the two clumped isotope records from Belgium – 29.8°C in Ampe Quarry but only 20°C in Kester borehole (Evans et al., 2018a) – is also noted. In other respects, the carbonate proxies exhibit a relatively consistent trend for all time slices: a shallow latitudinal gradient of <5°C for the Southern Hemisphere (to ~55°S) and a somewhat steeper gradient of 10–15°C in the Northern Hemisphere (to ~45°N). Carbonate proxy data are too sparse to generalize temperature differences between the time slices.

Geosci. Model Dev. Discuss., https://doi.org/10.5194/gmd-2018-309
Manuscript under review for journal Geosci. Model Dev.
Discussion started: 17 January 2019

When TEX_{86}-derived SSTs ($BAYSPAR_{SST}$ calibration) are added to the compilation (Fig. 8b), the range in SSTs increases markedly: the Southern Hemisphere gradient increases to >10°C and the Northern Hemisphere gradient increases to >15°C. There is also a distinct separation between the time slices: the PETM is ~5–10°C warmer than the LP and the EECO tends to be >5°C warmer than the LP, at least in middle–high latitudes. Interestingly, TEX_{86} values for the LP and EECO time slices overlap in low latitude sites. TEX_{86}-derived SSTs (average values) based on the BAYSPAR calibration tend to be ~5°C warmer than estimates derived from carbonate proxies at the same or proximal sites, notably in New Zealand and New Jersey. TEX_{86}-derived SSTs for low latitude sites are in better agreement with carbonate proxies, especially for the EECO.

Data coverage for land air temperature (LAT) is reasonable for high–middle southern and northern latitudes (Fig. 9) but there are only four low-latitude records, all in India. Available datasets for the PETM and LP are too locally restricted to observe any latitudinal patterns other than to note general similarities with the EECO. These EECO records exhibit a pattern similar to the SST record; in general LAT estimates are warmer in southern mid-latitudes than in northern mid-latitudes. However, there is considerable variability within estimates based on leaf physiognomy, some of which relates to the wide variety of methods employed. The nine different methods used for early Eocene leaf fossil assemblages range from LMA and CLAMP (each with multiple calibrations) to single or multiple linear regressions, and other statistical manipulations of leaf shape and size. Some methods consistently yield higher LATs than others (e.g. LMA using the Kowalski and Dilcher [2003] calibration) but there is as yet no consensus on a preferred methodology. Moreover, considerable local variability is also evident with the MBT/CBT proxy. As discussed previously, age control is poor in some terrestrial sections and some of the variability may relate to this; some sites may prove to be outside the EECO time slice.

Most of the proxies indicate that LAT ranges from ~5–10°C in high latitudes to ~25–28°C in middle and low latitudes, albeit with only four low-latitude sites to constrain the latitudinal range from 30°S to 30°N. LATs derived from paleosol or mammal $\delta^{18}O$ lie at the lower end of this range at several sites, notably Salta Basin, Argentina (Hyland et al., 2017), Wind River Basin, Wyoming (Hyland et al., 2013) and Ellesmere Island (Fricke and Wing, 2004). This suggests that these proxies may suffer from a cool bias in some circumstances. Conversely, LAT estimates from clumped isotopes are much higher than this range, which is consistent with the interpretation that they represent summer temperatures, at least in the Bighorn Basin (Snell et al., 2013). Low and middle latitude EECO records for the new brGDGT-based proxy (LAT_{PEAT}) also yield LATs significantly higher than other LAT estimates from the same region or similar latitudes (Naafs et al., 2018b). In New Zealand, a LAT_{PEAT} value of ~28°C at Otaio River contrasts with LATs of 16–20° based on NLR at nearby mid-Waipara River. In the Northern Hemisphere, a LAT_{PEAT} value of ~27°C from the Schöningen Lignite, Germany, is 2°C and 5°C warmer than the warmest LAT estimates derived by MBT'/CBT and LMA, respectively, at an equivalent latitude. These differences are within the error ranges for the proxies and this LAT_{PEAT} estimate is consistent with a LAT estimate of 28°C derived from mammal $\delta^{18}O$ from a site in the San Juan Basin, New Mexico (Fricke and Wing, 2004). It is also consistent with the summer temperatures inferred

for the Bighorn Basin (Snell et al., 2013). This agreement between proxies indicates that the LAT_{PEAT} proxy may help to resolve the long-standing issue of an apparent cool bias in other LAT proxies (Huber and Caballero, 2011; Pancost et al., 2013; Naafs et al., 2018b). Moreover, the two LAT_{PEAT} values for the EECO are within the range of SST estimates for the EECO (Fig. 9).

9 Conclusions and priorities for new data gathering

We have reviewed the primary ways in which temperature and atmospheric CO_2 may be reconstructed in the early Cenozoic. These proxies are in widely different stages of maturity, with several proxies in need of concerted effort to improve their reliability and reduce uncertainties. After considering the strengths and weaknesses of each of these climate proxies, we have provided recommendations on their future use, both in general terms and specifically in the context of the DeepMIP objective to reconstruct climate across three time slices: the latest Paleocene (LP), Paleocene-Eocene thermal maximum (PETM) and early Eocene climatic optimum (EECO). We applied these recommendations in a preliminary way to a compilation of existing sea surface and land air temperatures (SST and LAT).

We have determined that existing data coverage is very patchy and that there are considerable inconsistencies between temperature proxies. The same is true for the available CO_2 proxies. Over the past few years, researchers associated with the DeepMIP project have made great advances in recovering paleotemperature records from poorly sample regions, both in high (Frieling et al., 2014; Hollis et al, 2015; Schoon et al. 2015; Hines et al., 2017) and low latitudes (Inglis et al. 2015; Frieling et al., 2017, 2018; Cramwinckel et al., 2018; Evans et al., 2018a; Naafs et al. 2018a). Several of these studies have applied new methodologies to deep sea cores collected over 20 years ago (Hollis et al., 2015; Inglis et al. 2015; Cramwinckel et al., 2018). There is huge potential to apply new methods in $\delta^{18}O$ and Mg/Ca analysis (Kozdon et al., 2011, 2013; Evans and Müller 2012) to many other cores in our database that so far have only been analyzed by conventional $\delta^{18}O$ methods. There is also value in searching for new continental margin records in poorly sampled regions, where multi-proxy approaches to climate reconstruction can be applied (e.g. Sluijs et al., 2014; Frieling et al., 2017). For such records, the value of improving on existing calibrations for branched and isoprenoidal GDGTs (MBT–CBT and TEX_{86}) present in marine sediments cannot be underestimated as they have the potential to provide coupled SST and LAT records in well dated successions that can be compared with other proxies. For MBT–CBT, the challenges are to address the issue of calibration saturation at the upper temperature range and the effects of mixed sources of brGDGTs. For TEX_{86}, we have shown that the preferred alternative approach to BAYSPAR, TEX_{86}^{H}, is poorly formulated mathematically. It lacks a physiological basis as there is little evidence for the exponential increase in archaeal cyclopentane moieties in the upper temperature range, which is implicit in the calibration (Fig. 4a). Therefore, the challenge for TEX_{86} is to understand why BAYSPAR temperature estimates are consistently higher than other proxies in middle and high latitudes (Fig. 8b).

For terrestrial records, the major challenge is to improve age models through integrated stratigraphy – utilizing miospore biostratigraphy, carbon isotopes and magnetostratigraphy. This is a long-term objective, requiring significant taxonomic effort.

Researchers associated with the DeepMIP project have also generated several new CO_2 proxy records for the studied time intervals (Anagnostou et al., 2016; Foster et al. 2017). As with the temperature proxies, there is clearly value in finding locations where multiple CO_2 proxies can be applied to add confidence in the data generated. Work should also focus on reducing the structural uncertainty in the associated proxies (e.g., vital effects for $\delta^{11}B$).

Author contributions

CJH and TDJ compiled the text and tables; CJH prepared Figs. 1-4 and 8–9; KME, JCZ, PP, RK prepared the text on on oxygen isotopes; DA, CHL, RK and AT prepared the text on Mg/Ca ratios; DA, AT and NM prepared the text on clupbed isotopes; GNI, JT, AS, JF, MC, PKB and RDP prepared the text on TEX_{86}; BDAN and RDP prepared the text on brGDGTs and Fig. 5; EMK and UZ prepared the text on plant fossil-based temperate proxies; GLF, EA, YC, YE, DLR, BS, CW and YGZ prepared the text on CO2 proxies; GLF prepared fig. 6; HS compiled the paleolocations for all sites and prepared Fig. 7; TW and VL contributed to the text on geochronology; many of the above in addition to GRD, RS, PS, BW, MH and DL contributed to the overall text.

Competing interests

The authors declare that they have no conflict of interest.

Data availability

The data referenced in this manuscript are provided as Supplementary Data Files 1 to 8. In the final version, these files will form DeepMIP database version 0.1 and will be accessible online via a citable DOI reference.

Acknowledgements

DeepMIP is supported by the UK government through NERC grants NE/P01903X/1 and NE/N006828/1. Contributions from CJH, EMK and HS were supported by the GNS Science Global Change through Time Programme. The authors acknowledge helpful reviews of the manuscript by Erica Crouch, Sebastian Naeher (GNS Science).

References

Affek, H. P., and Zaarur, S.: Kinetic isotope effect in CO_2 degassing: insight from clumped and oxygen isotopes in laboratory precipitation experiments, Geochimica et Cosmochimica Acta, 143, 319-330, 2014.

Allen, K. A., Hönisch, B., Eggins, S. M., Haynes, L. L., Rosenthal, Y., and Yu, J.: Trace element proxies for surface ocean conditions: A synthesis of culture calibrations with planktic foraminifera, Geochimica et Cosmochimica Acta, 193, 197-221, https://doi.org/10.1016/j.gca.2016.08.015, 2016.

Anagnostou, E., John, E. H., Edgar, K. M., Foster, G. L., Ridgwell, A., Inglis, G. N., Pancost, R. D., Lunt, D. J., and Pearson, P. N.: Changing atmospheric CO_2 concentration was the primary driver of early Cenozoic climate, Nature, 533, 380-384, 10.1038/nature17423, http://www.nature.com/nature/journal/v533/n7603/abs/nature17423, 2016.

Anand, P., Elderfield, H., and Conte, M. H.: Calibration of Mg/Ca thermometry in planktonic foraminifera from a sediment trap time series, Paleoceanography, 18, 10.1029/2002PA000846, 2003.

Anand, P., and Elderfield, H.: Variability of Mg/Ca and Sr/Ca between and within the planktonic foraminifers Globigerina bulloides and Globorotalia truncatulinoides, Geochem. Geophys. Geosyst., 6, 10.1029/2004GC000811, 2005.

Aze, T., Pearson, P. N., Dickson, A. J., Badger, M. P. S., Bown, P. R., Pancost, R. D., Gibbs, S. J., Huber, B. T., Leng, M. J., Coe, A. L., Cohen, A. S., and Foster, G. L.: Extreme warming of tropical waters during the Paleocene–Eocene Thermal Maximum, Geology, 10.1130/g35637.1, 2014.

Bailey, I. W., and Sinnott, E. W.: A botanical index of Cretaceous and Tertiary climates, Science, 41, 831-834, 1915.

Bailey, I. W., and Sinnott, E. W.: The climatic distribution of certain types of angiosperm leaves, American Journal of Botany, 3, 24-39, 1916.

Baker, P. A., Gieskes, J. M., and Elderfield, H.: Diagenesis of carbonates in deep-sea sediments; evidence from Sr/Ca ratios and interstitial dissolved Sr^{2+} data, Journal of Sedimentary Research, 52, 71-82, 1982.

Barker, S., Greaves, M., and Elderfield, H.: A study of cleaning procedures used for foraminiferal Mg/Ca paleothermometry, Geochemistry Geophysics Geosystems, 4, 10.1029/2003gc000559, 2003.

Bartlein, P. J., Harrison, S. P., Brewer, S., Connor, S., Davis, B. A. S., Gajewski, K., Guiot, J., Harrison-Prentice, T. I., Henderson, A., Peyron, O., Prentice, I. C., Scholze, M., Seppä, H., Shuman, B., Sugita, S., Thompson, R. S., Viau, A. E., Williams, J., and Wu, H.: Pollen-based continental climate reconstructions at 6 and 21 ka: a global synthesis, Climate Dynamics, 37, 775-802, 10.1007/s00382-010-0904-1, 2011.

Beerling, D. J., Lake, J. A., Berner, R. A., Hickey, L. J., Taylor, D. W., and Royer, D. L.: Carbon isotope evidence implying high O_2/CO_2 ratios in the Permo-Carboniferous atmosphere, Geochimica et Cosmochimica Acta, 66, 3757-3767, https://doi.org/10.1016/S0016-7037(02)00901-8, 2002.

Beerling, D. J., Fox, A., and Anderson, C. W.: Quantitative uncertainty analyses of ancient atmospheric CO2 estimates from fossil leaves, 309, 775-787, 10.2475/09.2009.01, 2009.

Beerling, D. J., and Royer, D. L.: Convergent Cenozoic CO_2 history, Nature Geosci, 4, 418-420, 2011.

Bemis, B. E., Spero, H. J., Bijma, J., and Lea, D. W.: Reevaluation of the oxygen isotopic composition of planktonic foraminifera: Experimental results and revised paleotemperature equations, Paleoceanography, 13, 150-160, 10.1029/98PA00070, 1998.

Bendle, J. A., Weijers, J. W. H., Maslin, M. A., Sinninghe Damsté, J. S., Schouten, S., Hopmans, E. C., Boot, C. S., and Pancost, R. D.: Major changes in glacial and Holocene terrestrial temperatures and sources of organic carbon recorded in the Amazon fan by tetraether lipids, Geochem. Geophys. Geosyst., 11, Q12007, doi: 10.1029/2010gc003308, 2010.

Benthien, A., Zondervan, I., Engel, A., Hefter, J., Terbrüggen, A., and Riebesell, U.: Carbon isotopic fractionation during a mesocosm bloom experiment dominated by *Emiliania huxleyi*: Effects of CO_2 concentration and primary production, Geochimica et Cosmochimica Acta, 71, 1528-1541, 10.1016/j.gca.2006.12.015, 2007.

Bentov, S., and Erez, J.: Impact of biomineralization processes on the Mg content of foraminiferal shells: A biological perspective, Geochem. Geophys. Geosyst., 7, 10.1029/2005GC001015, 2006.

Bernasconi, S. M., Hu, B., Wacker, U., Fiebig, J., Breitenbach, S. F. M., and Rutz, T.: Background effects on Faraday collectors in gas-source mass spectrometry and implications for clumped isotope measurements, Rapid Communications in Mass Spectrometry, 27, 603-612, 10.1002/rcm.6490, 2013.

Bernasconi, S. M., Müller, I. A., Bergmann, K. D., Breitenbach, S. F. M., Fernandez, A., Hodell, D. A., Jaggi, M., Meckler, A. N., Millan, I., and Ziegler, M.: Reducing uncertainties in carbonate clumped isotope analysis through consistent carbonate-based standardization, Geochem. Geophys. Geosyst., 10.1029/2017GC007385, 2018.

Berner, R. A., Petsch, S. T., Lake, J. A., Beerling, D. J., Popp, B. N., Lane, R. S., Laws, E. A., Westley, M. B., Cassar, N., Woodward, F. I., and Quick, W. P.: Isotope fractionation and atmospheric oxygen: Implications for Phanerozoic O_2 evolution, 287, 1630-1633, 2000.

Bice, K. L., Birgel, D., Meyers, P. A., Dahl, K. A., Hinrichs, K.-U., and Norris, R. D.: A multiple proxy and model study of Cretaceous upper ocean temperatures and atmospheric CO_2 concentrations, 21, doi:10.1029/2005PA001203, 2006.

Bidigare, R. R., Fluegge, A., Freeman, K. H., Hanson, K. L., Hayes, J. M., Hollander, D., Jasper, J. P., King, L. L., Laws, E. A., Milder, J., Millero, F. J., Pancost, R., Popp, B. N., Steinberg, P. A., and Wakeham, S. G.: Consistent fractionation of ^{13}C in nature and in the laboratory: Growth-rate effects in some haptophyte algae, Global Biogeochemical Cycles, 11, 279-292, 10.1029/96GB03939, 1997.

Bijl, P. K., Schouten, S., Sluijs, A., Reichart, G.-J., Zachos, J. C., and Brinkhuis, H.: Early Palaeogene temperature evolution of the southwest Pacific Ocean, Nature, 461, 776-779, 2009.

Bijl, P. K., Houben, A. J. P., Schouten, S., Bohaty, S. M., Sluijs, A., Reichart, G.-J., Sinninghe Damsté, J. S., and Brinkhuis, H.: Transient Middle Eocene Atmospheric CO_2 and Temperature Variations, Science, 330, 819-821, 10.1126/science.1193654, 2010.

Bijl, P. K., Bendle, J. A. P., Bohaty, S. M., Pross, J., Schouten, S., Tauxe, L., Stickley, C. E., McKay, R. M., Röhl, U., Olney, M., Sluijs, A., Escutia, C., Brinkhuis, H., and Scientists, E.: Eocene cooling linked to early flow across the Tasmanian Gateway, Proceedings of the National Academy of Sciences, 110, 9645-9650, 10.1073/pnas.1220872110, 2013.

Bijma, J., Spero, H. J., and Lea, D. W.: Reassessing foraminiferal stable isotope geochemistry: Impact of the oceanic carbonate system (experimental results), in: Use of Proxies in Paleoceanography, edited by: Fischer, G., and Wefer, G., Springer Berlin Heidelberg, 489-512, 1999.

Birch, H., Coxall, H. K., Pearson, P. N., Kroon, D., and O'Regan, M.: Planktonic foraminifera stable isotopes and water column structure: Disentangling ecological signals, Marine Micropaleontology, 101, 127-145, 2013.

Blaga, C. I., Reichart, G.-J., Heiri, O., and Sinninghe Damsté, J. S.: Tetraether membrane lipid distributions in water-column particulate matter and sediments: a study of 47 European lakes along a north–south transect, Journal of Paleolimnology, 41, 523-540, 10.1007/s10933-008-9242-2, 2009.

Boller, A. J., Thomas, P. J., Cavanaugh, C. M., and Scott, K. M.: Low stable carbon isotope fractionation by coccolithophore RubisCO, Geochimica et Cosmochimica Acta, 75, 7200-7207, 10.1016/j.gca.2011.08.031, 2011.

Bolton, C. T., and Stoll, H. M.: Late Miocene threshold response of marine algae to carbon dioxide limitation, Nature, 500, 558-562, 2013.

Bolton, C. T., Hernandez-Sanchez, M. T., Fuertes, M.-A., Gonzalez-Lemos, S., Abrevaya, L., Mendez-Vicente, A., Flores, J.-A., Probert, I., Giosan, L., Johnson, J., and Stoll, H. M.: Decrease in coccolithophore calcification and CO_2 since the middle Miocene, Nature Communications, 7, 10284, 10.1038/ncomms10284, 2016.

Bonifacie, M., Calmels, D., Eiler, J. M., Horita, J., Chaduteau, C., Vasconcelos, C., Agrinier, P., Katz, A., Passey, B. H., Ferry, J. M., and Bourrand, J.-J.: Calibration of the dolomite clumped isotope thermometer from 25 to 350°C, and implications for a universal calibration for all (Ca, Mg, Fe)CO_3 carbonates, Geochimica et Cosmochimica Acta, 200, 255-279, https://doi.org/10.1016/j.gca.2016.11.028, 2017.

Bougeois, L., de Rafélis, M., Reichart, G.-J., de Nooijer, L. J., Nicollin, F., and Dupont-Nivet, G.: A high resolution study of trace elements and stable isotopes in oyster shells to estimate Central Asian Middle Eocene seasonality, Chemical Geology, 363, 200-212, https://doi.org/10.1016/j.chemgeo.2013.10.037, 2014.

Bowen, G. J., Beerling, D. J., Koch, P. L., Zachos, J. C., and Quattlebaum, T.: A humid climate state during the Palaeocene/Eocene thermal maximum, Nature, 432, 495, 10.1038/nature03115, 2004.

Boyle, E. A.: Manganese carbonate overgrowths on foraminifera tests, Geochimica et Cosmochimica Acta, 47, 1815-1819, https://doi.org/10.1016/0016-7037(83)90029-7, 1983.

Boyle, E. A., and Keigwin, L. D.: Comparison of Atlantic and Pacific paleochemical records for the last 215,000 years: changes in deep ocean circulation and chemical inventories, Earth and Planetary Science Letters, 76, 135-150, 1985.

Brassell, S. C., Eglinton, G., Marlowe, I. T., Pflaumann, U., and Sarnthein, M.: Molecular stratigraphy: a new tool for climatic assessment, Nature, 320, 129, 10.1038/320129a0, 1986.

Brassell, S. C.: Climatic influences on the Paleogene evolution of alkenones, Paleoceanography, 29, 255-272, doi:10.1002/2013PA002576, 2014.

Breecker, D. O., Sharp, Z. D., and McFadden, L. D.: Seasonal bias in the formation and stable isotopic composition of pedogenic carbonate in modern soils from central New Mexico, USA, Geological Society of America Bulletin, 121, 630-640, 2009.

Breecker, D. O., Sharp, Z. D., and McFadden, L. D.: Atmospheric CO_2 concentrations during ancient greenhouse climates were similar to those predicted for A.D. 2100, PNAS, 107, 576-580, 2010.

Breecker, D. O.: Quantifying and understanding the uncertainty of atmospheric CO_2 concentrations determined from calcic paleosols, Geochem, Geophys, Geosys, 14, 3210-3220, 2013.

Breecker, D. O., and Retallack, G. J.: Refining the pedogenic carbonate atmospheric CO_2 proxy and application to Miocene CO_2, Paleogeogr. Paleoclimatol. Paleoecol., 406, 1-8, 2014.

Brinkhuis, H., Schouten, S., Collinson, M. E., Sluijs, A., Damsté, J. S. S., Dickens, G. R., Huber, M., Cronin, T. M., Onodera, J., Takahashi, K., Bujak, J. P., Stein, R., van der Burgh, J., Eldrett, J. S., Harding, I. C., Lotter, A. F., Sangiorgi, F., Cittert, H. v. K.-v., de Leeuw, J. W., Matthiessen, J., Backman, J., Moran, K., and the Expedition, S.: Episodic fresh surface waters in the Eocene Arctic Ocean, Nature, 441, 606, 10.1038/nature04692.

Broecker, W. S.: The salinity contrast between the Atlantic and Pacific oceans during glacial time, Paleoceanography, 4, 207-212, 10.1029/PA004i002p00207, 1989.

Broecker, W., and Yu, J.: What do we know about the evolution of Mg to Ca ratios in seawater?, Paleoceanography, 26, PA3203, 10.1029/2011pa002120, 2011.

Brown, S. J., and Elderfield, H.: Variations in Mg/Ca and Sr/Ca ratios of planktonic foraminifera caused by postdepositional dissolution: Evidence of shallow Mg-dependent dissolution, Paleoceanography, 11, 543-551, 10.1029/96PA01491, 1996.

Bryan, S. P., and Marchitto, T. M.: Mg/Ca–temperature proxy in benthic foraminifera: New calibrations from the Florida Straits and a hypothesis regarding Mg/Li, Paleoceanography, 23, 10.1029/2007PA001553, 2008.

Caballero, R., and Huber, M.: State-dependent climate sensitivity in past warm climates and its implications for future climate projections, Proceedings of the National Academy of Sciences, 10.1073/pnas.1303365110, 2013.

Came, R. E., Eiler, J. M., Veizer, J., Azmy, K., Brand, U., and Weidman, C. R.: Coupling of surface temperatures and atmospheric CO_2 concentrations during the Palaeozoic era, Nature, 449, 198-201, 10.1038/nature06085, 2007.

Carmichael, M. J., Inglis, G. N., Badger, M. P. S., Naafs, B. D. A., Behrooz, L., Remmelzwaal, S., Monteiro, F. M., Rohrssen, M., Farnsworth, A., Buss, H. L., Dickson, A. J., Valdes, P. J., Lunt, D. J., and Pancost, R. D.: Hydrological and associated biogeochemical consequences of rapid global warming during the Paleocene-Eocene Thermal Maximum, Global and Planetary Change, 157, 114-138, https://doi.org/10.1016/j.gloplacha.2017.07.014, 2017.

Carpenter, R. J., Jordan, G. J., Macphail, M. K., and Hill, R. S.: Near-tropical Early Eocene terrestrial temperatures at the Australo-Antarctic margin, western Tasmania, Geology, 40, 267-270, 10.1130/G32584.1, 2012.

Casson, S., and Gray, J. E.: Influence of environmental factors on stomatal development, New Phytologist, 178, 9-23, 2008.

Cerling, T. E.: Carbon dioxide in the atmosphere: evidence from Cenozoic and Mesozoic paleosols, American Journal of Science, 291, 377-400, 1991.

Cerling, T. E.: Stable carbon isotopes in palaeosol carbonates, Special Publications of the International Association of Sedimentologists, 27, 43-60, 1999.

Church, M. J., Wai, B., Karl, D. M., and DeLong, E. F.: Abundances of crenarchaeal amoA genes and transcripts in the Pacific Ocean, Environmental Microbiology, 12, 679-688, doi:10.1111/j.1462-2920.2009.02108.x, 2010.

Coggon, R. M., Teagle, D. A. H., Smith-Duque, C. E., Alt, J. C., and Cooper, M. J.: Reconstructing Past Seawater Mg/Ca and Sr/Ca from Mid-Ocean Ridge Flank Calcium Carbonate Veins, Science, 327, 1114-1117, 10.1126/science.1182252, 2010.

Conte, M. H., and Eglinton, G.: Alkenone and alkenoate distributions within the euphotic zone of the eastern North Atlantic: correlation with production temperature, Deep Sea Research Part I: Oceanographic Research Papers, 40, 1935-1961, 10.1016/0967-0637(93)90040-A, 1993.

Conte, M. H., Thompson, A., Lesley, D., and Harris, R. P.: Genetic and Physiological Influences on the Alkenone/Alkenoate Versus Growth Temperature Relationship in *Emiliania huxleyi* and *Gephyrocapsa Oceanica*, Geochimica et Cosmochimica Acta, 62, 51-68, https://doi.org/10.1016/S0016-7037(97)00327-X, 1998.

Conte, M. H., Sicre, M.-A., Rühlemann, C., Weber, J. C., Schulte, S., Schulz-Bull, D., and Blanz, T.: Global temperature calibration of the alkenone unsaturation index (UK′37) in surface waters and comparison with surface sediments, Geochem. Geophys. Geosyst., 7, 10.1029/2005GC001054, 2006.

Costa, K. B., Toledo, F. A., Pivel, M. A., Moura, C. A., and Chemale Jr, F.: Evaluation of two genera of benthic foraminifera for down-core paleotemperature studies in the western South Atlantic, Brazilian Journal of Oceanography, 54, 75-84, 2006.

Cotton, J. M., and Sheldon, N. D.: New constraints on using paleosols to reconstruct atmospheric pCO_2, Geological Society of America Bulletin, 124, 1411-1423, 2012.

Cramer, B. S., Wright, J. D., Kent, D. V., and Aubry, M.-P.: Orbital climate forcing of $\delta^{13}C$ excursions in the late Paleocene-early Eocene (Chrons C24n-C25n), Paleoceanography, 18, 1097, doi: 1010.1029/2003PA000909, 2003.

Cramer, B. S., Toggweiler, J. R., Wright, J. D., Katz, M. E., and Miller, K. G.: Ocean overturning since the Late Cretaceous: Inferences from a new benthic foraminiferal isotope compilation, Paleoceanography, 24, PA4216, 10.1029/2008pa001683, 2009.

Cramer, B. S., Miller, K. G., Barrett, P. J., and Wright, J. D.: Late Cretaceous–Neogene trends in deep ocean temperature and continental ice volume: Reconciling records of benthic foraminiferal geochemistry ($\delta^{18}O$ and Mg/Ca) with sea level history, Journal of Geophysical Research: Oceans, 116, C12023, 10.1029/2011jc007255, 2011.

Cramwinckel, M. J., Huber, M., Kocken, I. J., Agnini, C., Bijl, P. K., Bohaty, S. M., Frieling, J., Goldner, A., Hilgen, F. J., Kip, E. L., Peterse, F., van der Ploeg, R., Röhl, U., Schouten, S., and Sluijs, A.: Synchronous tropical and polar temperature evolution in the Eocene, Nature, 559, 382-386, 10.1038/s41586-018-0272-2, 2018.

Creech, J. B., Baker, J. A., Hollis, C. J., Morgans, H. E. G., and Smith, E. G. C.: Eocene sea temperatures for the mid-latitude southwest Pacific from Mg/Ca ratios in planktonic and benthic foraminifera, Earth and planetary science letters, 299(3/4), 483-495; doi:410.1016/j.epsl.2010.1009.1039, 2010.

Cui, Y., and Schubert, B. A.: Quantifying uncertainty of past pCO_2 determined from changes in C3 plant carbon isotope fractionation, Geochimica et Cosmochimica Acta, 172, 127-138, https://doi.org/10.1016/j.gca.2015.09.032, 2016.

Cui, Y., and Schubert, B. A.: Atmospheric pCO_2 reconstructed across five early Eocene global warming events, Earth and Planetary Science Letters, 478, 225-233, https://doi.org/10.1016/j.epsl.2017.08.038, 2017.

Cui, Y., and Schubert, B. A.: Towards determination of the source and magnitude of atmospheric pCO_2 change across the early Paleogene hyperthermals, Global and Planetary Change, 170, 120-125, https://doi.org/10.1016/j.gloplacha.2018.08.011, 2018.

Daëron, M., Blamart, D., Peral, M., and Affek, H. P.: Absolute isotopic abundance ratios and the accuracy of Δ_{47} measurements, Chemical Geology, 442, 83-96, 2016.

Dallanave, E., Bachtadse, V., Agnini, C., Muttoni, G., Hollis, C. J., Hines, B. R., Morgans, H. E. G., Strong, C. P., Tauxe, L., and Crampton, J. S.: Early-middle Eocene magneto-biochronology of the Southern Pacific Ocean: new data from the South Island of New Zealand, Rendiconti Online, 31, 50-51, 2014.

Damsté, J. S. S., Kuypers, M. M. M., Pancost, R. D., and Schouten, S.: The carbon isotopic response of algae, (cyano)bacteria, archaea and higher plants to the late Cenomanian perturbation of the global carbon cycle: Insights from biomarkers in black shales from the Cape Verde Basin (DSDP Site 367), Organic Geochemistry, 39, 1703-1718, https://doi.org/10.1016/j.orggeochem.2008.01.012, 2008.

Dang, X., Yang, H., Naafs, B. D. A., Pancost, R. D., Evershed, R. P., and Xie, S.: Direct evidence of moisture control on the methylation of branched glycerol dialkyl glycerol tetraethers in semi-arid and arid soils, Geochimica et Cosmochimica Acta, 189, 24-36, doi: 10.1016/j.gca.2016.06.004, 2016.

De Jonge, C., Hopmans, E. C., Stadnitskaia, A., Rijpstra, W. I. C., Hofland, R., Tegelaar, E., and Sinninghe Damsté, J. S.: Identification of novel penta- and hexamethylated branched glycerol dialkyl glycerol tetraethers in peat using HPLC–MS^2, GC–MS and GC–SMB-MS, Organic Geochemistry, 54, 78-82, doi: 10.1016/j.orggeochem.2012.10.004, 2013.

De Jonge, C., Hopmans, E. C., Zell, C. I., Kim, J.-H., Schouten, S., and Sinninghe Damsté, J. S.: Occurrence and abundance of 6-methyl branched glycerol dialkyl glycerol tetraethers in soils: implications for palaeoclimate reconstruction, Geochimica et Cosmochimica Acta, 141, 97-112, doi: 10.1016/j.gca.2014.06.013, 2014.

de Nooijer, L. J., Hathorne, E. C., Reichart, G. J., Langer, G., and Bijma, J.: Variability in calcitic Mg/Ca and Sr/Ca ratios in clones of the benthic foraminifer Ammonia tepida, Marine Micropaleontology, 107, 32-43, https://doi.org/10.1016/j.marmicro.2014.02.002, 2014.

Defliese, W. F., Hren, M. T., and Lohmann, K. C.: Compositional and temperature effects of phosphoric acid fractionation on Δ_{47} analysis and implications for discrepant calibrations, Chemical Geology, 396, 51-60, 10.1016/j.chemgeo.2014.12.018, 2015.

Dekens, P. S., Lea, D. W., Pak, D. K., and Spero, H. J.: Core top calibration of Mg/Ca in tropical foraminifera: Refining paleotemperature estimation, 3, 1-29, doi:10.1029/2001GC000200, 2002.

Delaney, M. L., W.H., Bé, A., and Boyle, E. A.: Li, Sr, Mg, and Na in foraminiferal calcite shells from laboratory culture, sediment traps, and sediment cores, Geochimica et Cosmochimica Acta, 49, 1327-1341, https://doi.org/10.1016/0016-7037(85)90284-4, 1985.

Dennis, K. J., and Schrag, D. P.: Clumped isotope thermometry of carbonatites as an indicator of diagenetic alteration, Geochimica et Cosmochimica Acta, 74, 4110-4122, 2010.

Dennis, K. J., Affek, H. P., Passey, B. H., Schrag, D. P., and Eiler, J. M.: Defining an absolute reference frame for 'clumped' isotope studies of CO_2, Geochimica et Cosmochimica Acta, 75, 7117-7131, 2011.

D'Hondt, S., Zachos, J. C., and Schultz, G.: Stable isotopic signals and photosymbiosis in Late Paleocene planktic foraminifera, Paleobiology, 20, 391-406, doi:10.1017/S0094837300012847, 1994.

Dickens, G. R., O'Neil, J. R., Rea, D. K., and Owen, R. M.: Dissociation of oceanic methane hydrate as a cause of the carbon isotope excursion at the end of the Paleocene, Paleoceanography, 10, 965-972, 1995.

Diefendorf, A. F., Mueller, K. E., Wing, S. L., Koch, P. L., and Freeman, K. H.: Global patterns in leaf ^{13}C discrimination and implications for studies of past and future climate, Proceedings of the National Academy of Sciences, 107, 5738-5743, 10.1073/pnas.0910513107, 2010.

Dolph, G. E., and Dilcher, D. L.: Variation in leaf size with respect to climate in the tropics of the Western Hemisphere., Bulletin of the Torrey Botanical Club, 107, 154-162, 1980.

Doria, G., Royer, D. L., Wolfe, A. P., Fox, A., Westgate, J. A., and Beerling, D. J.: Declining atmospheric CO_2 during the late Middle Eocene climate transition, 311, 63-75, 10.2475/01.2011.03, 2011.

Douglas, P. M. J., Affek, H. P., Ivany, L. C., Houben, A. J. P., Sijp, W. P., Sluijs, A., Schouten, S., and Pagani, M.: Pronounced zonal heterogeneity in Eocene southern high-latitude sea surface temperatures, Proceedings of the National Academy of Sciences, 111, 6582-6587, 2014.

Dunkley Jones, T., Lunt, D. J., Schmidt, D. N., Ridgwell, A., Sluijs, A., Valdes, P. J., and Maslin, M.: Climate model and proxy data constraints on ocean warming across the Paleocene–Eocene Thermal Maximum, Earth-Science Reviews, 125, 123-145, http://dx.doi.org/10.1016/j.earscirev.2013.07.004, 2013.

Eagle, R., Risi, C., Mitchell, J. L., Eiler, J. M., Seibt, U., Neelin, J. D., Li, G., and Tripati, A. K.: High regional climate sensitivity over continental China constrained by glacial-recent changes in temperature and the hydrological cycle, Proceedings of the National Academy of Sciences, 110, 8813-8818, 2013.

Eagle, R. A., Eiler, J. M., Tripati, A. K., Ries, J. B., Freitas, P. S., Hiebenthal, C., Wanamaker Jr, A. D., Taviani, M., Elliot, M., and Marenssi, S.: The influence of temperature and seawater carbonate saturation state on ^{13}C-^{18}O bond ordering in bivalve mollusks, Biogeosciences, 10, 157-194, 2013a.

Edgar, K. M., Pälike, H., and Wilson, P. A.: Testing the impact of diagenesis on the $\delta^{18}O$ and $\delta^{13}C$ of benthic foraminiferal calcite from a sediment burial depth transect in the equatorial Pacific, Paleoceanography, 28, 468-480, 10.1002/palo.20045, 2013b.

Edgar, K. M., Anagnostou, E., Pearson, P. N., and Foster, G. L.: Assessing the impact of diagenesis on $\delta^{11}B$, $\delta^{13}C$, $\delta^{18}O$, Sr/Ca and B/Ca values in fossil planktic foraminiferal calcite, Geochimica et Cosmochimica Acta, 166, 189-209, http://dx.doi.org/10.1016/j.gca.2015.06.018, 2015.

Eggins, S., De Deckker, P., and Marshall, J.: Mg/Ca variation in planktonic foraminifera tests: implications for reconstructing palaeo-seawater temperature and habitat migration, Earth and Planetary Science Letters, 212, 291-306, https://doi.org/10.1016/S0012-821X(03)00283-8, 2003.

Eggins, S. M., Sadekov, A., and De Deckker, P.: Modulation and daily banding of Mg/Ca in Orbulina universa tests by symbiont photosynthesis and respiration: a complication for seawater thermometry?, Earth and Planetary Science Letters, 225, 411-419, https://doi.org/10.1016/j.epsl.2004.06.019, 2004.

Eiler, J., and Schauble, E.: $^{18}O^{13}C^{16}O$ in Earth's atmosphere, Geochimica et Cosmochemica Acta, 68, 4767-4777, 2004.

Eiler, J. M.: "Clumped-isotope" geochemistry-The study of naturally-occurring multiply-substituted isotopologues, Earth and Planetary Science Letters, 262, 309-327, 2007.

Elderfield, H., and Ganssen, G.: Past temperature and $\delta^{18}O$ of surface ocean waters inferred from foraminiferal Mg/Ca ratios, Nature, 405, 442, 10.1038/35013033, 2000.

Elderfield, H., Yu, J., Anand, P., Kiefer, T., and Nyland, B.: Calibrations for benthic foraminiferal Mg/Ca paleothermometry and the carbonate ion hypothesis, Earth and Planetary Science Letters, 250, 633-649, https://doi.org/10.1016/j.epsl.2006.07.041, 2006.

Elderfield, H., Greaves, M., Barker, S., Hall, I. R., Tripati, A., Ferretti, P., Crowhurst, S., Booth, L., and Daunt, C.: A record of bottom water temperature and seawater $\delta^{18}O$ for the Southern Ocean over the past 440 kyr based on Mg/Ca of benthic foraminiferal *Uvigerina* spp, Quaternary Science Reviews, 29, 160-169, https://doi.org/10.1016/j.quascirev.2009.07.013, 2010.

Eldrett, J. S., Greenwood, D. R., Harding, I. C., and Huber, M.: Increased seasonality through the Eocene to Oligocene transition in northern high latitudes, Nature, 459, 969, doi: 10.1038/nature08069, 2009.

Elling, F. J., Könneke, M., Lipp, J. S., Becker, K. W., Gagen, E. J., and Hinrichs, K.-U.: Effects of growth phase on the membrane lipid composition of the thaumarchaeon Nitrosopumilus maritimus and their implications for archaeal lipid distributions in the marine environment, Geochimica et Cosmochimica Acta, 141, 579-597, http://dx.doi.org/10.1016/j.gca.2014.07.005, 2014.

Elling, F. J., Könneke, M., Mußmann, M., Greve, A., and Hinrichs, K.-U.: Influence of temperature, pH, and salinity on membrane lipid composition and TEX_{86} of marine planktonic thaumarchaeal isolates, Geochimica et Cosmochimica Acta, 171, 238-255, https://doi.org/10.1016/j.gca.2015.09.004, 2015.

Evans, D., and Müller, W.: Deep time foraminifera Mg/Ca paleothermometry: Nonlinear correction for secular change in seawater Mg/Ca, Paleoceanography, 27, 10.1029/2012PA002315, 2012.

Evans, D., Müller, W., Oron, S., and Renema, W.: Eocene seasonality and seawater alkaline earth reconstruction using shallow-dwelling large benthic foraminifera, Earth and Planetary Science Letters, 381, 104-115, https://doi.org/10.1016/j.epsl.2013.08.035, 2013.

Evans, D., Bhatia, R., Stoll, H., and Müller, W.: LA-ICPMS Ba/Ca analyses of planktic foraminifera from the Bay of Bengal: Implications for late Pleistocene orbital control on monsoon freshwater flux, Geochem. Geophys. Geosyst., 16, 2598-2618, 10.1002/2015GC005822, 2015.

Evans, D., Brierley, C., Raymo, M. E., Erez, J., and Müller, W.: Planktic foraminifera shell chemistry response to seawater chemistry: Pliocene–Pleistocene seawater Mg/Ca, temperature and sea level change, Earth and Planetary Science Letters, 438, 139-148, https://doi.org/10.1016/j.epsl.2016.01.013, 2016a.

Evans, D., Wade, B., Henehan, M., Erez, J., and Müller, W.: Revisiting carbonate chemistry controls on planktic foraminifera Mg/Ca: implications for sea surface temperature and hydrology shifts over the Paleocene-Eocene Thermal Maximum and Eocene-Oligocene transition, Climate of the Past, 12, 819-835, doi.org/10.5194/cp-12-819-2016, 2016b.

Evans, D., Müller, W., and Erez, J.: Assessing foraminifera biomineralisation models through trace element data of cultures under variable seawater chemistry, Geochimica et Cosmochimica Acta, 236, 198-217, 10.1016/j.gca.2018.02.048, 2018.

Evans, D., Sagoo, N., Renema, W., Cotton, L. J., Müller, W., Todd, J. A., Saraswati, P. K., Stassen, P., Ziegler, M., Pearson, P. N., Valdes, P. J., and Affek, H. P.: Eocene greenhouse climate revealed by coupled clumped isotope-Mg/Ca thermometry, Proceedings of the National Academy of Sciences, 10.1073/pnas.1714744115, 2018.

Farquhar, G. D., and Sharkey, T. D.: Stomatal conductance and photosynthesis, Annual Review of Plant Physiology, 33, 317-345, 1982.

Farquhar, G. D., and Richards, R. A.: Isotopic composition of plant carbon correlates with water-use efficiency of wheat genotypes, Functional Plant Biology, 11, 539-552, 10.1071/PP9840539, 1984.

Fehrenbacher, J. S., and Martin, P. A.: Exploring the dissolution effect on the intrashell Mg/Ca variability of the planktic foraminifer Globigerinoides ruber, Paleoceanography, 29, 854-868, 10.1002/2013PA002571, 2014.

Fernandez, A., Müller, I. A., Rodríguez-Sanz, L., van Dijk, J., Looser, N., and Bernasconi, S. M.: A Reassessment of the Precision of Carbonate Clumped Isotope Measurements: Implications for Calibrations and Paleoclimate Reconstructions, 18, 4375-4386, doi:10.1002/2017GC007106, 2017.

Foster, G. L.: Seawater pH, pCO_2 and [CO_3^{2-}] variations in the Caribbean Sea over the last 130 kyr: A boron isotope and B/Ca study of planktic foraminifera, Earth Plan. Sci. Lett., 271, 254-266, doi:210.1016/j.epsl.2008.1004.1015, 2008.

Foster, G. L., Lear, C. H., and Rae, J. W. B.: The evolution of pCO_2, ice volume and climate during the middle Miocene, Earth Plan. Sci. Lett., 341-344, 243-254, 10.1016/j.epsl.2012.06.007, 2012.

Foster, G. L., and Rae, J. W. B.: Reconstructing Ocean pH with Boron Isotopes in Foraminifera, Annual Review of Earth and Planetary Sciences, 44, 207-237, 10.1146/annurev-earth-060115-012226, 2016.

Foster, G. L., Royer, D. L., and Lunt, D. J.: Future climate forcing potentially without precedent in the last 420 million years, Nature Communications, 8, 14845, 10.1038/ncomms14845, 2017.

Franks, P. J., and Royer, D. L.: Comment on "Was atmospheric CO_2 capped at 1000ppm over the past 300 million years?" by McElwain J. C. et al. [Palaeogeogr. Palaeoclimatol. Palaeoecol. 441 (2016) 653–658], Palaeogeography, Palaeoclimatology, Palaeoecology, 472, 256-259, https://doi.org/10.1016/j.palaeo.2017.01.015, 2017.

Franks, P. J., Royer, D. L., Beerling, D. J., Van de Water, P. K., Cantrill, D. J., Barbour, M. M., and Berry, J. A.: New constraints on atmospheric CO_2 concentration for the Phanerozoic, Geophys. Res. Lett., 41, 2014GL060457, 10.1002/2014gl060457, 2014.

Freeman, K. H., and Hayes, J. M.: Fractionation of carbon isotopes by phytoplankton and estimates of ancient CO2 levels, Global Biogeochemical Cycles, 6, 185-198, doi:10.1029/92GB00190, 1992.

Freeman, K. H., and Pagani, M.: Alkenone-based estimates of past CO_2 levels: A consideration of their utility based on an analysis of uncertainties, in: A history of atmospheric CO_2 and its effects on plants, animals, and ecosystems, edited by: Ehleringer, J. R., Cerling, T. E., and Dearing, M. D., Ecological Studies, Springer, New York, 2005.

Fricke, H. C., and Wing, S. L.: Oxygen isotope and paleobotanical estimates of temperature and $\delta^{18}O$–latitude gradients over North America during the early Eocene, American Journal of Science, 304, 612-635, doi: 10.2475/ajs.304.7.612, 2004.

Frieling, J., Iakovleva, A. I., Reichart, G.-J., Aleksandrova, G. N., Gnibidenko, Z. N., Schouten, S., and Sluijs, A.: Paleocene–Eocene warming and biotic response in the epicontinental West Siberian Sea, Geology, 42, 767-770, 2014.

Frieling, J., Gebhardt, H., Huber, M., Adekeye, O. A., Akande, S. O., Reichart, G.-J., Middelburg, J. J., Schouten, S., and Sluijs, A.: Extreme warmth and heat-stressed plankton in the tropics during the Paleocene-Eocene Thermal Maximum, Science Advances, 3, 10.1126/sciadv.1600891, 2017.

Frieling, J., Reichart, G. J., Middelburg, J. J., Röhl, U., Westerhold, T., Bohaty, S. M., and Sluijs, A.: Tropical Atlantic climate and ecosystem regime shifts during the Paleocene–Eocene Thermal Maximum, Clim. Past, 14, 39-55, 10.5194/cp-14-39-2018, 2018.

Frieling, J., and Sluijs, A.: Towards quantitative environmental reconstructions from ancient non-analogue microfossil assemblages: Ecological preferences of Paleocene – Eocene dinoflagellates, Earth-Science Reviews, 185, 956-973, 10.1016/j.earscirev.2018.08.014, 2018.

Frontalini, F., Coccioni, R., Catanzariti, R., Jovane, L., Savian, J., and Sprovieri, M.: The Eocene Thermal Maximum 3: Reading the environmental perturbations at Gubbio (Italy), 2016.

Garreta, V., Guiot, J., Mortier, F., Chadœuf, J., and Hély, C.: Pollen-based climate reconstruction: Calibration of the vegetation–pollen processes, Ecological Modelling, 235-236, 81-94, https://doi.org/10.1016/j.ecolmodel.2012.03.031, 2012.

Ghosh, P., Adkins, J., Affek, H., Balta, B., Guo, W., Schauble, E. A., Schrag, D., and Eiler, J. M.: ^{13}C–^{18}O bonds in carbonate minerals: A new kind of paleothermometer, Geochimica et Cosmochimica Acta, 70, 1439-1456, https://doi.org/10.1016/j.gca.2005.11.014, 2006.

Goericke, R., and Fry, B.: Variations of marine plankton $\delta^{13}C$ with latitude, temperature, and dissolved CO_2 in the world ocean, Global Biogeochemical Cycles, 8, 85-90, 10.1029/93GB03272, 1994.

Gradstein, F. M., Ogg, J. G., Schmitz, M., and Ogg, G.: The geologic time scale, Elsevier, Amsterdam, 1176 pp., 2012.

Grauel, A.-L., Schmid, T. W., Hu, B., Bergami, C., Capotondi, L., Zhou, L., and Bernasconi, S. M.: Calibration and application of the 'clumped isotope' thermometer to foraminifera for high-resolution climate reconstructions, Geochimica et Cosmochimica Acta, 2013.

Gray, W. R., Weldeab, S., Lea, D. W., Rosenthal, Y., Gruber, N., Donner, B., and Fischer, G.: The effects of temperature, salinity, and the carbonate system on Mg/Ca in *Globigerinoides ruber* (White): A global sediment trap calibration, Earth and Planetary Science Letters, 482, 607-620, https://doi.org/10.1016/j.epsl.2017.11.026, 2018.

Green, W. A.: Loosening the clamp: an exploratory graphical approach to the climate leaf analysis multivariate program, Palaeontologia Electronica, 9, 9A (17 p.), 2006.

Greenop, R., Hain, M. P., Sosdian, S. M., Oliver, K. I. C., Goodwin, P., Chalk, T. B., Lear, C. H., Wilson, P. A., and Foster, G. L.: A record of Neogene seawater $\delta^{11}B$ reconstructed from paired $\delta^{11}B$ analyses on benthic and planktic foraminifera, Clim. Past, 13, 149-170, 10.5194/cp-13-149-2017, 2017.

Greenwood, D. R., Moss, P., Rowett, A., Vadala, A. J., and Keefe, R.: Plant communities and climate change in southeastern Australia during the early Paleogene, in: Causes and Consequences of Globally Warm Climates in the Early Paleogene, edited by: Wing, S., Gingerich, P., Schmitz, B., and Thomas, E., Geological Society of America Special Paper, Boulder, Colorado, 365-390, 2003.

Greenwood, D. R., Wilf, P., Wing, S. L., and Christophel, D. C.: Paleotemperature estimates using Leaf-Margin Analysis: Is Australia different?, Palaios, 19, 129-142, 2004.

Greenwood, D. R., Archibald, S. B., Mathewes, R. W., and Moss, P. T.: Fossil biotas from the Okanagan Highlands, southern British Columbia and northeastern Washington State: climates and ecosystems across an Eocene landscape, Canadian Journal of Earth Sciences, 42, 167-185, doi:10.1139/e04-100, 2005.

Greenwood, D. R.: Fossil angiosperm leaves and climate: from Wolfe and Dilcher to Burnham and Wilf, Courier Forschungsinstitut Senckenberg, 258, 95-108, 2007.

Griffiths, N., Müller, W., Johnson, K. G., and Aguilera, O. A.: Evaluation of the effect of diagenetic cements on element/Ca ratios in aragonitic Early Miocene (~16Ma) Caribbean corals: Implications for 'deep-time' palaeo-environmental reconstructions, Palaeogeography, Palaeoclimatology, Palaeoecology, 369, 185-200, https://doi.org/10.1016/j.palaeo.2012.10.018, 2013.

Grimm, G. W., and Denk, T.: Reliability and resolution of the coexistence approach — A revalidation using modern-day data, Review of Palaeobotany and Palynology, 172, 33-47, 10.1016/j.revpalbo.2012.01.006, 2012.

Grimm, G. W., Bouchal, J. M., Denk, T., and Potts, A.: Fables and foibles: A critical analysis of the Palaeoflora database and the Coexistence Approach for palaeoclimate reconstruction, Review of Palaeobotany and Palynology, 233, 216-235, 10.1016/j.revpalbo.2016.07.001, 2016.

Gutjahr, M., Ridgwell, A., Sexton, P. F., Anagnostou, E., Pearson, P. N., Pälike, H., Norris, R. D., Thomas, E., and Foster, G. L.: Very large release of mostly volcanic carbon during the Palaeocene–Eocene Thermal Maximum, Nature, 548, 573-577, 10.1038/nature23646, 2017.

Hare, V. J., Loftus, E., Jeffrey, A., and Ramsey, C. B.: Atmospheric CO_2 effect on stable carbon isotope composition of terrestrial fossil archives, Nature Communications, 9, 252, 10.1038/s41467-017-02691-x, 2018.

Hasiuk, F. J., and Lohmann, K. C.: Application of calcite Mg partitioning functions to the reconstruction of paleocean Mg/Ca, Geochimica et Cosmochimica Acta, 74, 6751-6763, https://doi.org/10.1016/j.gca.2010.07.030, 2010.

Hathorne, E. C., Alard, O., James, R. H., and Rogers, N. W.: Determination of intratest variability of trace elements in foraminifera by laser ablation inductively coupled plasma-mass spectrometry, Geochem. Geophys. Geosyst., 4, 10.1029/2003GC000539, 2003.

He, B., Olack, G. A., and Colman, A. S.: Pressure baseline correction and high-precision CO2 clumped-isotope (Δ_{47}) measurements in bellows and micro-volume modes, Rapid Communications in Mass Spectrometry, 26, 2837-2853, 2012.

Henderiks, J., and Pagani, M.: Refining ancient carbon dioxide estimates: Significance of coccolithophore cell size for alkenone-based pCO_2 records, Paleoceanography, 22, PA3202, doi:10.1029/2006PA001399, 2007.

Henehan, M. J., Rae, J. W. B., Foster, G. L., Erez, J., Prentice, K. C., Kucera, M., Bostock, H. C., Martinez-Boti, M. A., Milton, J. A., Wilson, P. A., Marshall, B. J., and Elliott, T.: Calibration of the boron isotope proxy in the planktonic foraminifera *Globigerinoides ruber* for use in palaeo-CO_2 reconstruction, Earth Plan. Sci. Lett., 364, 111-122, 10.1016/j.epsl.2012.12.029, 2013.

Henehan, M. J., Foster, G. L., Bostock, H. C., Greenop, R., Marshall, B. J., and Wilson, P. A.: A new boron isotope-pH calibration for Orbulina universa, with implications for understanding and accounting for 'vital effects', Earth and Planetary Science Letters, 454, 282-292, http://dx.doi.org/10.1016/j.epsl.2016.09.024, 2016.

Henkes, G. A., Passey, B. H., Wanamaker, A. D., Grossman, E. L., Ambrose, W. G., and Carroll, M. L.: Carbonate clumped isotope compositions of modern marine mollusk and brachiopod shells, Geochimica et Cosmochimica Acta, 2013.

Henkes, G. A., Passey, B. H., Grossman, E. L., Shenton, B. J., Pérez-Huerta, A., and Yancey, T. E.: Temperature limits for preservation of primary calcite clumped isotope paleotemperatures, Geochimica et Cosmochimica Acta, 139, 362-382, 10.1016/j.gca.2014.04.040, 2014.

Herfort, L., Schouten, S., Boon, J. P., and Sinninghe Damsté, J. S.: Application of the TEX_{86} temperature proxy to the southern North Sea, Organic Geochemistry, 37, 1715-1726, 2006.

Herold, N., Buzan, J., Seton, M., Goldner, A., Green, J. A. M., Müller, R. D., Markwick, P., and Huber, M.: A suite of early Eocene (~55 Ma) climate model boundary conditions, Geosci. Model Dev., 7, 2077-2090, 10.5194/gmd-7-2077-2014, 2014.

Hill, P. S., Tripati, A. K., and Schauble, E. A.: Theoretical constraints on the effects of pH, salinity, and temperature on clumped isotope signatures of dissolved inorganic carbon species and precipitating carbonate minerals, Geochimica et Cosmochimica Acta, 125, 610-652, https://doi.org/10.1016/j.gca.2013.06.018, 2014.

Hines, B. R., Hollis, C. J., Atkins, C. B., Baker, J. A., Morgans, H. E. G., and Strong, C. P.: Reduction of oceanic temperature gradients in the early Eocene Southwest Pacific Ocean, Palaeogeography, Palaeoclimatology, Palaeoecology, 475, 41-54, https://doi.org/10.1016/j.palaeo.2017.02.037, 2017.

Hincke, A. J. C., Broere, T., Kürschner, W. M., Donders, T. H., and Wagner-Cremer, F.: Multi-Year Leaf-Level Response to Sub-Ambient and Elevated Experimental CO2 in Betula nana, PLOS ONE, 11, e0157400, 10.1371/journal.pone.0157400, 2016.

Hinojosa, L. F., and Villagran, C.: Did South American mixed paleofloras evolve under thermal equability or in the absence of an effective Andean barrier during the Cenozoic?, Palaeogeography, Palaeoclimatology, Palaeoecology 217, 1-23, 2005.

Hinojosa, L. F., Pesce, O., Yabe, A., Uemura, K., and Nishida, H.: Physiognomical analysis and paleoclimate of the Ligorio Márquez fossil flora, Ligorio Márquez Formation, 46º45' S, Chile, in: Post-Cretaceous Floristic Changes in Southern Patagonia, Chile, edited by: Nishida, H., Chuo University, Tokyo, 45-55, 2006.

Ho, S. L., and Laepple, T.: Flat meridional temperature gradient in the early Eocene in the subsurface rather than surface ocean, Nature Geosci, 9, 606, 10.1038/ngeo2763, 2016.

Hoins, M., Van de Waal, D. B., Eberlein, T., Reichart, G.-J., Rost, B., and Sluijs, A.: Stable carbon isotope fractionation of organic cyst-forming dinoflagellates: Evaluating the potential for a CO_2 proxy, Geochimica et Cosmochimica Acta, 160, 267-276, https://doi.org/10.1016/j.gca.2015.04.001, 2015.

Hoins, M., Eberlein, T., Groβmann, C. H., Brandenburg, K., Reichart, G.-J., Rost, B., Sluijs, A., and Van de Waal, D. B.: Combined effects of ocean acidification and light or nitrogen availabilities on ^{13}C fractionation in marine dinoflagellates, PLOS ONE, 11, e0154370, 10.1371/journal.pone.0154370, 2016a.

Hoins, M., Eberlein, T., Van de Waal, D. B., Sluijs, A., Reichart, G.-J., and Rost, B.: CO_2-dependent carbon isotope fractionation in dinoflagellates relates to their inorganic carbon fluxes, Journal of Experimental Marine Biology and Ecology, 481, 9-14, 10.1016/j.jembe.2016.04.001, 2016b.

Hollis, C. J., Handley, L., Crouch, E. M., Morgans, H. E. G., Baker, J. A., Creech, J., Collins, K. S., Gibbs, S. J., Huber, M., Schouten, S., Zachos, J. C., and Pancost, R. D.: Tropical sea temperatures in the high-latitude South Pacific during the Eocene, Geology, 37, 99-102, 10.1130/g25200a.1, 2009.

Hollis, C. J., Taylor, K. W. R., Handley, L., Pancost, R. D., Huber, M., Creech, J. B., Hines, B. R., Crouch, E. M., Morgans, H. E. G., Crampton, J. S., Gibbs, S., Pearson, P. N., and Zachos, J. C.: Early Paleogene temperature history of the Southwest Pacific Ocean: Reconciling proxies and models, Earth and Planetary Science Letters, 349–350, 53-66, http://dx.doi.org/10.1016/j.epsl.2012.06.024, 2012.

Hollis, C. J., Hines, B. R., Littler, K., Villasante-Marcos, V., Kulhanek, D. K., Strong, C. P., Zachos, J. C., Eggins, S. M., Nothcote, L., and Phillips, A.: The Paleocene-Eocene Thermal Maximum at DSDP Site 277, Campbell Plateau, southern Pacific Ocean, Climate of the Past, 11, 1009-1025, doi:1010.5194/cp-1011-1009-2015, 10.5194/cp-11-1009-2015, 2015.

Holtz, L.-M., Wolf-Gladrow, D., and Thoms, S.: Numerical cell model investigating cellular carbon fluxes in *Emiliania huxleyi*, Journal of Theoretical Biology, 364, 305-315, 10.1016/j.jtbi.2014.08.040, 2015.

Holtz, L.-M., Wolf-Gladrow, D., and Thoms, S.: Stable carbon isotope signals in particulate organic and inorganic carbon of coccolithophores – A numerical model study for *Emiliania huxleyi*, Journal of Theoretical Biology, 420, 117-127, 10.1016/j.jtbi.2017.01.030, 2017.

Hönisch, B., Bijma, J., Russell, A. D., Spero, H. J., Palmer, M. R., Zeebe, R. E., and Eisenhauer, A.: The influence of symbiont photosynthesis on the boron isotopic composition of foraminifera shells, Marine Micropaleontology, 49, 87-96, 10.1016/S0377-8398(03)00030-6, 2003.

Hönisch, B., Hemming, N. G., Archer, D., Siddall, M., and McManus, J. F.: Atmospheric carbon dioxide concentration across the Mid-Pleistocene transition, Science, 324, 1551-1554, 10.1126/science.1171477, 2009.

Hönisch, B., Ridgwell, A., Schmidt, D. N., Thomas, E., Gibbs, S. J., Sluijs, A., Zeebe, R., Kump, L., Martindale, R. C., Greene, S. E., Kiessling, W., Ries, J., Zachos, J. C., Royer, D. L., Barker, S., Marchitto, T. M., Moyer, R., Pelejero, C., Ziveri, P., Foster, G. L., and Williams, B.: The geological record of ocean acidification, Science, 335, 1058-1063, 10.1126/science.1208277, 2012.

Hönisch, B., Allen, K. A., Lea, D. W., Spero, H. J., Eggins, S. M., Arbuszewski, J., deMenocal, P., Rosenthal, Y., Russell, A. D., and Elderfield, H.: The influence of salinity on Mg/Ca in planktic foraminifers – Evidence from cultures, core-top sediments and complementary $\delta^{18}O$, Geochimica et Cosmochimica Acta, 121, 196-213, https://doi.org/10.1016/j.gca.2013.07.028, 2013.

Hopmans, E. C., Schouten, S., Pancost, R. D., van der Meer, M. T. J., and Sinninghe Damsté, J. S.: Analysis of intact tetraether lipids in archaeal cell material and sediments by high performance liquid chromatography/atmospheric pressure chemical ionization mass spectrometry, Rapid Communications in Mass Spectrometry, 14, 585-589, doi:10.1002/(SICI)1097-0231(20000415)14:7<585::AID-RCM913>3.0.CO;2-N, 2000.

Hopmans, E. C., Weijers, J. W. H., Schefuss, E., Herfort, L., Sinninghe Damsté, J. S., and Schouten, S.: A novel proxy for terrestrial organic matter in sediments based on branched and isoprenoid tetraether lipids, Earth and Planetary Science Letters, 224, 107-116, 2004.

Hopmans, E. C., Schouten, S., and Sinninghe Damsté, J. S.: The effect of improved chromatography on GDGT-based palaeoproxies, Organic Geochemistry, 93, 1-6, https://doi.org/10.1016/j.orggeochem.2015.12.006, 2016.

Horita, J., Zimmermann, H., and Holland, H. D.: Chemical evolution of seawater during the Phanerozoic: Implications from the record of marine evaporites, Geochimica et Cosmochimica Acta, 66, 3733-3756, 2002.

Huber, M., and Caballero, R.: The early Eocene equable climate problem revisited, Climate of the Past, 7, 603-633, doi:10.5194/cp-7-603-2011, 2011.

Huguet, C., Schimmelmann, A., Thunell, R., Lourens, L. J., Sinninghe Damsté, J. S., and Schouten, S.: A study of the TEX_{86} paleothermometer in the water column and sediments of the Santa Barbara Basin, California, Paleoceanography, 22, PA3203, 10.1029/2006PA001310, 2007.

Huguet, A., Fosse, C., Laggoun-Défarge, F., Delarue, F., and Derenne, S.: Effects of a short-term experimental microclimate warming on the abundance and distribution of branched GDGTs in a French peatland, Geochimica et Cosmochimica Acta, 105, 294-315, doi: 10.1016/j.gca.2012.11.037, 2013.

Huguet, A., Francez, A.-J., Jusselme, M. D., Fosse, C., and Derenne, S.: A climatic chamber experiment to test the short term effect of increasing temperature on branched GDGT distribution in *Sphagnum* peat, Organic Geochemistry, 73, 109-112, doi: 10.1016/j.orggeochem.2014.05.010, 2014.

Huntington, K. W., Eiler, J. M., Affek, H. P., Guo, W., Bonifacie, M., Yeung, L. Y., Thiagarajan, N., Passey, B., Tripati, A., and Daëron, M.: Methods and limitations of 'clumped' CO_2 isotope (Δ^{47}) analysis by gas-source isotope ratio mass spectrometry, Journal of Mass Spectrometry, 44, 1318-1329, 2009.

Hurley, S. J., Elling, F. J., Könneke, M., Buchwald, C., Wankel, S. D., Santoro, A. E., Lipp, J. S., Hinrichs, K.-U., and Pearson, A.: Influence of ammonia oxidation rate on thaumarchaeal lipid composition and the TEX_{86} temperature proxy, Proceedings of the National Academy of Sciences, 113, 7762-7767, 10.1073/pnas.1518534113, 2016.

Hyland, E., Sheldon, N. D., and Fan, M.: Terrestrial paleoenvironmental reconstructions indicate transient peak warming during the early Eocene climatic optimum, Geological Society of America Bulletin, 125, 1338-1348, doi: 10.1130/B30761.1, 2013.

Hyland, E. G., and Sheldon, N. D.: Coupled CO_2-climate response during the Early Eocene Climatic Optimum, Palaeogeography, Palaeoclimatology, Palaeoecology, 369, 125-135, doi: 10.1016/j.palaeo.2012.10.011, 2013.

Hyland, E. G., Sheldon, N. D., and Cotton, J. M.: Constraining the early Eocene climatic optimum: A terrestrial interhemispheric comparison, Geological Society of America Bulletin, 129, 244-252, doi: 10.1130/B31493.1, 2017.

Inglis, G. N., Farnsworth, A., Lunt, D., Foster, G. L., Hollis, C. J., Pagani, M., Jardine, P. E., Pearson, P. N., Markwick, P., Galsworthy, A. M. J., Raynham, L., Taylor, K. W. R., and Pancost, R. D.: Descent toward the Icehouse: Eocene sea surface cooling inferred from GDGT distributions, Paleoceanography, 30, 1000-1020, 10.1002/2014pa002723, 2015.

Inglis, G. N., Collinson, M. E., Riegel, W., Wilde, V., Farnsworth, A., Lunt, D. J., Valdes, P., Robson, B. E., Scott, A. C., Lenz, O. K., Naafs, B. D. A., and Pancost, R. D.: Mid-latitude continental temperatures through the early Eocene in western Europe, Earth and Planetary Science Letters, 460, 86-96, doi: 10.1016/j.epsl.2016.12.009, 2017.

IPCC: The Physical Science Basis. Working Group I Contribution to the IPCC Fifth Assessment Report of the Intergovernmental Panel on Climate Change. IPCC Fifth Assessment Report., 2013.

Jacques, F. M. B., Su, T., Spicer, R. A., Xing, Y., Huang, Y., Wang, W., and Zhou, Z.: Leaf physiognomy and climate: Are monsoon climates different?, Global and Planetary Change, 76, 56–62, 2011.

Jagniecki, E. A., Lowenstein, T. K., Jenkins, D. M., and Demicco, R. V.: Eocene atmospheric CO_2 from the nahcolite proxy, Geology, 43, 1075-1078, 10.1130/G36886.1, 2015.

Jaramillo, C., and Cárdenas, A.: Global Warming and Neotropical Rainforests: A Historical Perspective, Annual Review of Earth and Planetary Sciences, 41, 741-766, 10.1146/annurev-earth-042711-105403, 2013.

Jasper, J. P., Hayes, J. M., Mix, A. C., and Prahl, F. G.: Photosynthetic fractionation of ^{13}C and concentrations of dissolved CO_2 in the central equatorial Pacific during the last 255,000 years, Paleoceanography, 9, 781-798, 10.1029/94PA02116, 1994.

John, C. M., Bohaty, S. M., Zachos, J. C., Sluijs, A., Gibbs, S., Brinkhuis, H., and Bralower, T. J.: North American continental margin records of the Paleocene-Eocene thermal maximum: Implications for global carbon and hydrological cycling, Paleoceanography, 23, 10.1029/2007pa001465, 2008.

John, E. H., Pearson, P. N., Coxall, H. K., Birch, H., Wade, B. S., and Foster, G. L.: Warm ocean processes and carbon cycling in the Eocene, Philosophical Transactions of the Royal Society A: Mathematical, Physical and Engineering Sciences, 371, 2013.

Keating-Bitonti, C. R., Ivany, L. C., Affek, H. P., Douglas, P., and Samson, S. D.: Warm, not super-hot, temperatures in the early Eocene subtropics, Geology, 39, 771-774, 10.1130/g32054.1, 2011.

Kele, S., Breitenbach, S. F. M., Capezzuoli, E., Meckler, A. N., Ziegler, M., Millan, I. M., Kluge, T., Deák, J., Hanselmann, K., John, C. M., Yan, H., Liu, Z., and Bernasconi, S. M.: Temperature dependence of oxygen- and clumped isotope fractionation in carbonates: A study of travertines and tufas in the 6–95°C temperature range, Geochimica et Cosmochimica Acta, 168, 172-192, https://doi.org/10.1016/j.gca.2015.06.032, 2015.

Kelson, J. R., Huntington, K. W., Schauer, A. J., Saenger, C., and Lechler, A. R.: Toward a universal carbonate clumped isotope calibration: Diverse synthesis and preparatory methods suggest a single temperature relationship, Geochimica et Cosmochimica Acta, 197, 104-131, 10.1016/j.gca.2016.10.010, 2017.

Kennedy, E. M., Arens, N. C., Reichgelt, T., Spicer, R. A., Spicer, T. E. V., Stranks, L., and Yang, J.: Deriving temperature estimates from Southern Hemisphere leaves, Palaeogeography, Palaeoclimatology, Palaeoecology, 412, 80-90, http://dx.doi.org/10.1016/j.palaeo.2014.07.015, 2014.

Kershaw, A. P., and Nix, H. A.: Quantitative palaeoclimatic estimates from pollen data usigf bioclimatic profiles of extant taxa., Journal of Biogeography, 15, 589–602, 1988.

Khan, M. A., Spicer, R. A., Bera, S., Ghosh, R., Yang, J., Spicer, T. E. V., Guo, S.-x., Su, T., Jacques, F., and Grote, P. J.: Miocene to Pleistocene floras and climate of the Eastern Himalayan Siwaliks, and new palaeoelevation estimates for the Namling–Oiyug Basin, Tibet, Global and Planetary Change, 113, 1-10, http://dx.doi.org/10.1016/j.gloplacha.2013.12.003, 2014.

Kim, S.-T., and O'Neil, J. R.: Equilibrium and nonequilibrium oxygen isotope effects in synthetic carbonates, Geochimica et Cosmochimica Acta, 61, 3461-3475, http://dx.doi.org/10.1016/S0016-7037(97)00169-5, 1997.

Kim, J.-H., Schouten, S., Hopmans, E. C., Donner, B., and Sinninghe Damsté, J. S.: Global sediment core-top calibration of the TEX_{86} paleothermometer in the ocean, Geochimica et Cosmochimica Acta, 72, 1154-1173, 2008.

Kim, J.-H., van der Meer, J., Schouten, S., Helmke, P., Willmott, V., Sangiorgi, F., Koç, N., Hopmans, E. C., and Sinninghe Damsté, J. S.: New indices and calibrations derived from the distribution of crenarchaeal isoprenoid tetraether lipids: Implications for past sea surface temperature reconstructions, Geochimica et Cosmochimica Acta, 74, 4639-4654, 2010.

Kim, J.-H., Schouten, S., Rodrigo-Gámiz, M., Rampen, S., Marino, G., Huguet, C., Helmke, P., Buscail, R., Hopmans, E. C., and Pross, J.: Influence of deep-water derived isoprenoid tetraether lipids on the paleothermometer in the Mediterranean Sea, Geochimica et Cosmochimica Acta, 150, 125-141, 2015.

Kirtland Turner, S., Sexton, P. F., Charles, C. D., and Norris, R. D.: Persistence of carbon release events through the peak of early Eocene global warmth, Nature Geosci, 7, 748-751, 10.1038/ngeo2240, 2014.

Kısakürek, B., Eisenhauer, A., Böhm, F., Garbe-Schönberg, D., and Erez, J.: Controls on shell Mg/Ca and Sr/Ca in cultured planktonic foraminiferan, Globigerinoides ruber (white), Earth and Planetary Science Letters, 273, 260-269, https://doi.org/10.1016/j.epsl.2008.06.026, 2008.

Kluge, T., John, C. M., Jourdan, A.-L., Davis, S., and Crawshaw, J.: Laboratory calibration of the calcium carbonate clumped isotope thermometer in the 25–250°C temperature range, Geochimica et Cosmochimica Acta, 157, 213-227, https://doi.org/10.1016/j.gca.2015.02.028, 2015.

Koch, P. L., Zachos, J. C., and Gingerich, P. D.: Correlation between isotope records in marine and continental carbon reservoirs near the Palaeocene/Eocene boundary, Nature, 358, 319, 10.1038/358319a0, 1992.

Konrad, W., Roth-Nebelsick, A., and Grein, M.: Modelling of stomatal density response to atmospheric CO_2, Journal of Theoretical Biology, 253, 638-658, 2008.

Konrad, W., Katul, G., Roth-Nebelsick, A., and Grein, M.: A reduced order model to analytically infer atmospheric CO_2 concentration from stomatal and climate data, Advances in Water Resources, 104, 145-157, 2017.

Kowalczyk, J. B., Royer, D. L., Miller, I. M., Anderson, C. W., Beerling, D. J., Franks, P. J., Grein, M., Konrad, W., Roth-Nebelsick, A., Bowring, S. A., Johnson, K. R., and Ramezani, J.: Multiple proxy estimates of atmospheric CO_2 from an early Paleocene rainforest, 0, doi:10.1029/2018PA003356, 2018.

Kowalski, E. A., and Dilcher, D. L.: Warmer paleotemperatures for terrestrial ecosystems, Proceedings of the National Academy of Sciences of the United States of America, 100, 167-170, 2003.

Kozdon, R., Kelly, D. C., Kita, N. T., Fournelle, J. H., and Valley, J. W.: Planktonic foraminiferal oxygen isotope analysis by ion microprobe technique suggests warm tropical sea surface temperatures during the Early Paleogene, Paleoceanography, 26, PA3206, 10.1029/2010PA002056, 2011.

Kozdon, R., Kelly, D. C., Kitajima, K., Strickland, A., Fournelle, J. H., and Valley, J. W.: In situ $\delta^{18}O$ and Mg/Ca analyses of diagenetic and planktic foraminiferal calcite preserved in a deep-sea record of the Paleocene-Eocene thermal maximum, Paleoceanography, 28, 517-528, 10.1002/palo.20048, 2013.

Lake, J. A., Woodward, F. I., and Quick, W. P.: Long-distance CO_2 signalling in plants, Journal of Experimental Botany, 53, 183-193, 2002.

Lauretano, V., Littler, K., Polling, M., Zachos, J. C., and Lourens, L. J.: Frequency, magnitude and character of hyperthermal events at the onset of the Early Eocene Climatic Optimum, Clim. Past, 11, 1313-1324, 10.5194/cp-11-1313-2015, 2015.

Lauretano, V., Zachos, J. C., and Lourens, L. J.: Orbitally Paced Carbon and Deep-Sea Temperature Changes at the Peak of the Early Eocene Climatic Optimum, Paleoceanography and Paleoclimatology, 33, 1-16, doi:10.1029/2018PA003422, 2018.

Laws, E. A., Popp, B. N., Bidigare, R. R., Kennicutt, M. C., and Macko, S. A.: Dependence of phytoplankton carbon isotopic composition on growth rate and $[CO_2]_{aq}$ Theoretical considerations and experimental results, Geochimica et Cosmochimica Acta, 59, 1131-1138, 10.1016/0016-7037(95)00030-4, 1995.

Lazartigues, A. V., Sirois, P., and Savard, D.: LA-ICP-MS Analysis of Small Samples: Carbonate Reference Materials and Larval Fish Otoliths, Geostandards and Geoanalytical Research, 38, 225-240, 10.1111/j.1751-908X.2013.00248.x, 2014.

Lea, D. W., Mashiotta, T. A., and Spero, H. J.: Controls on magnesium and strontium uptake in planktonic foraminifera determined by live culturing, Geochimica Et Cosmochimica Acta, 63, 2369-2379, http://dx.doi.org/10.1016/S0016-7037(99)00197-0, 1999.

Lear, C. H., Elderfield, H., and Wilson, P.: Cenozoic deep-sea temperatures and global ice volumes from Mg/Ca in benthic foraminiferal calcite, Science, 287, 269-272, 2000.

Lear, C. H., Rosenthal, Y., and Slowey, N.: Benthic foraminiferal Mg/Ca-paleothermometry: a revised core-top calibration, Geochimica et Cosmochimica Acta, 66, 3375-3387, https://doi.org/10.1016/S0016-7037(02)00941-9, 2002.

Lear, C. H., Mawbey, E. M., and Rosenthal, Y.: Cenozoic benthic foraminiferal Mg/Ca and Li/Ca records: Toward unlocking temperatures and saturation states, Paleoceanography, 25, n/a-n/a, 10.1029/2009PA001880, 2010.

Lear, C. H., Coxall, H. K., Foster, G. L., Lunt, D. J., Mawbey, E. M., Rosenthal, Y., Sosdian, S. M., Thomas, E., and Wilson, P. A.: Neogene ice volume and ocean temperatures: Insights from infaunal foraminiferal Mg/Ca paleothermometry, Paleoceanography, 30, 1437-1454, 10.1002/2015PA002833, 2015.

LeGrande, A. N., and Schmidt, G. A.: Global gridded data set of the oxygen isotopic composition in seawater, Geophysical Research Letters, 33, doi:10.1029/2006GL026011, 2006.

Lemarchand, D., Gaillardet, J., Lewin, E., and Allegre, C. J.: The influence of rivers on marine boron isotopes and implications for reconstructing past ocean pH, Nature, 408, 951-954, 2000.

Lemarchand, D., Gaillardet, J., Lewin, É., and Allègre, C. J.: Boron isotope systematics in large rivers: implications for the marine boron budget and paleo-pH reconstruction over the Cenozoic, Chemical Geology, 190, 123-140, http://dx.doi.org/10.1016/S0009-2541(02)00114-6, 2002.

Li, C., Peng, P. a., Sheng, G., Fu, J., and Yan, Y.: A molecular and isotopic geochemical study of Meso- to Neoproterozoic (1.73–0.85 Ga) sediments from the Jixian section, Yanshan Basin, North China, Precambrian Research, 125, 337-356, https://doi.org/10.1016/S0301-9268(03)00111-6, 2003.

Littler, K., Röhl, U., Westerhold, T., and Zachos, J. C.: A high-resolution benthic stable-isotope record for the South Atlantic: Implications for orbital-scale changes in Late Paleocene–Early Eocene climate and carbon cycling, Earth and Planetary Science Letters, 401, 18-30, https://doi.org/10.1016/j.epsl.2014.05.054, 2014.

Lourens, L. J., Sluijs, A., Kroon, D., Zachos, J. C., Thomas, E., Rohl, U., Bowles, J., and Raffi, I.: Astronomical pacing of late Palaeocene to early Eocene global warming events, Nature (London), 435, 1083-1087, 2005.

Lowenstein, T. K., and Demicco, R. V.: Elevated Eocene atmospheric CO_2 and its subsequent decline, Science, 313, 1928-1928, 10.1126/science.1129555, 2006.

Loyd, S. J., Sample, J., Tripati, R. E., Defliese, W. F., Brooks, K., Hovland, M., Torres, M., Marlow, J., Hancock, L. G., Martin, R., Lyons, T., and Tripati, A. E.: Methane seep carbonates yield clumped isotope signatures out of equilibrium with formation temperatures, Nature Communications, 7, 12274, 10.1038/ncomms12274, 2016.

Luciani, V., Dickens, G. R., Backman, J., Fornaciari, E., Giusberti, L., Agnini, C., and D'Onofrio, R.: Major perturbations in the global carbon cycle and photosymbiont-bearing planktic foraminifera during the early Eocene, Clim. Past, 12, 981-1007, 10.5194/cp-12-981-2016, 2016.

Luciani, V., D'Onofrio, R., Dickens, G. R., and Wade, B. S.: Planktic foraminiferal response to early Eocene carbon cycle perturbations in the southeast Atlantic Ocean (ODP Site 1263), Global and Planetary Change, 158, 119-133, https://doi.org/10.1016/j.gloplacha.2017.09.007, 2017.

Lunt, D. J., Dunkley Jones, T., Heinemann, M., Huber, M., LeGrande, A., Winguth, A., Loptson, C., Marotzke, J., Tindall, J., Valdes, P., and Winguth, C.: A model-data comparison for a multi-model ensemble of early Eocene atmosphere-ocean simulations: EoMIP, Clim. Past Discuss., 8, 1229-1273, 10.5194/cpd-8-1229-2012, 2012.

Lunt, D. J., Huber, M., Anagnostou, E., Baatsen, M. L. J., Caballero, R., DeConto, R., Dijkstra, H. A., Donnadieu, Y., Evans, D., Feng, R., Foster, G. L., Gasson, E., von der Heydt, A. S., Hollis, C. J., Inglis, G. N., Jones, S. M., Kiehl, J., Kirtland Turner, S., Korty, R. L., Kozdon, R., Krishnan, S., Ladant, J. B., Langebroek, P., Lear, C. H., LeGrande, A. N., Littler, K., Markwick, P., Otto-Bliesner, B., Pearson, P., Poulsen, C. J., Salzmann, U., Shields, C., Snell, K., Stärz, M., Super, J., Tabor, C., Tierney, J. E., Tourte, G. J. L., Tripati, A., Upchurch, G. R., Wade, B. S., Wing, S. L., Winguth, A. M. E., Wright, N. M., Zachos, J. C., and Zeebe, R. E.: The DeepMIP contribution to PMIP4: experimental design for model simulations of the EECO, PETM, and pre-PETM (version 1.0), Geosci. Model Dev., 10, 889-901, 10.5194/gmd-10-889-2017, 2017.

Lynch-Stieglitz, J., Curry, W. B., and Slowey, N.: A geostrophic transport estimate for the Florida Current from the oxygen isotope composition of benthic foraminifera, Paleoceanography, 14, 360-373, 1999.

Mackensen, A.: On the use of benthic foraminiferal $\delta^{13}C$ in palaeoceanography: constraints from primary proxy relationships, Geological Society, London, Special Publications, 303, 121-133, 2008.

MacRae, R. A., Fensome, R. A., and Williams, G. L.: Fossil dinoflagellate diversity, originations, and extinctions and their significance, Canadian Journal of Botany, 74, 1687-1694, 10.1139/b96-205, 1996.

Makarova, M., Wright, J. D., Miller, K. G., Babila, T. L., Rosenthal, Y., and Park, J. I.: Hydrographic and ecologic implications of foraminiferal stable isotopic response across the U.S. mid-Atlantic continental shelf during the Paleocene-Eocene Thermal Maximum, Paleoceanography, 32, 56-73, doi:10.1002/2016PA002985, 2017.

Martinez-Boti, M. A., Foster, G. L., Chalk, T. B., Rohling, E. J., Sexton, P. F., Lunt, D. J., Pancost, R. D., Badger, M. P. S., and Schmidt, D. N.: Plio-Pleistocene climate sensitivity evaluated using high-resolution CO_2 records, Nature, 518, 49-54, 10.1038/nature14145, 2015.

Matthews, K., Maloney, K., Zahirovic, S., Williams, S., Seton, M., and Müller, D.: Global plate boundary evolution and kinematics since the late Paleozoic, 2016.

Mawbey, E. M., and Lear, C. H.: Carbon cycle feedbacks during the Oligocene-Miocene transient glaciation, Geology, 41, 963-966, 10.1130/G34422.1, 2013.

Maxbauer, D. P., Royer, D. L., and LePage, B. A.: High Arctic forests during the middle Eocene supported by moderate levels of atmospheric CO_2, Geology, 42, 1027-1030, 10.1130/G36014.1, 2014.

McClelland, H. L. O., Bruggeman, J., Hermoso, M., and Rickaby, R. E. M.: The origin of carbon isotope vital effects in coccolith calcite, Nature Communications, 8, 1-16, 2017.

McCorkle, D. C., Bernhard, J. M., Hintz, C. J., Blanks, J. K., Chandler, G. T., and Shaw, T. J.: The carbon and oxygen stable isotopic composition of cultured benthic foraminifera, Geological Society, London, Special Publications, 303, 135-154, 2008.

McElwain, J. C., and Chaloner, W. G.: Stomatal density and index of fossil plants track atmospheric carbon dioxide in the Palaeozoic, Annals of Botany, 76, 389-395, 1995.

McElwain, J. C., Montañez, I., White, J. D., Wilson, J. P., and Yiotis, C.: Was atmospheric CO_2 capped at 1000ppm over the past 300 million years?, Palaeogeography, Palaeoclimatology, Palaeoecology, 441, 653-658, https://doi.org/10.1016/j.palaeo.2015.10.017, 2016a.

McElwain, J. C., Yiotis, C., and Lawson, T.: Using modern plant trait relationships between observed and theoretical maximum stomatal conductance and vein density to examine patterns of plant macroevolution, The New phytologist, 209, 94-103, 10.1111/nph.13579, 2016b.

McElwain, J. C., Montañez, I. P., White, J. D., Wilson, J. P., and Yiotis, C.: Reply to comment on "Was atmospheric CO_2 capped at 1000ppm over the past 300 million years?" [Palaeogeogr. Palaeoclimatol. Palaeoecol. 441 (2016) 653–658], Palaeogeography, Palaeoclimatology, Palaeoecology, 472, 260-263, https://doi.org/10.1016/j.palaeo.2017.01.020, 2017.

McInerney, F. A., and Wing, S. L.: The Paleocene-Eocene Thermal Maximum: A Perturbation of Carbon Cycle, Climate, and Biosphere with Implications for the Future, Annual Review of Earth and Planetary Sciences, 39, 489-516, doi:10.1146/annurev-earth-040610-133431, 2011.

Meckler, A. N., Ziegler, M., Millán, M. I., Breitenbach, S. F. M., and Bernasconi, S. M.: Long-term performance of the Kiel carbonate device with a new correction scheme for clumped isotope measurements, Rapid Communications in Mass Spectrometry, 28, 1705-1715, 2014.

Menges, J., Huguet, C., Alcañiz, J. M., Fietz, S., Sachse, D., and Rosell-Melé, A.: Influence of water availability in the distributions of branched glycerol dialkyl glycerol tetraether in soils of the Iberian Peninsula, Biogeosciences, 11, 2571-2581, doi: 10.5194/bg-11-2571-2014, 2014.

Meyers, S. R.: Astrochron: An R Package for Astrochronology., https://cran.r-project.org/package=astrochron, 2014.

Miller, K. G., Fairbanks, R. G., and Mountain, G. S.: Tertiary oxygen isotope synthesis, sea level history, and continental margin erosion, Paleoceanography, 2, 1-19, 1987.

Miller, K. G., Kominz, M. A., Browning, J. V., Wright, J. D., Mountain, G. S., Katz, M. E., Sugarman, P. J., Cramer, B. S., Christie-Blick, N., and Pekar, S. F.: The Phanerozoic Record of Global Sea-Level Change, Science, 310, 1293-1298, 10.1126/science.1116412, 2005.

Miller, I. M., Brandon, M. T., and Hickey, L. J.: Using leaf margin analysis to estimate the mid-Cretaceous (Albian) paleolatitude of the Baja BC block., Earth and Planetary Science Letters, 245, 95-114, 2006.

Miller, K. G., Mountain, G. S., Wright, J. D., and Browning, J. V.: A 180-million-year record of sea level and ice volume variations from continental margin and deep-sea isotopic records, Oceanography, 24, 40-53, http://dx.doi.org/10.5670/oceanog.2011.26., 2011.

Montañez, I. P.: Modern soil system constraints on reconstructing deep-time atmospheric CO_2, Geochim. Cosmochim. Acta, 101, 57-75, 2013.

Montañez, I. P., McElwain, J. C., Poulsen, C. J., White, J. D., DiMichele, William A., Wilson, J. P., Griggs, G., and Hren, M. T.: Climate, pCO_2 and terrestrial carbon cycle linkages during late Palaeozoic glacial–interglacial cycles, Nature Geosci, 9, 824, 10.1038/ngeo2822, 2016.

Mosbrugger, V., and Utescher, T.: The coexistence approach — a method for quantitative reconstructions of Tertiary terrestrial palaeoclimate data using plant fossils, Palaeogeography, Palaeoclimatology, Palaeoecology, 134, 61-86, https://doi.org/10.1016/S0031-0182(96)00154-X, 1997.

Muller, W., Shelley, M., Miller, P., and Broude, S.: Initial performance metrics of a new custom-designed ArF excimer LA-ICPMS system coupled to a two-volume laser-ablation cell, Journal of Analytical Atomic Spectrometry, 24, 10.1039/B805995K, 2009.

Müller, I. A., Fernandez, A., Radke, J., Dijk, J., Bowen, D., Schwieters, J., and Bernasconi, S. M.: Carbonate clumped isotope analyses with the long-integration dual-inlet (LIDI) workflow: scratching at the lower sample weight boundaries, Rapid Communications in Mass Spectrometry, 31, 1057-1066, 10.1002/rcm.7878, 2017.

Naafs, B. D. A., Castro, J. M., De Gea, G. A., Quijano, M. L., Schmidt, D. N., and Pancost, R. D.: Gradual and sustained carbon dioxide release during Aptian Oceanic Anoxic Event 1a, Nature Geosci, 9, 135, 10.1038/ngeo2627, 2016.

Naafs, B. D. A., and Pancost, R. D.: Sea-surface temperature evolution across Aptian Oceanic Anoxic Event 1a, Geology, 44, 959-962, 10.1130/G38575.1, 2016.

Naafs, B. D. A., Gallego-Sala, A. V., Inglis, G. N., and Pancost, R. D.: Refining the global branched glycerol dialkyl glycerol tetraethers (brGDGTs) soil temperature calibration, Organic Geochemistry, accepted, 2017a.

Naafs, B. D. A., Inglis, G. N., Zheng, Y., Amesbury, M. J., Biester, H., Bindler, R., Blewett, J., Burrows, M. A., del Castillo Torres, D., Chambers, F. M., Cohen, A. D., Evershed, R. P., Feakins, S. J., Gałka, M., Gallego-Sala, A., Gandois, L., Gray, D. M., Hatcher, P. G., Honorio Coronado, E. N., Hughes, P. D. M., Huguet, A., Könönen, M., Laggoun-Défarge,

F., Lähteenoja, O., Lamentowicz, M., Marchant, R., McClymont, E., Pontevedra-Pombal, X., Ponton, C., Pourmand, A., Rizzuti, A. M., Rochefort, L., Schellekens, J., De Vleeschouwer, F., and Pancost, R. D.: Introducing global peat-specific temperature and pH calibrations based on brGDGT bacterial lipids, Geochimica et Cosmochimica Acta, 208, 285-301, doi: 10.1016/j.gca.2017.01.038, 2017b.

Naafs, B. D. A., Rohrssen, M., Inglis, G. N., Lähteenoja, O., Feakins, S. J., Collinson, M. E., Kennedy, E. M., Singh, P. K., Singh, M. P., Lunt, D. J., and Pancost, R. D.: High temperatures in the terrestrial mid-latitudes during the early Palaeogene, Nature Geosci, 11, 766-771, 10.1038/s41561-018-0199-0, 2018a.

Naafs, B. D. A., McCormick, D., Inglis, G. N., and Pancost, R. D.: Archaeal and bacterial H-GDGTs are abundant in peat and their relative abundance is positively correlated with temperature, Geochimica et Cosmochimica Acta, 227, 156-170, doi: 10.1016/j.gca.2018.02.025, 2018b.

Naeher, S., Niemann, H., Peterse, F., Smittenberg, R. H., Zigah, P. K., and Schubert, C. J.: Tracing the methane cycle with lipid biomarkers in Lake Rotsee (Switzerland), Organic Geochemistry, 66, 174-181, https://doi.org/10.1016/j.orggeochem.2013.11.002, 2014.

Nicolo, M. J., Dickens, G. R., and Hollis, C. J.: South Pacific intermediate water oxygen depletion at the onset of the Paleocene-Eocene thermal maximum as depicted in New Zealand margin sections, Paleoceanography, 25, PA4210, doi:4210.1029/2009PA001904, 2010.

Nunes, F., and Norris, R. D.: Abrupt reversal in ocean overturning during the Palaeocene/Eocene warm period, Nature (London), 439, 60-63, 2006.

O'Brien, C. L., Robinson, S. A., Pancost, R. D., Sinninghe Damsté, J. S., Schouten, S., Lunt, D. J., Alsenz, H., Bornemann, A., Bottini, C., Brassell, S. C., Farnsworth, A., Forster, A., Huber, B. T., Inglis, G. N., Jenkyns, H. C., Linnert, C., Littler, K., Markwick, P., McAnena, A., Mutterlose, J., Naafs, B. D. A., Püttmann, W., Sluijs, A., van Helmond, N. A. G. M., Vellekoop, J., Wagner, T., and Wrobel, N. E.: Cretaceous sea-surface temperature evolution: Constraints from TEX_{86} and planktonic foraminiferal oxygen isotopes, Earth-Science Reviews, 172, 224-247, https://doi.org/10.1016/j.earscirev.2017.07.012, 2017.

Pagani, M.: The alkenone-CO_2 proxy and ancient atmospheric carbon dioxide, Philosophical Transactions of the Royal Society A: Mathematical, Physical and Engineering Sciences, 360, 609-632, 2002.

Pagani, M., Zachos, J. C., Freeman, K. H., Tipple, B., and Bohaty, S.: Marked decline in atmospheric carbon dioxide concentrations during the Paleogene, Science, 309, 600-603, 10.1126/science.1110063, 2005.

Pagani, M., Pedentchouk, N., Huber, M., Sluijs, A., Schouten, S., Brinkhuis, H., Sinninghe Damsté, J. S., Dickens, G. R., and Expedition, S.: Arctic hydrology during global warming at the Palaeocene/Eocene thermal maximum, Nature, 442, 671-675, http://www.nature.com/nature/journal/v442/n7103/suppinfo/nature05043_S1.html, 2006.

Pagani, M., Huber, M., Liu, Z., Bohaty, S. M., Henderiks, J., Sijp, W., Krishnan, S., and DeConto, R. M.: The Role of Carbon Dioxide During the Onset of Antarctic Glaciation, Science, 334, 1261-1264, 10.1126/science.1203909, 2011.

Pagani, M.: 12.13 Biomarker-based inferences of past climate: The alkenone pCO_2 proxy, in: Treatise on Geochemistry, edited by: Holland, H. D., and Turekian, K. K., Elsevier, Oxford, 361-378, 2014.

PALAEOSENS Project Members: Making sense of palaeoclimate sensitivity, Nature, 491, 683, 10.1038/nature11574, 2012.

Pälike, H., Lyle, M. W., Nishi, H., Raffi, I., Ridgwell, A., Gamage, K., Klaus, A., Acton, G., Anderson, L., Backman, J., Baldauf, J., Beltran, C., Bohaty, S. M., BownPaul, Busch, W., Channell, J. E. T., Chun, C. O. J., Delaney, M., Dewangan, P., Dunkley Jones, T., Edgar, K. M., Evans, H., Fitch, P., Foster, G. L., Gussone, N., Hasegawa, H., Hathorne, E. C., Hayashi, H., Herrle, J. O., Holbourn, A., Hovan, S., Hyeong, K., Iijima, K., Ito, T., Kamikuri, S.-i., Kimoto, K., Kuroda, J., Leon-Rodriguez, L., Malinverno, A., Moore Jr, T. C., Murphy, B. H., Murphy, D. P., Nakamura, H., Ogane, K., Ohneiser, C., Richter, C., Robinson, R., Rohling, E. J., Romero, O., Sawada, K., Scher, H., Schneider, L., Sluijs, A., Takata, H., Tian, J., Tsujimoto, A., Wade, B. S., Westerhold, T., Wilkens, R., Williams, T., Wilson, P. A., Yamamoto, Y., Yamamoto, S., Yamazaki, T., and Zeebe, R. E.: A Cenozoic record of the equatorial Pacific carbonate compensation depth, Nature, 488, 609-614, 10.1038/nature11360, 2012.

Pancost, R. D., Hopmans, E. C., and Sinninghe Damsté, J. S.: Archaeal lipids in Mediterranean cold seeps: molecular proxies for anaerobic methane oxidation, Geochimica et Cosmochimica Acta, 65, 1611-1627, https://doi.org/10.1016/S0016-7037(00)00562-7, 2001.

Pancost, R. D., Taylor, K. W. R., Inglis, G. N., Kennedy, E. M., Handley, L., Hollis, C. J., Crouch, E. M., Pross, J. r., Huber, M., Schouten, S., Pearson, P. N., Morgans, H. E. G., and Raine, J. I.: Early Paleogene evolution of terrestrial climate in the SW Pacific, Southern New Zealand, Geochem. Geophys. Geosyst., 14, 5413-5429, doi: 10.1002/2013GC004935, 2013.

Passey, B. H., Levin, N. E., Cerling, T. E., Brown, F. H., and Eiler, J. M.: High-temperature environments of human evolution in East Africa based on bond ordering in paleosol carbonates, PNAS, 107, 11245-11249, 2010.

Passey, B. H., and Henkes, G. A.: Carbonate clumped isotope bond reordering and geospeedometry, Earth and Planetary Science Letters, 351-352, 223-236, 10.1016/j.epsl.2012.07.021, 2012.

Pearson, P. N., and Palmer, M. R.: Middle Eocene seawater pH and atmospheric carbon dioxide concentrations, Science, 284, 1824-1826, 10.1126/science.284.5421.1824, 1999.

Pearson, P. N., and Palmer, M. R.: Atmospheric carbon dioxide concentrations over the past 60 million years, Nature, 406, 695-699, 2000.

Pearson, P. N., Ditchfield, P. W., Singano, J., Harcourt-Brown, K. G., Nicholas, C. J., Olsson, R. K., Shackleton, N. J., and Hall, M. A.: Warm tropical sea surface temperatures in the Late Cretaceous and Eocene epochs, Nature, 413, 481-487, http://www.nature.com/nature/journal/v413/n6855/suppinfo/413481a0_S1.html, 2001.

Pearson, P. N., Nicholas, C. J., Singano, J. M., Bown, P. R., Coxall, H. K., van Dongen, B. E., Huber, B. T., Karega, A., Lees, J. A., Msaky, E., Pancost, R. D., Pearson, M., and Roberts, A. P.: Paleogene and cretaceous sediment cores from the Kilwa and Lindi areas of coastal Tanzania: Tanzania Drilling Project Sites 1-5, Journal of African Earth Sciences, 39, 25-62, 10.1016/j.jafrearsci.2004.05.001, 2004.

Pearson, P. N., van Dongen, B. E., Nicholas, C. J., Pancost, R. D., Schouten, S., Singano, J. M., and Wade, B. S.: Stable warm tropical climate through the Eocene Epoch, Geology, 35, 211-214, 10.1130/g23175a.1, 2007.

Pearson, P. N., and Burgess, C. E.: Foraminifer test preservation and diagenesis: comparison of high latitude Eocene sites, Geological Society, London, Special Publications, 303, 59-72, 10.1144/sp303.5, 2008.

Pearson, P. N., Foster, G. L., and Wade, B. S.: Atmospheric carbon dioxide through the Eocene-Oligocene climate transition, Nature, 461, 1110-1113, 2009.

Pearson, P. N.: Oxygen Isotopes in Foraminifera: Overview and Historical Review, in: Reconstructing Earth's Deep Time Climate - The State of the Art in 2012, edited by: Ivany, L. C., and Huber, B. T., The Paleontological Society Papers, 1-38, 2012.

Pena, L. D., Cacho, I., Calvo, E., Pelejero, C., Eggins, S., and Sadekov, A.: Characterization of contaminant phases in foraminifera carbonates by electron microprobe mapping, Geochem. Geophys. Geosyst., 9, n/a-n/a, 10.1029/2008GC002018, 2008.

Penman, D. E., Hönisch, B., Zeebe, R. E., Thomas, E., and Zachos, J. C.: Rapid and sustained surface ocean acidification during the Paleocene-Eocene Thermal Maximum, Paleoceanography, 29, 2014PA002621, 10.1002/2014pa002621, 2014.

Peppe, D. J., Royer, D. L., Cariglino, B., Oliver, S. Y., Newman, S., Leight, E., Enikolopov, G., Fernandez-Burgos, M., Herrera, F., Adams, J. M., Correa, E., Currano, E. D., Erickson, J. M., Hinojosa, L. F., Hoganson, J. W., Iglesias, A., Jaramillo, C. A., Johnson, K. R., Jordan, G. J., Kraft, N. J. B., Lovelock, E. C., Lusk, C. H., Niinemets, Ü., Peñuelas, J., Rapson, G., Wing, S. L., and Wright, I. J.: Sensitivity of leaf size and shape to climate: global patterns and paleoclimatic applications, New Phytologist, 190, 724-739, 10.1111/j.1469-8137.2010.03615.x, 2011.

Peterse, F., van der Meer, J., Schouten, S., Weijers, J. W. H., Fierer, N., Jackson, R. B., Kim, J.-H., and Sinninghe Damsté, J. S.: Revised calibration of the MBT–CBT paleotemperature proxy based on branched tetraether membrane lipids in surface soils, Geochimica et Cosmochimica Acta, 96, 215-229, http://dx.doi.org/10.1016/j.gca.2012.08.011, 2012.

Pitcher, A., Rychlik, N., Hopmans, E. C., Spieck, E., Rijpstra, W. I. C., Ossebaar, J., Schouten, S., Wagner, M., and Sinninghe Damsté, J. S.: Crenarchaeol dominates the membrane lipids of *Candidatus Nitrososphaera gargensis*, a thermophilic Group I.1b Archaeon, The Isme Journal, 4, 542, 10.1038/ismej.2009.138, 2009.

Popp, B. N., Takigiku, R., Hayes, J. M., Louda, J. W., and Baker, E. W.: The post-Paleozoic chronology and mechanism of ^{13}C depletion in primary marine organic matter, 289, 436-454, 10.2475/ajs.289.4.436, 1989.

Popp, B. N., Laws, E. A., Bidigare, R. R., Dore, J. E., Hanson, K. L., and Wakeham, S. G.: Effect of Phytoplankton Cell Geometry on Carbon Isotopic Fractionation, Geochimica et Cosmochimica Acta, 62, 69-77, doi:10.1016/s0016-7037(97)00333-5, 1998.

Porter, A. S., Yiotis, C., Montañez, I. P., and McElwain, J. C.: Evolutionary differences in $\Delta^{13}C$ detected between spore and seed bearing plants following exposure to a range of atmospheric O_2:CO_2 ratios; implications for paleoatmosphere reconstruction, Geochimica et Cosmochimica Acta, 213, 517-533, https://doi.org/10.1016/j.gca.2017.07.007, 2017.

Pound, M. J., and Salzmann, U.: Heterogeneity in global vegetation and terrestrial climate change during the late Eocene to early Oligocene transition, Scientific Reports, 7, 43386, 10.1038/srep43386, https://www.nature.com/articles/srep43386#supplementary-information, 2017.

Povey, D. A. R., Spicer, R. A., and England, P. C.: Palaeobotanical investigation of early tertiary palaeoelevations in northeastern Nevada: initial results, Review of Palaeobotany and Palynology, 81, 1-10, http://dx.doi.org/10.1016/0034-6667(94)90122-8, 1994.

Pross, J., Klotz, S., and Mosbrugger, V.: Reconstructing palaeotemperatures for the early and middle Pleistocene using the mutual climatic range method based on plant fossils, Quaternary Science Reviews, 19, 1785-1799, 2000.

Pross, J., Contreras, L., Bijl, P. K., Greenwood, D. R., Bohaty, S. M., Schouten, S., Bendle, J. A., Rohl, U., Tauxe, L., Raine, J. I., Huck, C. E., van de Flierdt, T., Jamieson, S. S. R., Stickley, C. E., van de Schootbrugge, B., Escutia, C., and Brinkhuis, H.: Persistent near-tropical warmth on the Antarctic continent during the early Eocene epoch, Nature, 488, 73-77, doi: 10.1038/nature11300, 2012.

Qin, W., Carlson, L. T., Armbrust, E. V., Devol, A. H., Moffett, J. W., Stahl, D. A., and Ingalls, A. E.: Confounding effects of oxygen and temperature on the TEX_{86} signature of marine Thaumarchaeota, Proceedings of the National Academy of Sciences, 112, 10979-10984, 2015.

Rablen, S., Affek, H., Tripati, A., Defliese, W., and Freedman, P.: Advances in 'clumped isotope' measurement techniques using the Nu Perspective IS and Nu Carb Carbonate Preparation Unit, Goldschmidt Conference, 2015,

Raitzsch, M., and Hönisch, B.: Cenozoic boron isotope variations in benthic foraminifers, Geology, 41, 591-594, 10.1130/g34031.1, 2013.

Rau, G. H., Takahashi, T., and Des Marais, D. J.: Latitudinal variations in plankton $\delta^{13}C$: Implications for CO_2 and productivity in past oceans, Nature, 341, 516-518, 1989.

Rau, G. H., Riebesell, U., and Wolf-Gladrow, D.: A model of photosynthetic ^{13}C fractionation by marine phytoplankton based on diffusive molecular CO_2 uptake, Marine Ecology Progress Series, 133, 275-285, 1996.

Raven, J. A., and Hurd, C. L.: Ecophysiology of photosynthesis in macroalgae, Photosynthesis Research, 113, 105-125, 10.1007/s11120-012-9768-z, 2012.

Raven, J. A., and Beardall, J.: CO_2 concentrating mechanisms and environmental change, Aquatic Botany, 118, 24-37, 10.1016/j.aquabot.2014.05.008, 2014.

Regenberg, M., Steph, S., Nürnberg, D., Tiedemann, R., and Garbe-Schönberg, D.: Calibrating Mg/Ca ratios of multiple planktonic foraminiferal species with δ18O-calcification temperatures: Paleothermometry for the upper water column, Earth and Planetary Science Letters, 278, 324-336, https://doi.org/10.1016/j.epsl.2008.12.019, 2009.

Regenberg, M., Regenberg, A., Garbe-Schönberg, D., and Lea, D. W.: Global dissolution effects on planktonic foraminiferal Mg/Ca ratios controlled by the calcite-saturation state of bottom waters, Paleoceanography, 29, 127-142, 10.1002/2013PA002492, 2014.

Richey, J. D., Upchurch, G. R., Montañez, I. P., Lomax, B. H., Suarez, M. B., Crout, N. M. J., Joeckel, R. M., Ludvigson, G. A., and Smith, J. J.: Changes in CO2 during Ocean Anoxic Event 1d indicate similarities to other carbon cycle perturbations, Earth and Planetary Science Letters, 491, 172-182, https://doi.org/10.1016/j.epsl.2018.03.035, 2018.

Ridgwell, A.: A Mid Mesozoic Revolution in the regulation of ocean chemistry, Mar Geol, 217, 339-357, 10.1016/j.margeo.2004.10.036, 2005.

Ridgwell, A., and Zeebe, R. E.: The role of the global carbonate cycle in the regulation and evolution of the Earth system, Earth Plan. Sci. Lett., 234, 299-315, 10.1016/j.epsl.2005.03.006, 2005.

Riebesell, U., Revill, A. T., Holdsworth, D. G., and Volkman, J. K.: The effects of varying CO_2 concentration on lipid composition and carbon isotope fractionation in *Emiliania huxleyi*, Geochimica et Cosmochimica Acta, 64, 4179-4192, 10.1016/S0016-7037(00)00474-9, 2000.

Ries, J.: Effect of ambient Mg/Ca ratio on Mg fractionation in calcareous marine invertebrates: A record of the oceanic Mg/Ca ratio over the Phanerozoic, Geology, 32, 981-984, 10.1130/G20851.1, 2004.

Roberts, C. D., LeGrande, A. N., and Tripati, A. K.: Sensitivity of seawater oxygen isotopes to climatic and tectonic boundary conditions in an early Paleogene simulation with GISS ModelE-R, Paleoceanography, 26, PA4203, 10.1029/2010pa002025, 2011.

Rohling, E. J.: Oxygen isotope composition of seawater, Encyclopedia of Quaternary Science, 2, 915-922, 2013.

Roij, L., Sluijs, A., Laks, J. J., and Reichart, G.-J.: Stable carbon isotope analyses of nanogram quantities of particulate organic carbon (pollen) with laser ablation nano combustion gas chromatography/isotope ratio mass spectrometry, Rapid Communications in Mass Spectrometry, 31, 47-58, 10.1002/rcm.7769, 2016.

Rollion-Bard, C., and Erez, J.: Intra-shell boron isotope ratios in the symbiont-bearing benthic foraminiferan Amphistegina lobifera: Implications for $\delta^{11}B$ vital effects and paleo-pH reconstructions, Geochimica et Cosmochimica Acta, 74, 1530-1536, http://dx.doi.org/10.1016/j.gca.2009.11.017, 2010.

Rosenthal, Y., Boyle, E. A., and Slowey, N.: Temperature control on the incorporation of magnesium, strontium, fluorine, and cadmium into benthic foraminiferal shells from Little Bahama Bank: Prospects for thermocline paleoceanography, Geochimica et Cosmochimica Acta, 61, 3633-3643, https://doi.org/10.1016/S0016-7037(97)00181-6, 1997.

Rosenthal, Y., and Lohmann, G. P.: Accurate estimation of sea surface temperatures using dissolution-corrected calibrations for Mg/Ca paleothermometry, Paleoceanography, 17, 16-11-16-16, 10.1029/2001PA000749, 2002.

Rosenthal, Y., Lear, C. H., Oppo, D. W., and Linsley, B. K.: Temperature and carbonate ion effects on Mg/Ca and Sr/Ca ratios in benthic foraminifera: Aragonitic species Hoeglundina elegans, Paleoceanography, 21, 10.1029/2005PA001158, 2006.

Roth-Nebelsick, A., Utescher, T., Mosbrugger, V., Diester-Haass, L., and Walther, H.: Changes in atmospheric CO2 concentrations and climate from the Late Eocene to Early Miocene: palaeobotanical reconstruction based on fossil floras from Saxony, Germany, Palaeogeography, Palaeoclimatology, Palaeoecology, 205, 43-67, https://doi.org/10.1016/j.palaeo.2003.11.014, 2004.

Royer, D. L.: Stomatal density and stomatal index as indicators of paleoatmospheric CO_2 concentration, Review of Palaeobotany and Palynology, 114, 1-28, 2001.

Royer, D. L., Berner, R. A., and Beerling, D. J.: Phanerozoic atmospheric CO_2 change: evaluating geochemical and paleobiological approaches, Earth-Science Reviews, 54, 349, 2001.

Royer, D. L.: Estimating latest Cretaceous and Tertiary atmospheric CO_2 concentration from stomatal indices, in: Causes and Consequences of Globally Warm Climates in the Early Paleogene, edited by: Wing, S. L., Gingerich, P. D., Schmitz, B., and Thomas, E., Geological Society of America Special Paper 369, Boulder, 2003.

Royer, D. L.: CO2-forced climate thresholds during the Phanerozoic, Geochimica et Cosmochimica Acta, 70, 5665-5675, https://doi.org/10.1016/j.gca.2005.11.031, 2006.

Royer, D. L.: Atmospheric CO_2 and O_2 during the Phanerozoic: tools, patterns, and impacts, in: Treatise on Geochemistry (Second Edition), edited by: Holland, H. D. a. T., K. K. , Elsevier, Oxford, 251-267, 2014.

Russell, A. D., and Spero, H. J.: isotopes in planktonic foraminifera, Paleoceanography, 15, 43-52, 2000.

Russell, A. D., Honisch, B., Spero, H. J., and Lea, D. W.: Effects of seawater carbonate ion concentration and temperature on shell U, Mg, and Sr in cultured planktonic foraminifera, Geochimica Et Cosmochimica Acta, 68, 4347-4361, 10.1016/j.gca.2004.03.013, 2004.

Sadekov, A. Y., Eggins, S. M., Klinkhammer, G. P., and Rosenthal, Y.: Effects of seafloor and laboratory dissolution on the Mg/Ca composition of Globigerinoides sacculifer and Orbulina universa tests — A laser ablation ICPMS microanalysis perspective, Earth and Planetary Science Letters, 292, 312-324, https://doi.org/10.1016/j.epsl.2010.01.039, 2010.

Saenger, C., Affek, H. P., Felis, T., Thiagarajan, N., Lough, J. M., and Holcomb, M.: Carbonate clumped isotope variability in shallow water corals: Temperature dependence and growth-related vital effects, Geochimica et Cosmochimica Acta, 99, 224-242, 10.1016/j.gca.2012.09.035, 2012.

Salzmann, U., Dolan, A. M., Haywood, A. M., Chan, W.-L., Voss, J., Hill, D. J., Abe-Ouchi, A., Otto-Bliesner, B., Bragg, F. J., Chandler, M. A., Contoux, C., Dowsett, H. J., Jost, A., Kamae, Y., Lohmann, G., Lunt, D. J., Pickering, S. J., Pound, M. J., Ramstein, G., Rosenbloom, N. A., Sohl, L., Stepanek, C., Ueda, H., and Zhang, Z.: Challenges in quantifying Pliocene terrestrial warming revealed by data–model discord, Nature Climate Change, 3, 969-974, 10.1038/nclimate2008, 2013.

Sangiorgi, F., van Soelen Els, E., Spofforth David, J. A., Pälike, H., Stickley Catherine, E., St. John, K., Koç, N., Schouten, S., Sinninghe Damsté Jaap, S., and Brinkhuis, H.: Cyclicity in the middle Eocene central Arctic Ocean sediment record: Orbital forcing and environmental response, Paleoceanography, 23, 10.1029/2007PA001487, 2008.

Sanyal, A., Hemming, N. G., Broecker, W. S., Lea, D. W., Spero, H. J., and Hanson, G. N.: Oceanic pH control on the boron isotopic composition of foraminifera: Evidence from culture experiments, Paleoceanography, 11, 513-517, 1996.

Sanyal, A., Bijma, J., Spero, H., and Lea, D. W.: Empirical relationship between pH and the boron isotopic composition of *Globigerinoides sacculifer*: Implications for the boron isotope paleo-pH proxy, Paleoceanography, 16, 515-519, 2001.

Schauble, E., Ghosh, P., and M. Eiler, J.: Preferential formation of 13C-18O bonds in carbonate minerals, estimated using first-principles lattice dynamics, 2510-2529 pp., 2006.

Schauer, A. J., Kelson, J., Saenger, C., and Huntington, K. W.: Choice of 17O correction affects clumped isotope (Δ_{47}) values of CO2 measured with mass spectrometry, Rapid Communications in Mass Spectrometry, 30, 2607-2616, 10.1002/rcm.7743, 2016.

Schoon, P. L., Heilmann-Clausen, C., Schultz, B. P., Sinninghe Damsté, J. S., and Schouten, S.: Warming and environmental changes in the eastern North Sea Basin during the Palaeocene–Eocene Thermal Maximum as revealed by biomarker lipids, Organic Geochemistry, 78, 79-88, 2015.

Schouten, S., Klein Breteler, W. C. M., Blokker, P., Schogt, N., Rijpstra, W. I. C., Grice, K., Baas, M., and Sinninghe Damsté, J. S.: Biosynthetic effects on the stable carbon isotopic compositions of algal lipids: implications for deciphering the carbon isotopic biomarker record, Geochimica et Cosmochimica Acta, 62, 1397-1406, https://doi.org/10.1016/S0016-7037(98)00076-3, 1998.

Schouten, S., Hopmans, E. C., Schefuß, E., and Sinninghe Damsté, J. S.: Distributional variations in marine crenarchaeotal membrane lipids: a new tool for reconstructing ancient sea water temperatures? Earth and Planetary Science Letters, 204, 265-274, 2002.

Schouten, S., Hopmans, E. C., and Sinninghe Damsté, J. S.: The effect of maturity and depositional redox conditions on archaeal tetraether lipid palaeothermometry, Organic Geochemistry, 35, 567-571, https://doi.org/10.1016/j.orggeochem.2004.01.012, 2004.

Schouten, S., Forster, A., Panoto, F. E., and Sinninghe Damsté, J. S.: Towards calibration of the TEX_{86} palaeothermometer for tropical sea surface temperatures in ancient greenhouse worlds, Organic Geochemistry, 38, 1537-1546, 2007.

Schouten, S., Hopmans, E. C., and Sinninghe Damsté, J. S.: The organic geochemistry of glycerol dialkyl glycerol tetraether lipids: A review, Organic Geochemistry, 54, 19-61, doi: 10.1016/j.orggeochem.2012.09.006, 2013.

Schouten, S., Hopmans Ellen, C., Rosell-Melé, A., Pearson, A., Adam, P., Bauersachs, T., Bard, E., Bernasconi Stefano, M., Bianchi Thomas, S., Brocks Jochen, J., Carlson Laura, T., Castañeda Isla, S., Derenne, S., Selver Ayça, D., Dutta, K., Eglinton, T., Fosse, C., Galy, V., Grice, K., Hinrichs, K. U., Huang, Y., Huguet, A., Huguet, C., Hurley, S., Ingalls, A., Jia, G., Keely, B., Knappy, C., Kondo, M., Krishnan, S., Lincoln, S., Lipp, J., Mangelsdorf, K., Martínez-García, A., Ménot, G., Mets, A., Mollenhauer, G., Ohkouchi, N., Ossebaar, J., Pagani, M., Pancost Richard, D., Pearson Emma, J., Peterse, F., Reichart, G. J., Schaeffer, P., Schmitt, G., Schwark, L., Shah Sunita, R., Smith Richard, W., Sinninghe Damsté Jaap, S., Smittenberg Rienk, H., Summons Roger, E., Takano, Y., Talbot Helen, M., Taylor Kyle, W. R., Tarozo, R., Uchida, M., Dongen Bart, E., Mooy Benjamin, A. S., Wang, J., Warren, C., Weijers Johan, W. H., Werne Josef, P., Woltering, M., Xie, S., Yamamoto, M., Yang, H., Zhang Chuanlun, L., Zhang, Y., and Zhao, M.: An interlaboratory study of TEX_{86} and BIT analysis of sediments, extracts, and standard mixtures, Geochem. Geophys. Geosyst., 14, 5263-5285, 10.1002/2013GC004904, 2013.

Schrag, D. P., DePaolo, D. J., and Richter, F. M.: Reconstructing past sea surface temperatures: Correcting for diagenesis of bulk marine carbonate, Geochimica Et Cosmochimica Acta, 59, 2265-2278, 10.1016/0016-7037(95)00105-9, 1995.

Schrag, D. P.: Effect of diagenesis on the isotopic record of late Paleogene tropical sea surface temperatures, Chemical Geology, 161, 215-224, 1999.

Schubert, B. A., and Jahren, A. H.: The effect of atmospheric CO2 concentration on carbon isotope fractionation in C3 land plants, Geochimica et Cosmochimica Acta, 96, 29-43, https://doi.org/10.1016/j.gca.2012.08.003, 2012.

Schubert, B. A., and Hope Jahren, A.: Reconciliation of marine and terrestrial carbon isotope excursions based on changing atmospheric CO2 levels, Nature Communications, 4, 1653, 10.1038/ncomms2659, https://www.nature.com/articles/ncomms2659#supplementary-information, 2013.

Schubert, B. A., and Jahren, A. H.: Global increase in plant carbon isotope fractionation following the Last Glacial Maximum caused by increase in atmospheric pCO2, Geology, 43, 435-438, 10.1130/G36467.1, 2015.

Schubert, B. A., and Jahren, A. H.: Incorporating the effects of photorespiration into terrestrial paleoclimate reconstruction, Earth-Science Reviews, 177, 637-642, https://doi.org/10.1016/j.earscirev.2017.12.008, 2018.

Seki, O., Foster, G. L., Schmidt, D. N., Mackensen, A., Kawamura, K., and Pancost, R. D.: Alkenone and boron-based Pliocene pCO_2 records, Earth Plan. Sci. Lett., 292, 201-211, 10.1016/j.epsl.2010.01.037, 2010.

Sexton, P. F., Wilson, P. A., and Pearson, P. N.: Microstructural and geochemical perspectives on planktic foraminiferal preservation: "Glassy" versus "Frosty", Geochemistry Geophysics Geosystems, 7, 10.1029/2006gc001291, 2006.

Sexton, P. F., Norris, R. D., Wilson, P. A., Palike, H., Westerhold, T., Rohl, U., Bolton, C. T., and Gibbs, S.: Eocene global warming events driven by ventilation of oceanic dissolved organic carbon, Nature, 471, 349-352, 2011.

Shackleton, N., Corfield, R. M., and Hall, M. A.: Stable isotope data and the ontogeny of Paleocene planktonic foraminifera, Journal of Foraminiferal Research, 15, 321-336, 1985.

Shackleton, N. J.: Paleogene stable isotope events, Palaeogeography, Palaeoclimatology, Palaeoecology, 57, 91-102, 1986.

Sharkey, T. D., and Berry, J. A.: Carbon isotope fractionation of algae as influenced by an inducible CO2 concentrating mechanism, in: Inorganic Carbon Uptake by Aquatic Photosynthetic Organisms, edited by: Lucas, W. J., and Berry, J. A., The American Society of Plant Physiologists, Rockville, MD, USA, 389-401, 1985.

Shenton, B. J., Grossman, E. L., Passey, B. H., Henkes, G. A., Becker, T. P., Laya, J. C., Perez-Huerta, A., Becker, S. P., and Lawson, M.: Clumped isotope thermometry in deeply buried sedimentary carbonates: The effects of bond reordering and recrystallization, GSA Bulletin, 127, 1036-1051, 10.1130/B31169.1, 2015.

Sinninghe Damsté, J. S., Hopmans, E. C., Pancost, R. D., Schouten, S., and Geenevasen, J. A. J.: Newly discovered non-isoprenoid glycerol dialkyl glycerol tetraether lipids in sediments, Chem. Commun., 1683-1684, doi: 10.1039/B004517I, 2000.

Sinninghe Damsté, J. S., Rijpstra, W. I. C., Hopmans, E. C., Weijers, J. W. H., Foesel, B. U., Overmann, J., and Dedysh, S. N.: 13,16-Dimethyl Octacosanedioic Acid (*iso*-Diabolic Acid), a Common Membrane-Spanning Lipid of *Acidobacteria* Subdivisions 1 and 3, Appl. Environ. Microb., 77, 4147-4154, doi: 10.1128/AEM.00466-11, 2011.

Sinninghe Damsté, J. S.: Spatial heterogeneity of sources of branched tetraethers in shelf systems: The geochemistry of tetraethers in the Berau River delta (Kalimantan, Indonesia), Geochimica et Cosmochimica Acta, 186, 13-31, doi: 10.1016/j.gca.2016.04.033, 2016.

Slotnick, B. S., Dickens, G. R., Nicolo, M., Hollis, C. J., Crampton, J. S., Zachos, J. C., and Sluijs, A.: Numerous large amplitude variations in carbon cycling and terrestrial weathering throughout the latest Paleocene and earliest Eocene Journal of Geology, 120, 487-505, 2012.

Slotnick, B. S., Dickens, G. R., Hollis, C. J., Crampton, J. S., Percy Strong, C., and Phillips, A.: The onset of the Early Eocene Climatic Optimum at Branch Stream, Clarence River valley, New Zealand, New Zealand Journal of Geology and Geophysics, 58, 262-280, 10.1080/00288306.2015.1063514, 2015.

Sluijs, A., Pross, J., and Brinkhuis, H.: From greenhouse to icehouse; organic-walled dinoflagellate cysts as paleoenvironmental indicators in the Paleogene, Earth-Science Reviews, 68, 281-315, 10.1016/j.earscirev.2004.06.001, 2005.

Sluijs, A., Schouten, S., Pagani, M., Woltering, M., Brinkhuis, H., Sinninghe Damsté, J. S., Dickens, G. R., Huber, M., Reichart, G.-J., and Stein, R.: Subtropical Arctic Ocean temperatures during the Palaeocene/Eocene thermal maximum, Nature, 441, 610-613, 2006.

Sluijs, A., Bowen, G., Brinkhuis, H., Lourens, L., and Thomas, E.: The Palaeocene-Eocene Thermal Maximum super greenhouse: biotic and geochemical signatures, age models and mechanisms of global change, in: Deep time perspectives on climate change: marrying the signal fromcomputer models and biological proxies, edited by: Willliams, M., Haywood, A. M., Gregory, F. J., and Schmidt, D. N., The Geological Society of London, Special Publication, 323-347, 2007.

Sluijs, A., Brinkhuis, H., Schouten, S., Bohaty, S. M., John, C. M., Zachos, J. C., Reichart, G.-J., Sinninghe Damsté, J. S., Crouch, E. M., and Dickens, G. R.: Environmental precursors to rapid light carbon injection at the Palaeocene/Eocene boundary, Nature, 450, 1218-1221, 2007.

Sluijs, A., Röhl, U., Schouten, S., Brumsack, H.-J., Sangiorgi, F., Sinninghe Damsté, J. S., and Brinkhuis, H.: Arctic late Paleocene-early Eocene paleoenvironments with special emphasis on the Paleocene-Eocene thermal maximum (Lomonosov Ridge, Integrated Ocean Drilling Program Expedition 302), Paleoceanography, 23, PA1S11, 10.1029/2007pa001495, 2008.

Sluijs, A., Schouten, S., Donders, T. H., Schoon, P. L., Rohl, U., Reichart, G.-J., Sangiorgi, F., Kim, J.-H., Sinninghe Damsté, J. S., and Brinkhuis, H.: Warm and wet conditions in the Arctic region during Eocene Thermal Maximum 2, Nature Geosci, 2, 777-780, 2009.

Sluijs, A., Bijl, P., Schouten, S., Röhl, U., Reichart, G.-J., and Brinkhuis, H.: Southern Ocean warming, sea level and hydrological change during the Paleocene-Eocene thermal maximum, Climate of the Past, 7, 2011.

Sluijs, A., and Dickens, G. R.: Assessing offsets between the $\delta^{13}C$ of sedimentary components and the global exogenic carbon pool across early Paleogene carbon cycle perturbations, Global Biogeochemical Cycles, 26, GB4005, doi: 4010.1029/2011gb004224, 10.1029/2011gb004224, 2012.

Sluijs, A., van Roij, L., Harrington, G. J., Schouten, S., Sessa, J. A., LeVay, L. J., Reichart, G. J., and Slomp, C. P.: Warming, euxinia and sea level rise during the Paleocene–Eocene Thermal Maximum on the Gulf Coastal Plain: implications for ocean oxygenation and nutrient cycling, Clim. Past, 10, 1421-1439, 10.5194/cp-10-1421-2014, 2014.

Sluijs, A., van Roij, L., Frieling, J., Laks, J., and Reichart, G.-J.: Single-species dinoflagellate cyst carbon isotope ecology across the Paleocene-Eocene Thermal Maximum, Geology, 46, 79-82, 10.1130/G39598.1, 2017.

Smith, R. Y., Greenwood, D. R., and Basinger, J. F.: Estimating paleoatmospheric pCO2 during the Early Eocene Climatic Optimum from stomatal frequency of Ginkgo, Okanagan Highlands, British Columbia, Canada, Palaeogeography, Palaeoclimatology, Palaeoecology, 293, 120-131, https://doi.org/10.1016/j.palaeo.2010.05.006, 2010.

Snell, K. E., Thrasher, B. L., Eiler, J. M., Koch, P. L., Sloan, L. C., and Tabor, N. J.: Hot summers in the Bighorn Basin during the early Paleogene, Geology, 41, 55-58, 2013.

Sosdian, S. M., Greenop, R., Hain, M. P., Foster, G. L., Pearson, P. N., and Lear, C. H.: Constraining the evolution of Neogene ocean carbonate chemistry using the boron isotope pH proxy, Earth and Planetary Science Letters, 498, 362-376, https://doi.org/10.1016/j.epsl.2018.06.017, 2018.

Speijer, R. P., Scheibner, C., Stassen, P., and Morsi, A.-M. M.: Response of marine ecosystems to deep-time global warming: a synthesis of biotic patterns across the Paleocene-Eocene thermal maximum (PETM), Austrian Journal of Earth Sciences, 105, 6-16, 2012.

Spero, H., and Williams, D. F.: Extracting environmental information from planktonic foraminiferal δ13C data, Nature, 335, 717-719, 1988.

Spero, H. J., Bijma, J., Lea, D. W., and Bemis, B. E.: Effect of seawater carbonate concentration on foraminiferal carbon and oxygen isotopes, Nature, 390, 497-500, 1997.

Spero, H. J., Eggins, S. M., Russell, A. D., Vetter, L., Kilburn, M. R., and Hönisch, B.: Timing and mechanism for intratest Mg/Ca variability in a living planktic foraminifer, Earth and Planetary Science Letters, 409, 32-42, http://dx.doi.org/10.1016/j.epsl.2014.10.030, 2015.

Spicer, R. A., Herman, A. B., and Kennedy, E. M.: Foliar physiognomic record of climatic conditions during dormancy: Climate Leaf Analysis Multivariate Program (CLAMP) and the Cold Month Mean Temperature., The Journal of Geology, 112, 685-702, 2004.

Spicer, R. A., Herman, A. B., and Kennedy, E. M.: The sensitivity of CLAMP to taphonomic loss of foliar physiognomic characters., Palaios, 20, 429-438, 2005.

Spicer, R. A., Valdes, P. J., Spicer, T. E. V., Craggs, H. J., Srivastava, G., Mehrotra, R. C., and Yang, J.: New developments in CLAMP: Calibration using global gridded meteorological data, Palaeogeography, Palaeoclimatology, Palaeoecology, 283, 91-98, 2009.

Spicer, R. A., and Yang, J.: Quantification of uncertainties in fossil leaf paleoaltimetry: does leaf size matter?, Tectonics, 29, TC6001, 10.1029/2010TC002741, 2010.

Spicer, R. A., Bera, S., De Bera, S., Spicer, T. E. V., Srivastava, G., Mehrotra, R., Mehrotra, N., and Yang, J.: Why do foliar physiognomic climate estimates sometimes differ from those observed? Insights from taphonomic information loss and a CLAMP case study from the Ganges Delta, Palaeogeography, Palaeoclimatology, Palaeoecology, 302, 381-395, 10.1016/j.palaeo.2011.01.024, 2011.

Spooner, P. T., Guo, W., Robinson, L. F., Thiagarajan, N., Hendry, K. R., Rosenheim, B. E., and Leng, M. J.: Clumped isotope composition of cold-water corals: A role for vital effects?, Geochimica et Cosmochimica Acta, 179, 123-141, 2016.

Steart, D. C., Spicer, R. A., and Bamford, M. K.: Is southern Africa different? An investigation of the relationship between leaf physiognomy and climate in southern African mesic vegetation., Review of Palaeobotany and Palynology, 162, 607–620, 2010.

Steinthorsdottir, M., Vajda, V., and Pole, M.: Significant transient pCO_2 perturbation at the New Zealand Oligocene-Miocene transition recorded by fossil plant stomata, Palaeogeography, Palaeoclimatology, Palaeoecology, https://doi.org/10.1016/j.palaeo.2018.01.039, 2018.

Stolper, D. A., Eiler, J. M., and Higgins, J. A.: Modeling the effects of diagenesis on carbonate clumped-isotope values in deep- and shallow-water settings, Geochimica et Cosmochimica Acta, 227, 264-291, 10.1016/j.gca.2018.01.037, 2018.

Stranks, L., and England, P.: The use of a resemblance function in the measurement of climatic parameters from the physiognomy of woody dicotyledons, Palaeogeography, Palaeoclimatology, Palaeoecology, 131, 15-28, 10.1016/S0031-0182(96)00147-2, 1997.

Suan, G., Popescu, S.-M., Suc, J.-P., Schnyder, J., Fauquette, S., Baudin, F., Yoon, D., Piepjohn, K., Sobolev, N. N., and Labrousse, L.: Subtropical climate conditions and mangrove growth in Arctic Siberia during the early Eocene, Geology, 45, 539-542, 10.1130/G38547.1, 2017.

Super, J. R., Thomas, E., Pagani, M., Huber, M., O'Brien, C., and Hull, P. M.: North Atlantic temperature and pCO_2 coupling in the early-middle Miocene, Geology, 46, 519-522, 10.1130/G40228.1, 2018.

Tang, J., Dietzel, M., Fernandez, A., Tripati, A. K., and Rosenheim, B. E.: Evaluation of kinetic effects on clumped isotope fractionation (Δ47) during inorganic calcite precipitation, Geochimica et Cosmochimica Acta, 134, 120-136, 10.1016/j.gca.2014.03.005, 2014.

Taylor, K. W., Huber, M., Hollis, C. J., Hernandez-Sanchez, M. T., and Pancost, R. D.: Re-evaluating modern and Palaeogene GDGT distributions: Implications for SST reconstructions, Global and Planetary Change, 108, 158-174, 2013.

Taylor, K. W. R., Willumsen, P. S., Hollis, C. J., and Pancost, R. D.: South Pacific evidence for the long-term climate impact of the Cretaceous/Paleogene boundary event, Earth-Science Reviews, 179, 287-302, https://doi.org/10.1016/j.earscirev.2018.02.012, 2018.

Thiagarajan, N., Adkins, J., and Eiler, J.: Carbonate clumped isotope thermometry of deep-sea corals and implications for vital effects, Geochimica et Cosmochimica Acta, 75, 4416-4425, 2011.

Thompson, R. S., Anderson, K. H., Pelltier, R. T., Strickland, L. E., Bartlein, P. J., and Shafer, S. L.: Quantitative estimation of climatic parameters from vegetation data in North America by the mutual climatic range technique., Quaternary Science Reviews, 51, 18–39, 2012.

Tierney, J. E., and Tingley, M. P.: A Bayesian, spatially-varying calibration model for the TEX< sub> 86</sub> proxy, Geochimica et Cosmochimica Acta, 127, 83-106, 2014.

Tierney, J. E., and Tingley, M. P.: A TEX_{86} surface sediment database and extended Bayesian calibration, Scientific data, 2, 2015.

Tierney, J. E., Sinninghe Damsté, J. S., Pancost, R. D., Sluijs, A., and Zachos, J. C.: Eocene temperature gradients, Nature Geosci, 10, 538, 10.1038/ngeo2997, https://www.nature.com/articles/ngeo2997#supplementary-information, 2017.

Tindall, J., Flecker, R., Valdes, P., Schmidt, D. N., Markwick, P., and Harris, J.: Modelling the oxygen isotope distribution of ancient seawater using a coupled ocean–atmosphere GCM: Implications for reconstructing early Eocene climate, Earth and Planetary Science Letters, 292, 265-273, http://dx.doi.org/10.1016/j.epsl.2009.12.049, 2010.

Tipple, B. J., Meyers, S. R., and Pagani, M.: Carbon isotope ratio of Cenozoic CO_2: A comparative evaluation of available geochemical proxies, 25, doi:10.1029/2009PA001851, 2010.

Traiser, C., Klotz, S., Uhl, D., and Mosbrugger, V.: Environmental signals from leaves – a physiognomic analysis of European vegetation, New Phytologist, 166, 465-484, 10.1111/j.1469-8137.2005.01316.x, 2005.

Tripati, A. K., Delaney, M. L., Zachos, J. C., Anderson, L. D., Kelly, D. C., and Harry, E.: Tropical sea-surface temperature reconstruction for the early Paleogene using Mg/Ca ratios of planktonic foraminifera, Paleoceanography, 18, 1101, doi:1110.1029/2003PA000937, 2003.

Tripati, A. K., and Elderfield, H.: Abrupt hydrographic changes in the equatorial Pacific and subtropical Atlantic from foraminiferal Mg/Ca indicate greenhouse origin for the thermal maximum at the Paleocene-Eocene Boundary, Geochem. Geophys. Geosyst., 5, doi:10.1029/2003GC000631, 2004.

Tripati, A., and Elderfield, H.: Deep-Sea Temperature and Circulation Changes at the Paleocene-Eocene Thermal Maximum, Science, 308, 1894-1898, 10.1126/science.1109202, 2005.

Tripati, A. K., Eagle, R. A., Thiagarajan, N., Gagnon, A. C., Bauch, H., Halloran, P. R., and Eiler, J. M.: $^{13}C–^{18}O$ isotope signatures and 'clumped isotope'thermometry in foraminifera and coccoliths, Geochimica et Cosmochimica Acta, 74, 5697-5717, 2010.

Tripati, A. K., Sahany, S., Pittman, D., Eagle, R. A., Neelin, J. D., Mitchell, J. L., and Beaufort, L.: Modern and glacial tropical snowlines controlled by sea surface temperature and atmospheric mixing, Nature Geosci, 7, 205-209, 10.1038/ngeo2082, 2014.

Tripati, A. K., Hill, P. S., Eagle, R. A., Mosenfelder, J. L., Tang, J., Schauble, E. A., Eiler, J. M., Zeebe, R. E., Uchikawa, J., Coplen, T. B., Ries, J. B., and Henry, D.: Beyond temperature: Clumped isotope signatures in dissolved inorganic carbon species and the influence of solution chemistry on carbonate mineral composition, Geochimica et Cosmochimica Acta, 166, 344-371, 10.1016/j.gca.2015.06.021, 2015.

Tyrrell, T., and Zeebe, R. E.: History of carbonate ion concentration over the last 100 million years, Geochim. Cosmochim. Acta, 68, 3521-3530, 10.1016/j.gca.2004.02.018, 2004.

Uchikawa, J., and Zeebe, R. E.: Examining possible effects of seawater pH decline on foraminiferal stable isotopes during the Paleocene-Eocene Thermal Maximum, Paleoceanography, 25, 10.1029/2009PA001864, 2010.

Uhl, D., Mosbrugger, V., Bruch, A., and Utescher, T.: Reconstructing palaeotemperatures using leaf floras-case studies for a comparison of leaf margin analysis and the coexistence approach., Review of Palaeobotany and Palynology, 126, 49-64, 2003.

Urey, H. C., Lowenstam, A., Epstein, S., McKinney, C.R.: Measurement of paleotemperatures and temperatures of the upper Cretaceous of England, Denmark, and the Southeastern United States, Bull. Geol. Soc. America, 62, 399-416, 1951.

Utescher, T., and Mosbrugger, V.: The Palaeoflora Database, Senckenberg Research Institute, Frankfurt, 2015.

Utescher, T., Bruch, A. A., Erdei, B., François, L., Ivanov, D., Jacques, F. M. B., Kern, A. K., Liu, Y. S., Mosbrugger, V., and Spicer, R. A.: The Coexistence Approach—Theoretical background and practical considerations of using plant fossils for climate quantification, Palaeogeography, Palaeoclimatology, Palaeoecology, 410, 58-73, https://doi.org/10.1016/j.palaeo.2014.05.031, 2014.

van der Meer, M. T. J., Baas, M., Rijpstra, W. I. C., Marino, G., Rohling, E. J., Sinninghe Damsté, J. S., and Schouten, S.: Hydrogen isotopic compositions of long-chain alkenones record freshwater flooding of the Eastern Mediterranean at the onset of sapropel deposition, Earth and Planetary Science Letters, 262, 594-600, 10.1016/j.epsl.2007.08.014, 2007.

van Hinsbergen, D. J. J., de Groot, L. V., van Schaik, J., Spakman, W., Bijl, P. K., Sluijs, A., Langereis, C. G., and Brinkhuis, H.: A Paleolatitude Calculator for Paleoclimate Studies, PLoS ONE, 10, 10.1371/journal. pone.0126946, 2015.

van Roij, L., Sluijs, A., Laks, J. J., and Reichart, G.-J.: Stable carbon isotope analyses of nanogram quantities of particulate organic carbon (pollen) with laser ablation nano combustion gas chromatography/isotope ratio mass spectrometry, 31, 47-58, doi:10.1002/rcm.7769, 2017.

Vengosh, A., Kolodny, Y., Starinsky, A., Chivas, A. R., and McCulloch, M. T.: Coprecipitation and isotopic fractionation of boron in modern biogenic carbonates, Geochimica et Cosmochimica Acta, 55, 2901-2910, 1991.

Voigt, J., Hathorne, E. C., Frank, M., and Holbourn, A.: Minimal influence of recrystallization on middle Miocene benthic foraminiferal stable isotope stratigraphy in the eastern equatorial Pacific, Paleoceanography, 31, 98-114, 10.1002/2015PA002822, 2016.

Volkman, J. K., Eglinton, G., Corner, E. D. S., and Forsberg, T. E. V.: Long-chain alkenes and alkenones in the marine coccolithophorid Emiliania huxleyi, Phytochemistry, 19, 2619-2622, https://doi.org/10.1016/S0031-9422(00)83930-8, 1980.

Wacker, U., Fiebig, J., Tödter, J., Schöne, B. R., Bahr, A., Friedrich, O., Tütken, T., Gischler, E., and Joachimski, M. M.: Empirical calibration of the clumped isotope paleothermometer using calcites of various origins, Geochimica et Cosmochimica Acta, 141, 127-144, 10.1016/j.gca.2014.06.004, 2014.

Warden, L., van der Meer, M. T. J., Moros, M., and Sinninghe Damsté, J. S.: Sedimentary alkenone distributions reflect salinity changes in the Baltic Sea over the Holocene, Organic Geochemistry, 102, 30-44, 10.1016/j.orggeochem.2016.09.007, 2016.

Weber, Y., De Jonge, C., Rijpstra, W. I. C., Hopmans, E. C., Stadnitskaia, A., Schubert, C. J., Lehmann, M. F., Sinninghe Damsté, J. S., and Niemann, H.: Identification and carbon isotope composition of a novel branched GDGT isomer in lake sediments: Evidence for lacustrine branched GDGT production, Geochimica et Cosmochimica Acta, 154, 118-129, doi: 10.1016/j.gca.2015.01.032, 2015.

Weijers, J. W., Schouten, S., Spaargaren, O. C., and Sinninghe Damsté, J. S.: Occurrence and distribution of tetraether membrane lipids in soils: Implications for the use of the TEX_{86} proxy and the BIT index, Organic Geochemistry, 37, 1680-1693, 2006.

Weijers, J. W. H., Schouten, S., Sluijs, A., Brinkhuis, H., and Sinninghe Damsté, J. S.: Warm Arctic continents during the Palaeocene–Eocene thermal maximum, Earth and Planetary Science Letters, 261, 230-238, doi: 10.1016/j.epsl.2007.06.033, 2007.

Weijers, J. W. H., Panoto, E., van Bleijswijk, J., Schouten, S., Rijpstra, W. I. C., Balk, M., Stams, A. J. M., and Sinninghe Damsté, J. S.: Constraints on the Biological Source(s) of the Orphan Branched Tetraether Membrane Lipids, Geomicrobiol. J., 26, 402-414, doi: 10.1080/01490450902937293, 2009.

Weijers, J. W. H., Steinmann, P., Hopmans, E. C., Schouten, S., and Sinninghe Damsté, J. S.: Bacterial tetraether membrane lipids in peat and coal: Testing the MBT-CBT temperature proxy for climate reconstruction, Organic Geochemistry, 42, 477-486, doi: 10.1016/j.orggeochem.2011.03.013, 2011.

Weijers, J. W. H., Schefuß, E., Kim, J.-H., Sinninghe Damsté, J. S., and Schouten, S.: Constraints on the sources of branched tetraether membrane lipids in distal marine sediments, Organic Geochemistry, 72, 14-22, doi: 10.1016/j.orggeochem.2014.04.011, 2014.

Weldeab, S., Arce, A., and Kasten, S.: Mg/Ca-$\Delta CO_3^{2-}{}_{porewater}$–temperature calibration for *Globobulimina* spp.: A sensitive paleothermometer for deep-sea temperature reconstruction, Earth and Planetary Science Letters, 438, 95-102, 10.1016/j.epsl.2016.01.009, 2016.

Westerhold, T., Röhl, U., Raffi, I., Fornaciari, E., Monechi, S., Reale, V., Bowles, J., and Evans, H. F.: Astronomical calibration of the Paleocene time, Palaeogeography, Palaeoclimatology, Palaeoecology, 257, 377-403, https://doi.org/10.1016/j.palaeo.2007.09.016, 2008.

Westerhold, T., Röhl, U., Donner, B., McCarren, H. K., and Zachos, J. C.: A complete high-resolution Paleocene benthic stable isotope record for the central Pacific (ODP Site 1209), Paleoceanography, 26, PA2216, 10.1029/2010pa002092, 2011.

Westerhold, T., Röhl, U., Frederichs, T., Agnini, C., Raffi, I., Zachos, J. C., and Wilkens, R. H.: Astronomical calibration of the Ypresian Time Scale: Implications for seafloor spreading rates and the chaotic behaviour of the Solar System?, Clim. Past Discuss., 2017, 1-34, 10.5194/cp-2017-15, 2017.

Westerhold, T., Röhl, U., Donner, B., and Zachos, J. C.: Global extent of early Eocene hyperthermal events: A new Pacific benthic foraminiferal isotope record from Shatsky Rise (ODP Site 1209), Paleoceanography and Paleoclimatology, 33, 626-642, doi:10.1029/2017PA003306, 2018.

Wiemann, M. C., Manchester, S. R., Dilcher, D. D., Hinojosa, L. F., and Wheeler, E. A.: Estimation of temperature and precipitation from morphological characters of dicotyledonous leaves., American Journal of Botany, 85, 1796-1802, 1998.

Wilf, P.: When are leaves good thermometers? A new case for Leaf Margin Analysis., Paleobiology, 23, 373-390, 1997.

Wilf, P., Wing, S. L., Greenwood, D. R., and Greenwood, C. L.: Using fossil leaves as paleoprecipitation indicators; an Eocene example, Geology (Boulder), 26, 203-206, 1998.

Wilke, I., Bickert, T., and Peeters, F. J.: The influence of seawater carbonate ion concentration [CO_3^{2-}] on the stable carbon isotope composition of the planktic foraminifera species Globorotalia inflata, Marine Micropaleontology, 58, 243-258, 2006.

Wilkes, E. B., Carter, S. J., and Pearson, A.: CO2-dependent carbon isotope fractionation in the dinoflagellate Alexandrium tamarense, Geochimica et Cosmochimica Acta, 212, 48-61, 10.1016/j.gca.2017.05.037, 2017.

Williams, G. L., Brinkhuis, H., Pearce, M. A., Fensome, R. A., and Weegink, J. W.: Southern Ocean and global dinoflagellate cyst events compared; index events for the Late Cretaceous-Neogene, in: The Tasmanian gateway: Cenozoic climatic and oceanographic development, covering Leg 189 of the cruises of the drilling vessel *JOIDES Resolution*, Hobart, Tasmania, to Sydney, Australia; Sites 1168-1172; 11 March-6 May 2000, edited by: Exon, N. F., Kennett, J. P., and Malone, M. J., Proceedings of the Ocean Drilling Program, Texas A&M University, College Station, Texas, 98 p., 2004.

Wing, S. L., and Greenwood, D. R.: Fossils and fossil climate: the case for equable continental interiors in the Eocene., Philosophical transactions of the Royal Society of London B, 341, 243-252, 1993.

Witkowski, C., Weijers, J. W. H., Blais, B., Schouten, S., and Sinninghe Damsté, J., S.S.: Molecular fossils from phytoplankton reveal secular pCO_2 trend over the Phanerozoic, Science Advances, 4, eaat4556, 2018.

Wolfe, J. A.: Temperature parameters of humid to Mesic forests of Eastern Asia and relation to forests of other regions of the Northern Hemisphere and Australasia., Geological Survey Professional Paper, 1106, 1-37, 1979.

Wolfe, J. A.: A method of obtaining climatic parameters from leaf assemblages., U.S. Geological Survey Bulletin, 2040, 71pp, 1993.

Woodward, F. I.: Stomatal numbers are sensitive to increases in CO_2 from pre-industrial levels, Nature, 327, 617-618, 1987.

Wuchter, C., Schouten, S., Coolen, M. J. L., and Sinninghe Damsté, J. S.: Temperature-dependent variation in the distribution of tetraether membrane lipids of marine Crenarchaeota: Implications for TEX86 paleothermometry, Paleoceanography, 19, doi:10.1029/2004PA001041, 2004.

Wycech, J. B., Kelly, D. C., Kozdon, R., Orland, I. J., Spero, H. J., and Valley, J. W.: Comparison of δ18O analyses on individual planktic foraminifer (Orbulina universa) shells by SIMS and gas-source mass spectrometry, Chemical Geology, 483, 119-130, https://doi.org/10.1016/j.chemgeo.2018.02.028, 2018.

Wynn, J. G.: Towards a physically based model of CO_2-induced stomatal frequency response, New Phytologist, 157, 391-398, 2003.

Yang, J., Wang, Y.-F., Spicer, R. A., Mosbrugger, V., Li, C.-S., and Sun, Q.-G.: Climatic reconstruction at the Miocene Shanwang basin, China, using leaf margin analysis, CLAMP, coexistence approach, and overlapping distribution analysis, American Journal of Botany, 94, 599-608, 10.3732/ajb.94.4.599, 2007.

Yang, J., Spicer, R., Spicer, T. V., and Li, C.-S.: 'CLAMP Online': a new web-based palaeoclimate tool and its application to the terrestrial Paleogene and Neogene of North America, Palaeobio Palaeoenv, 91, 163-183, 10.1007/s12549-011-0056-2, 2011.

Yang, J., Spicer, R. A., Spicer, T. E. V., Arens, N. C., Jacques, F. M. B., Su, T., Kennedy, E. M., Herman, A. B., Steart, D. C., Srivastava, G., Mehrotra, R. C., Valdes, P. J., Mehrotra, N. C., Zhou, Z.-K., and Lai, J.-S.: Leaf form–climate relationships on the global stage: an ensemble of characters, Global Ecology and Biogeography, 24, 1113-1125, 10.1111/geb.12334, 2015.

Yu, J., and Elderfield, H.: Benthic foraminiferal B/Ca ratios reflect deep water carbonate saturation state, Earth and Planetary Science Letters, 258, 73-86, 2007.

Yu, J., Elderfield, H., Greaves, M., and Day, J.: Preferential dissolution of benthic foraminiferal calcite during laboratory reductive cleaning, Geochem. Geophys. Geosyst., 8, 10.1029/2006GC001571, 2007.

Zaarur, S., Affek, H. P., and Brandon, M. T.: A revised calibration of the clumped isotope thermometer, Earth and Planetary Science Letters, 382, 47-57, 10.1016/j.epsl.2013.07.026, 2013.

Zachos, J. C., Stott, L. D., and Lohmann, K. C.: Evolution of early Cenozoic marine temperatures, Paleoceanography, 9, 353-387, 1994.

Zachos, J. C., Pagani, M., Sloan, L. C., Thomas, E., and Billups, K.: Trends, rhythms, and aberrations in global climate 65[thinsp]Ma to present, Science, 292, 686-693, 2001.

Zachos, J. C., Wara, M. W., Bohaty, S., Delaney, M. L., Petrizzo, M. R., Brill, A., Bralower, T. J., and Premoli-Silva, I.: A transient rise in tropical sea surface temperature during the Paleocene-Eocene thermal maximum, Science, 302, 1551-1554, 2003.

Zachos, J. C., Schouten, S., Bohaty, S., Quattlebaum, T., Sluijs, A., Brinkhuis, H., Gibbs, S., and Bralower, T.: Extreme warming of mid-latitude coastal ocean during the Paleocene-Eocene Thermal Maximum: Inferences from TEX86 and isotope data, Geology, 34, 737-740, 2006.

Zachos, J. C., Dickens, G. R., and Zeebe, R. E.: An early Cenozoic perspective on greenhouse warming and carbon-cycle dynamics, Nature, 451, 279-283, 2008.

Zeebe, R. E.: An explanation of the effect of seawater carbonate concentration on foraminiferal oxygen isotopes, Geochimica et Cosmochimica Acta, 63, 2001-2007, https://doi.org/10.1016/S0016-7037(99)00091-5, 1999.

Zeebe, R. E., Bijima, J., and Wolf-Gladow, D. A.: A diffusion-reaction model of carbon isotope fractionation in foraminifera, Marine Chemistry, 64, 1999.

Zeebe, R. E.: Seawater pH and isotopic paleotemperatures of Cretaceous oceans, Palaeogeography, Palaeoclimatology, Palaeoecology, 170, 49-57, http://dx.doi.org/10.1016/S0031-0182(01)00226-7, 2001.

Zeebe, R. E.: An expression for the overall oxygen isotope fractionation between the sum of dissolved inorganic carbon and water, Geochem. Geophys. Geosyst., 8, doi:10.1029/2007GC001663, 2007.

Zeebe, R. E.: Modeling CO_2 chemistry, $\delta^{13}C$, and oxidation of organic carbon and methane in sediment porewater: Implications for paleo-proxies in benthic foraminifera, Geochimica et Cosmochimica Acta, 71, 3238-3256, https://doi.org/10.1016/j.gca.2007.05.004, 2007.

Zeebe, R. E.: Time-dependent climate sensitivity and the legacy of anthropogenic greenhouse gas emissions, Proceedings of the National Academy of Sciences, 10.1073/pnas.1222843110, 2013.

Zell, C., Kim, J. H., Balsinha, M., Dorhout, D., Fernandes, C., Baas, M., and Sinninghe Damsté, J. S.: Transport of branched tetraether lipids from the Tagus River basin to the coastal ocean of the Portuguese margin: consequences for the interpretation of the MBT'/CBT paleothermometer, Biogeosciences, 11, 5637-5655, doi: 10.5194/bg-11-5637-2014, 2014.

Zhang, Y. G., Zhang, C. L., Liu, X.-L., Li, L., Hinrichs, K.-U., and Noakes, J. E.: Methane Index: a tetraether archaeal lipid biomarker indicator for detecting the instability of marine gas hydrates, Earth and Planetary Science Letters, 307, 525-534, 2011.

Zhang, Y. G., Pagani, M., Liu, Z., Bohaty, S. M., and DeConto, R.: A 40-million-year history of atmospheric CO_2, Philosophical Transactions of the Royal Society of London Series a-Mathematical Physical and Engineering Sciences, 371, 20130096, 2013.

Zhang, Y. G., Pagani, M., and Wang, Z.: Ring Index: A new strategy to evaluate the integrity of TEX86 paleothermometry, Paleoceanography, 31, 220-232, 10.1002/2015PA002848, 2016.

Zonneveld, K. A. F., Marret, F., Versteegh, G. J. M., Bogus, K., Bonnet, S., Bouimetarhan, I., Crouch, E., de Vernal, A., Elshanawany, R., Edwards, L., Esper, O., Forke, S., Grøsfjeld, K., Henry, M., Holzwarth, U., Kielt, J.-F., Kim, S.-Y., Ladouceur, S., Ledu, D., Chen, L., Limoges, A., Londeix, L., Lu, S. H., Mahmoud, M. S., Marino, G., Matsouka, K., Matthiessen, J., Mildenhall, D. C., Mudie, P., Neil, H. L., Pospelova, V., Qi, Y., Radi, T., Richerol, T., Rochon, A., Sangiorgi, F., Solignac, S., Turon, J.-L., Verleye, T., Wang, Y., Wang, Z., and Young, M.: Atlas of modern dinoflagellate cyst distribution based on 2405 data points, Review of Palaeobotany and Palynology, 191, 1-197, 10.1016/j.revpalbo.2012.08.003, 2013.

FIGURE CAPTIONS

Geosci. Model Dev. Discuss., https://doi.org/10.5194/gmd-2018-309
Manuscript under review for journal Geosci. Model Dev.
Discussion started: 17 January 2019

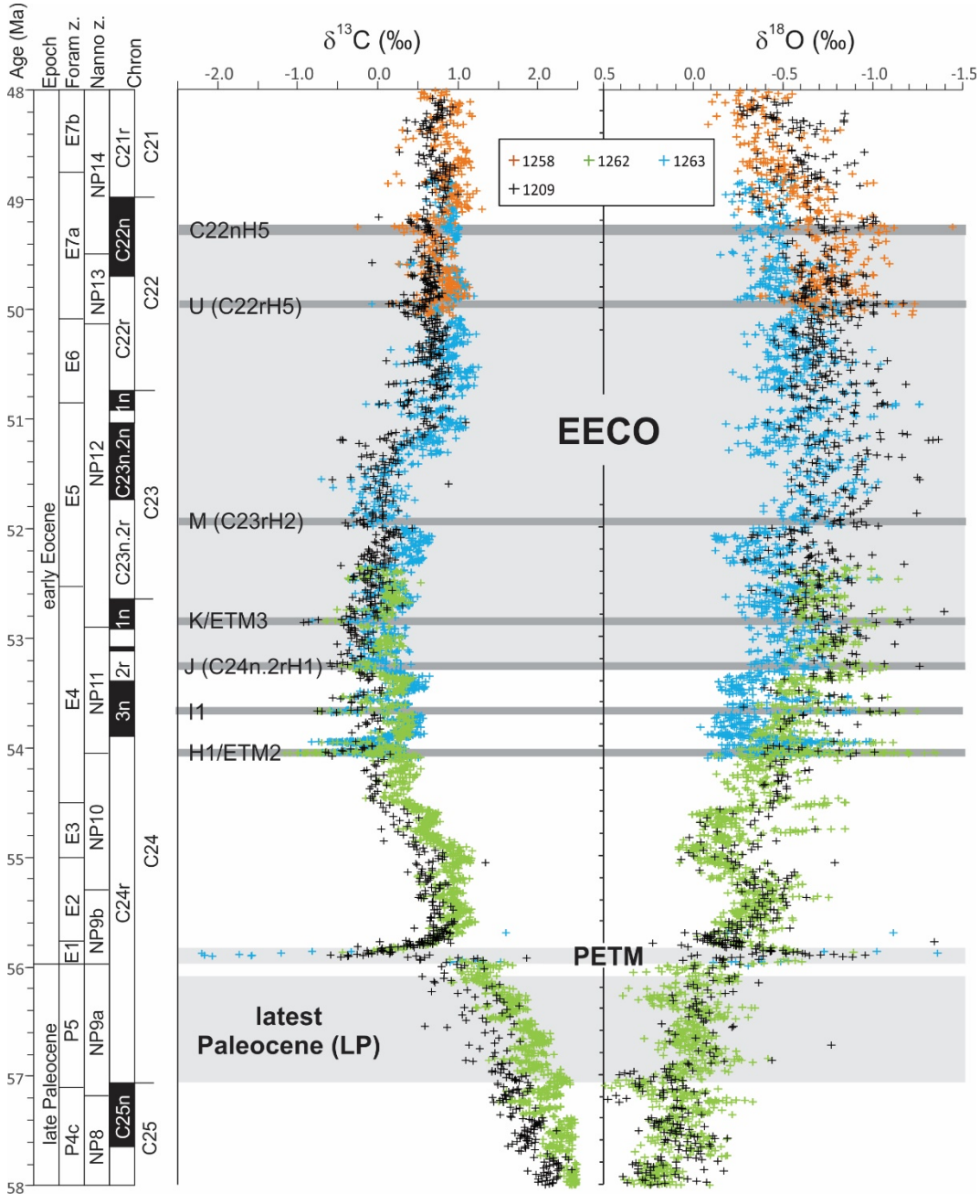

Figure 1: Benthic foraminiferal carbon and oxygen stable isotope records from ODP sites 1209, 1258, 1262 and 1263 (Littler et al., 2014; Lauretano et al., 2016, 2018; Westerhold et al., 2011, 2017, 2018) calibrated to the timescale of Westerhold et al. (2017). Calcareous nannofossil and planktic foraminiferal biozone boundaries are recalibrated from Gradstein et al. (2012).

Geosci. Model Dev. Discuss., https://doi.org/10.5194/gmd-2018-309
Manuscript under review for journal Geosci. Model Dev.
Discussion started: 17 January 2019

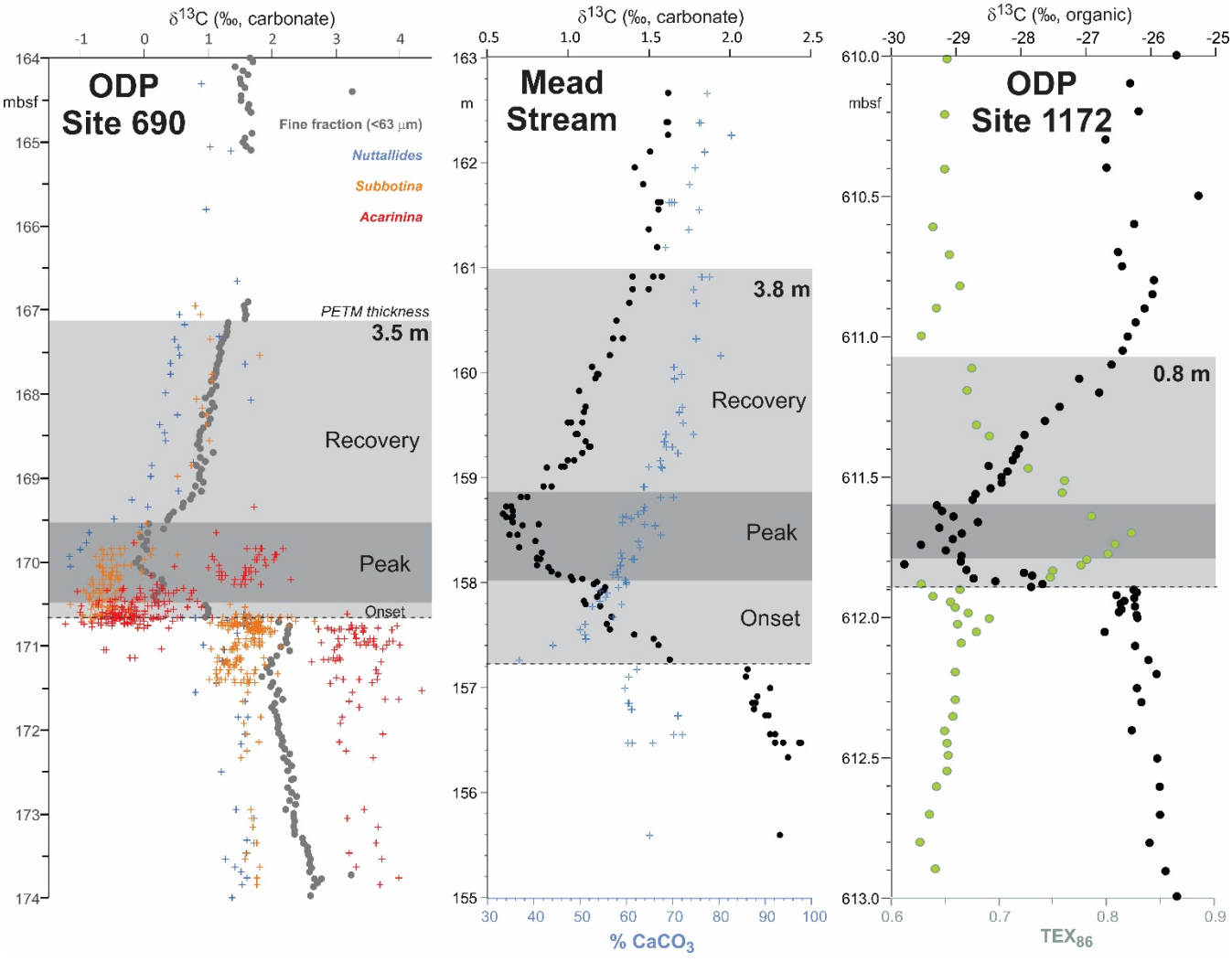

Figure 2. Three high-resolution records through the Paleocene-Eocene thermal maximum (PETM): ODP Site 690, Maud Rise, South Atlantic (Kennett and Stott, 1991; Bains et al., 1999; Thomas et al., 2002; Nunes and Norris, 2006); Mead Stream, New Zealand, South Pacific (Nicolo et al., 2010); ODP Site 1172, East Tasman Plateau, Tasman Sea (Sluijs et al., 2011).

Geosci. Model Dev. Discuss., https://doi.org/10.5194/gmd-2018-309
Manuscript under review for journal Geosci. Model Dev.
Discussion started: 17 January 2019

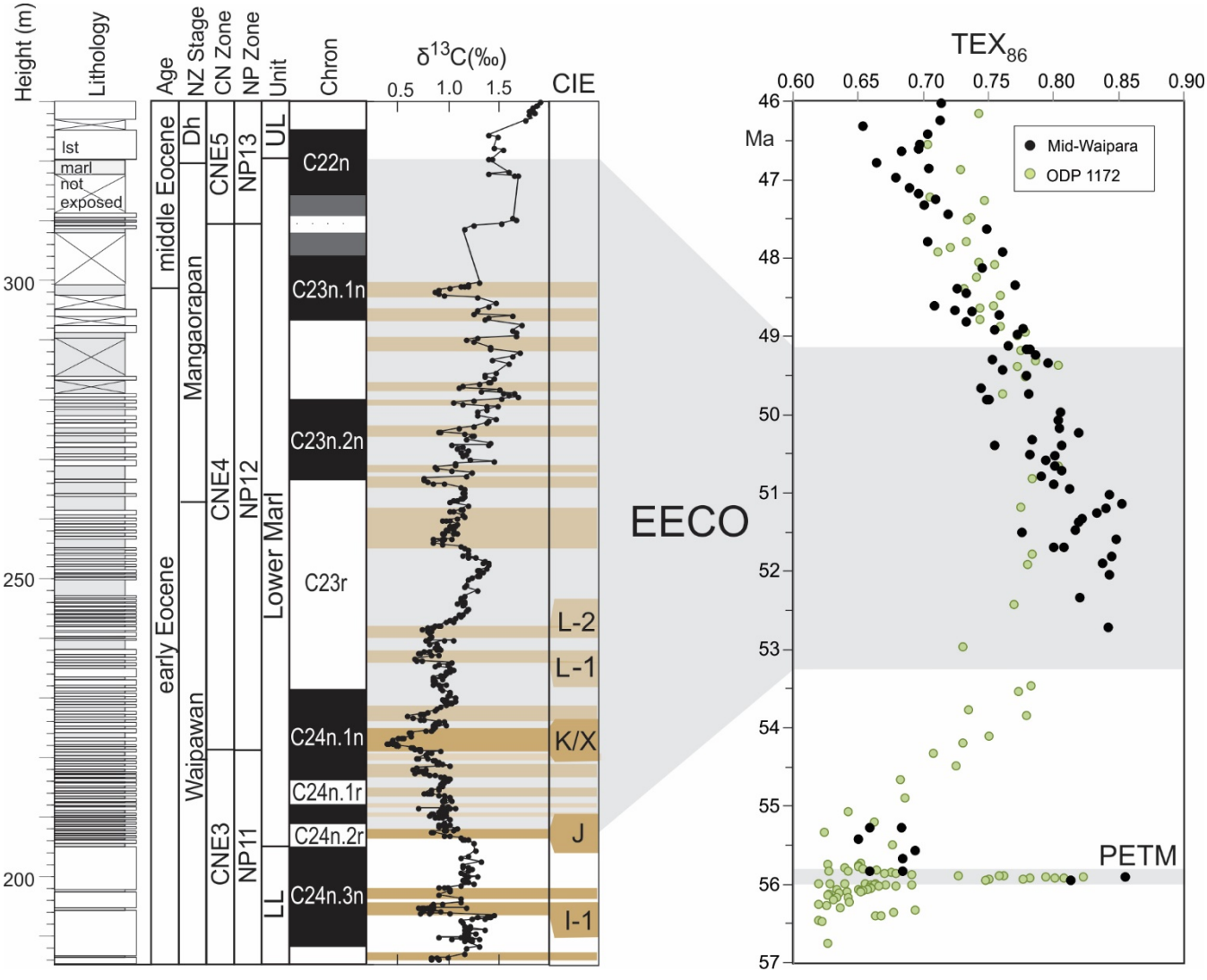

Figure 3. Eocene carbon isotopes and lithostratigraphy at Mead Stream, New Zealand (Slotnick et al., 2012), compared with indicators of relative changes in sea surface temperatures: TEX_{86} for ODP Site 1172 (Bijl et al., 2009) and mid-Waipara (Hollis et al., 2012; Crouch et al., in prep.). Grey shading = EECO interval as defined by Westerhold et al. (2018).

Geosci. Model Dev. Discuss., https://doi.org/10.5194/gmd-2018-309
Manuscript under review for journal Geosci. Model Dev.
Discussion started: 17 January 2019

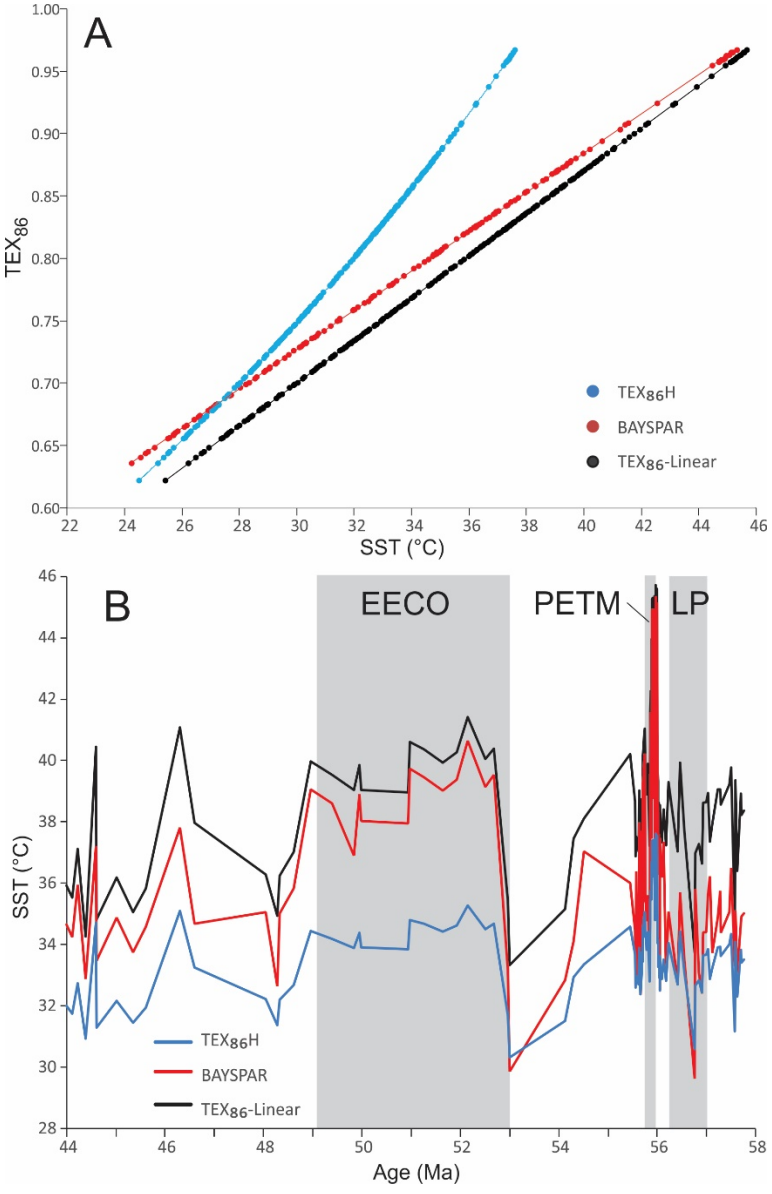

Figure 4: Relationships between TEX_{86} calibrations and sea surface temperature for low-latitude Paleocene-Eocene sites (data from Cramwinckel et al., 2018). A) Comparison of the exponential TEX_{86}^{H} calibration (Kim et al. 2010), the linear TEX_{86} (O'Brien et al., 2017) and BAYSPAR calibrations (Tierney and Tingley, 2014, 2015). Because of the spatially varying regression used for BAYSPAR only one site (ODP Site 959) is plotted for this calibration. B) Comparison of SST reconstructions from late Paleocene to early middle Eocene for the three calibrations. The timescale of Gradstein et al. (2012) is used in this figure. Approximate locations of the three targeted time intervals are also shown: latest Paleocene (LP), Paleocene-Eocene thermal maximum (PETM) and early Eocene climatic optimum (EECO).

Geosci. Model Dev. Discuss., https://doi.org/10.5194/gmd-2018-309
Manuscript under review for journal Geosci. Model Dev.
Discussion started: 17 January 2019

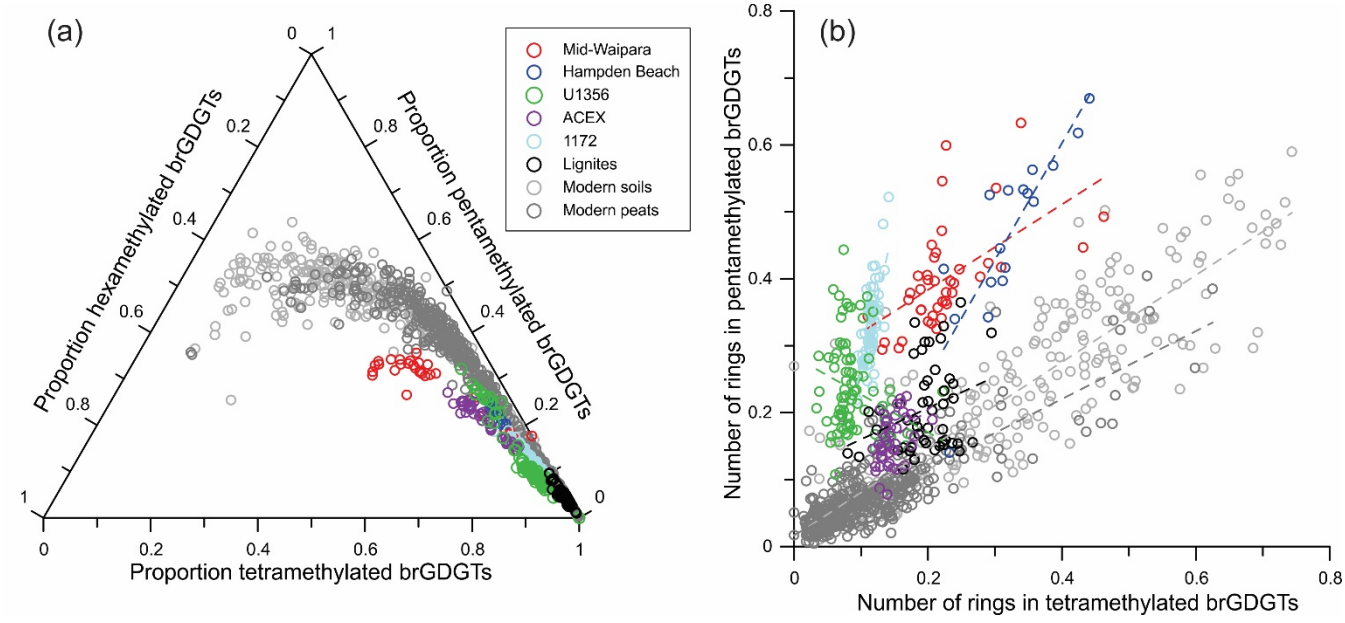

Figure 5. Distribution of brGDGTs in present-day mineral soils (Naafs et al., 2017a) and peats (Naafs et al., 2017b), compared to that in early Paleogene marine sediments (Weijers et al., 2007; Bijl et al., 2013; Pancost et al., 2013) and terrestrial lignites (Naafs et al., 2018): (a) a ternary plot showing relative proportions of tetra-, penta- and hexamethylated brGRGDTs; (b) a cross plot showing the average number of cyclopentane moieties (rings) for tetra- and pentamethylated brGDGTs.

Geosci. Model Dev. Discuss., https://doi.org/10.5194/gmd-2018-309
Manuscript under review for journal Geosci. Model Dev.
Discussion started: 17 January 2019

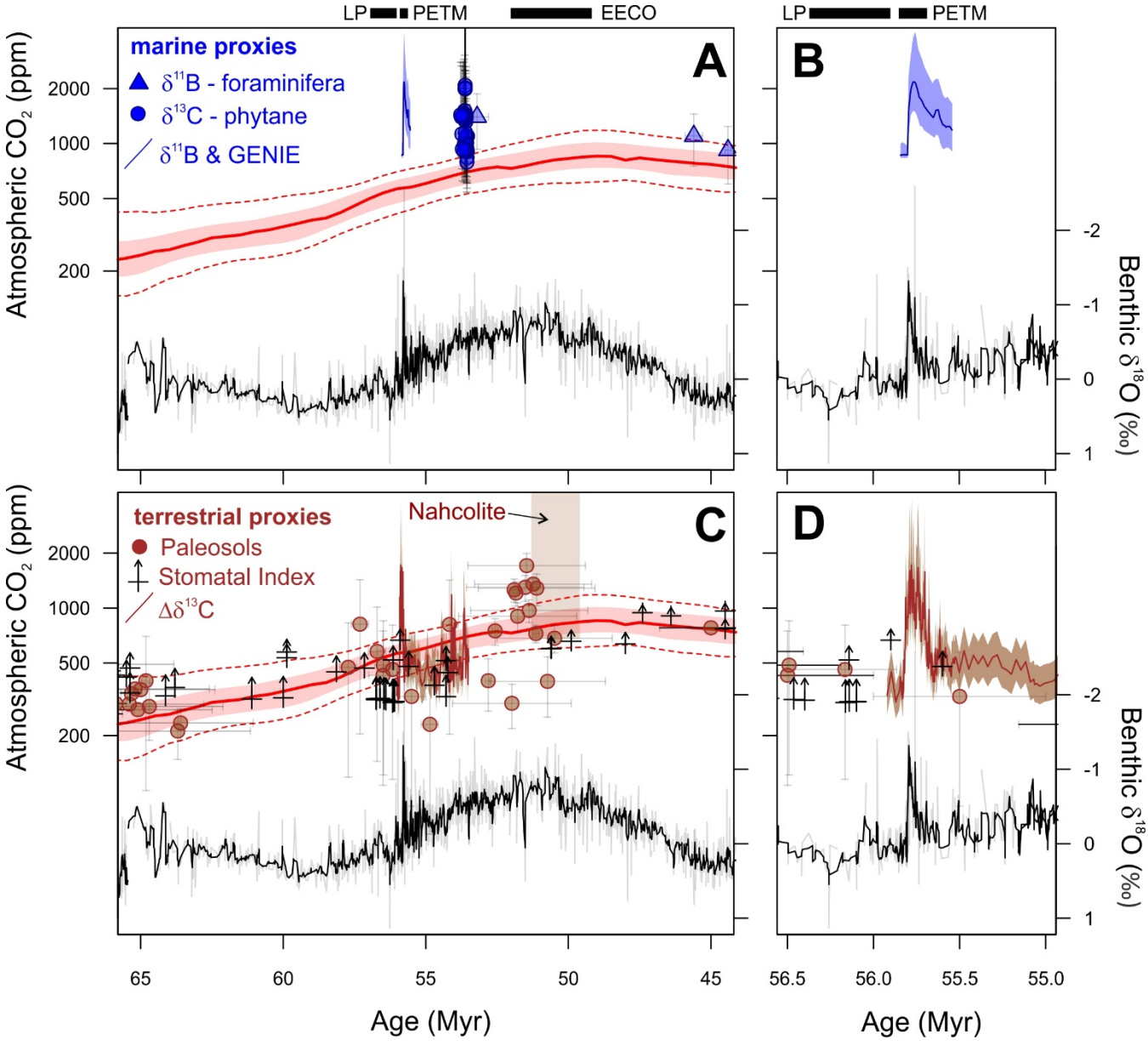

Figure 6. Reconstruction of atmospheric CO_2 from marine (A and B) and terrestrial (C and D) proxies for the early Paleocene to early middle Eocene (A and C), and an expanded reconstruction across the Paleocene-Eocene boundary (B and D). The CO_2 estimates plotted here are summarised with appropriate references in Supplementary Data File 8. The red line is a LOESS smoother from Foster et al. (2017), the red band is 68% confidence and the dashed red lines are 95% confidence around that long-term trend. The timescale of Gradstein et al. (2004) is used in this figure. Approximate locations of the three targeted time intervals are also shown: latest Paleocene (LP), Paleocene-Eocene thermal maximum (PETM) and early Eocene climatic optimum (EECO). Note that stomatal index and the nahcolite are plotted with an unbounded upper CO_2 and so represent minimum estimates. See the text for a discussion of the methodologies used.

Geosci. Model Dev. Discuss., https://doi.org/10.5194/gmd-2018-309
Manuscript under review for journal Geosci. Model Dev.
Discussion started: 17 January 2019

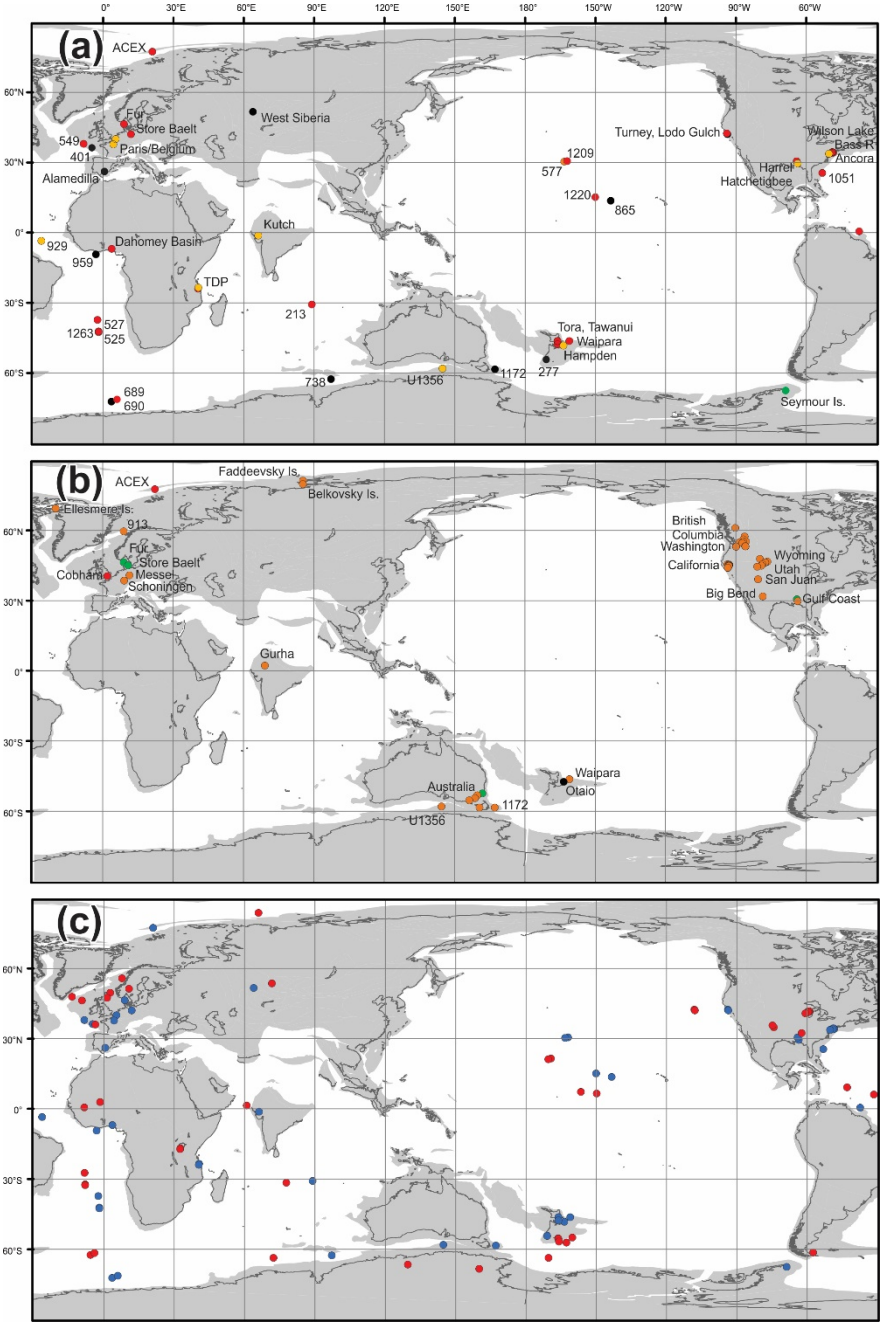

Figure 7. Sites with latest Paleocene–early Eocene temperature estimates on a 52 Ma paleogeographic reconstruction using relative plate motions from Matthews et al. (2016) with the paleomagnetic reference frame of Torsvik et al. (2012). (a) Marine sites with time intervals indicated as follows: black circles, all three time intervals represented; red circles, PETM ± LP intervals; orange circles, EECO interval; green circle, middle Eocene (Seymour Island). (b) Terrestrial sites with time intervals indicated as in (A) and green circles, LP only. (c) Comparison between reference frames; blue circles are marine sites plotted using the same paleomagnetic reference frame as in (A); red circles are plotted using a moving hot-spot reference frame (Matthews et al., 2016). Sites locations and paleolocations are tabulated in Supplementary Data File 2.

Geosci. Model Dev. Discuss., https://doi.org/10.5194/gmd-2018-309
Manuscript under review for journal Geosci. Model Dev.
Discussion started: 17 January 2019

Geoscientific Model Development Discussions
Open Access
EGU

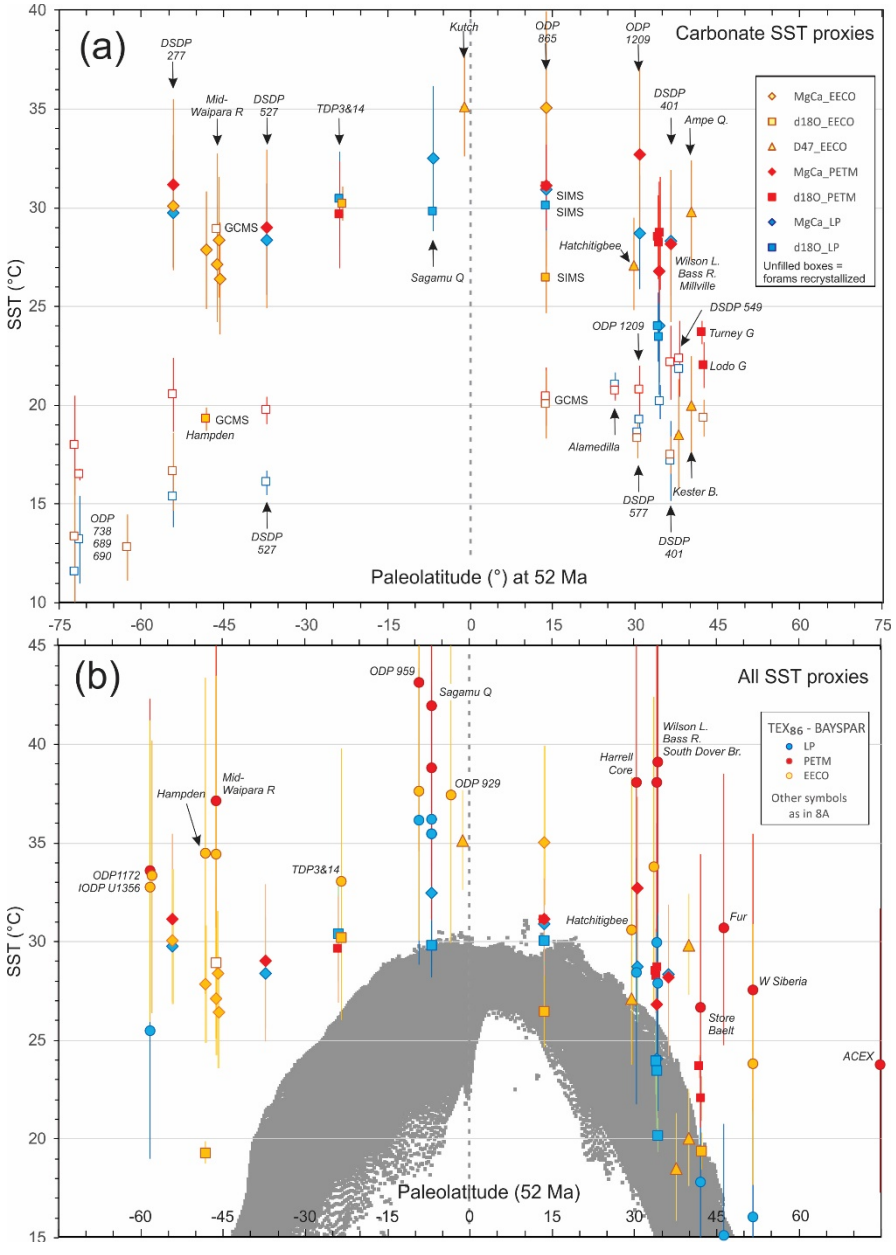

Figure 8. SST estimates derived from (a) carbonate proxies and (b) all proxies for three time slices: latest Paleocene (LP), PETM and EECO. Deep sea δ18O records that are inferred to be affected by diagenesis are omitted from Fig. 8B. These data are tabulated in Supplementary Data Files 3–6. Grey data cloud in Fig. 8B represents modern SST measurements derived from European Centre for Medium-Range Weather Forecasts (2017), ERA5 Reanalysis Monthly Means, https://doi.org/10.5065/D63B5XW1, Research Data Archive at the National Center for Atmospheric Research, Computational and Information Systems Laboratory, Boulder, Colo. (Updated monthly.) Accessed 8-11-2018.

Geosci. Model Dev. Discuss., https://doi.org/10.5194/gmd-2018-309
Manuscript under review for journal Geosci. Model Dev.
Discussion started: 17 January 2019

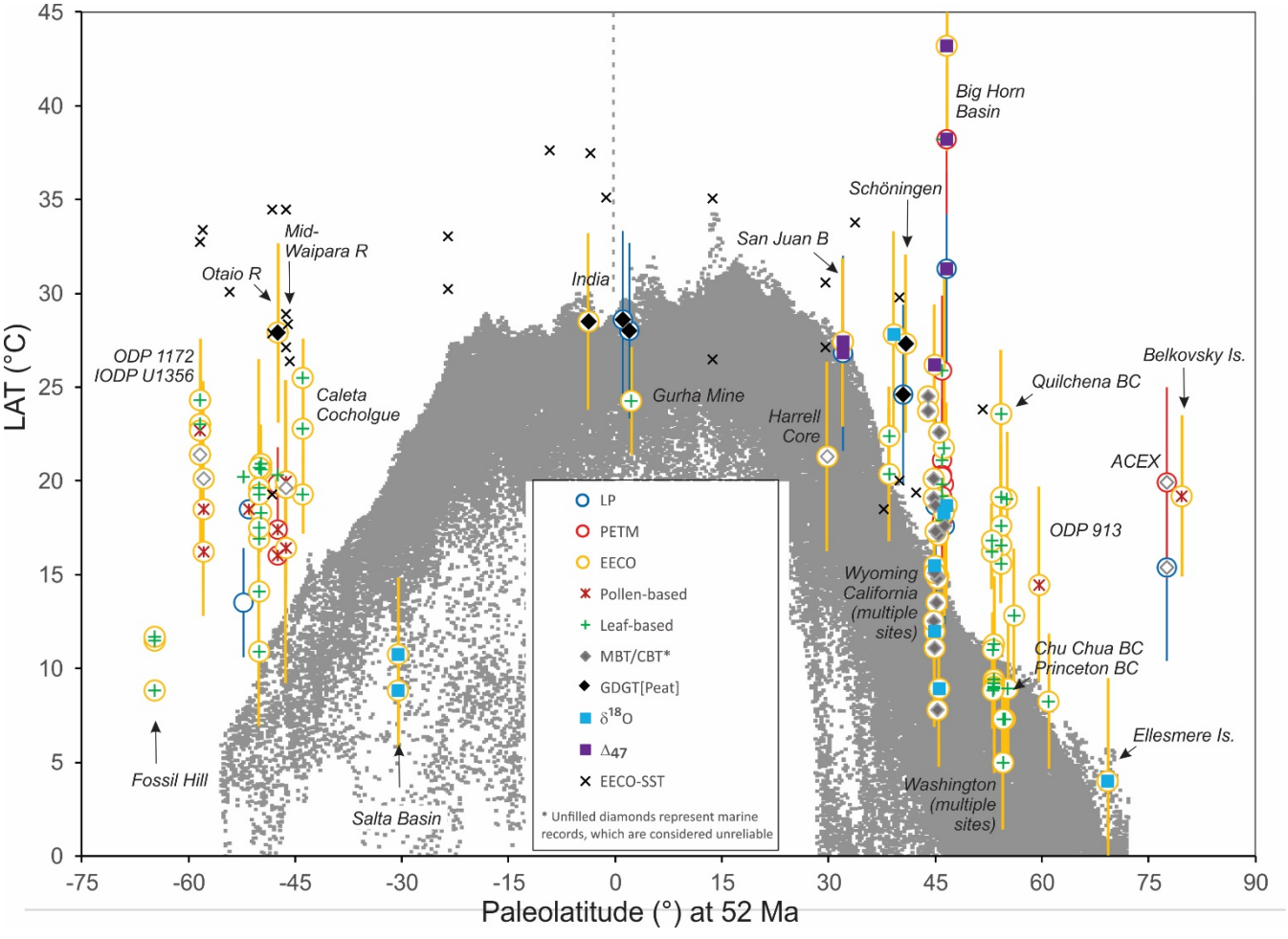

Figure 9. LAT estimates for the three time slices differentiated by broad proxy categories. These data are tabulated in Supplementary Data File 7. The SST data for the EECO is shown for comparison. Grey data cloud represents modern LAT measurements derived from same source cited for Figure 8B.